HHS Public Access

Author manuscript

Chem Rev. Author manuscript; available in PMC 2021 September 23.

Published in final edited form as:

Chem Rev. 2020 October 14; 120(19): 11093–11127. doi:10.1021/acs.chemrev.0c00145.

Solid Organ Bioprinting: Strategies to Achieve Organ Function

Adam M Jorgensen[1], **James J Yoo**[1], **Anthony Atala**[1,*]

[1]Wake Forest Institute for Regenerative Medicine, Wake Forest School of Medicine, Winston-Salem, North Carolina, USA.

Abstract

The field of tissue engineering has advanced over the last decade, but the largest impact on human health should be achieved with the transition of engineered solid organs to the clinic. The number of patients suffering from solid organ disease continues to increase, with over 100,000 patients on the US national waitlist and approximately 730,000 deaths in the United States resulting from end-stage organ disease annually. While flat, tubular, and hollow non-tubular engineered organs have already been implanted in patients, *in vitro* formation of a fully functional solid organ at a translatable scale has not yet been achieved. Thus, one major goal is to bioengineer complex, solid organs for transplantation, composed of patient-specific cells. Among the myriad of approaches attempted to engineer solid organs, 3D bioprinting offers unmatched potential. This review highlights the structural complexity which must be engineered at nano-, micro-, and mesostructural scales to enable organ function. We showcase key advances in bioprinting solid organs with complex vascular networks and functioning microstructures, advances in biomaterials science that have enabled this progress, the regulatory hurdles the field has yet to overcome, and cutting edge technologies that bring us closer to the promise of engineered solid organs.

Graphical Abstract

[*]Anthony Atala, MD; Wake Forest Institute for Regenerative Medicine, Wake Forest School of Medicine, Winston-Salem, Richard H. Dean Biomedical Building, 391 Technology Way, Winston-Salem, NC, USA 27101; Telephone: 336-713-7293; Fax: 336-713-7290; aatala@wakehealth.edu.

Adam M Jorgensen; Wake Forest Institute for Regenerative Medicine, Wake Forest School of Medicine, Winston-Salem, Richard H. Dean Biomedical Building, 391 Technology Way, Winston-Salem, NC, USA 27101; Telephone: 336-713-7293; Fax: 336-713-7290.

James J Yoo, MD/PhD; Wake Forest Institute for Regenerative Medicine, Wake Forest School of Medicine, Winston-Salem, Richard H. Dean Biomedical Building, 391 Technology Way, Winston-Salem, NC, USA 27101; Telephone: 336-713-7293; Fax: 336-713-7290.

The authors declare no competing financial interest

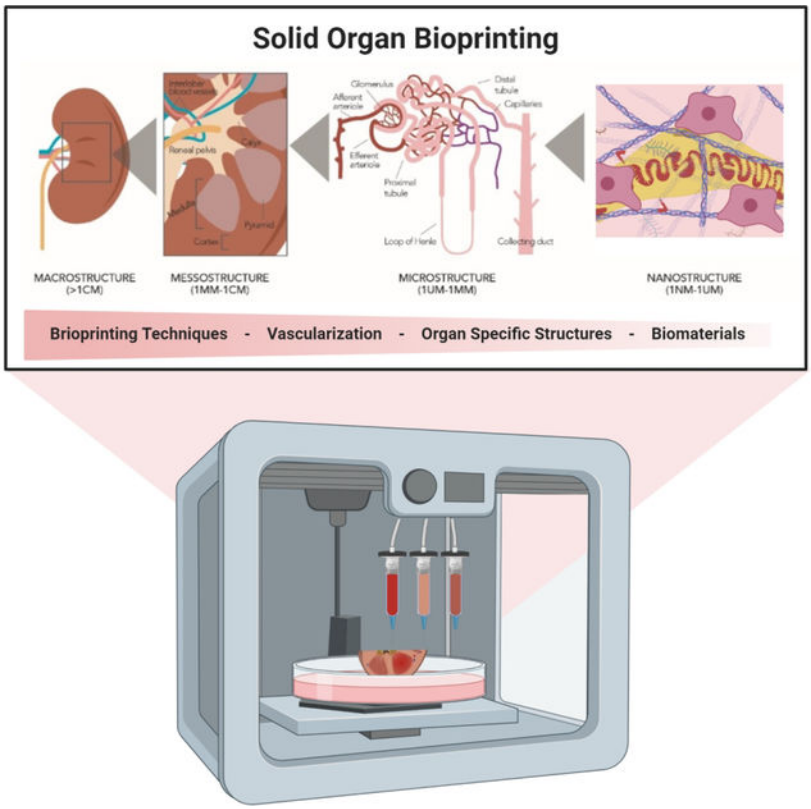

1. Introduction

The field of tissue engineering is maturing toward creating opportunities that provide complex tissues and organs to impact human health more significantly. The total patients suffering from end-stage solid organ disease continues to increase, with a patient being added to the national transplant waiting list every ten minutes. Whole-organ transplantation remains the gold standard for treatment of end-stage organ disease. However, only select patients receive functional organ transplants, and it is exceptionally difficult to obtain a histocompatibility, requiring permanent use of immunosuppressive agents. Despite the herculean efforts of UNOS and transplant centers across the country to provide over 30,000 organ transplants per year, over 100,000 patients on average with end-stage organ disease remain on the national waitlist year-over-year[1–3]. Furthermore, end-stage organ disease is responsible for approximately 730,000 US deaths annually[4].

To address these, and other unmet clinical needs, regenerative medicine has made major strides over the last decade with 1,028 clinical trials underway by the end of 2018, and 41 specific to tissue engineering[5].These efforts have led to a significant need to improve reproducibility, increase the specificity of cell placement, improve manufacturing techniques, and engineer more extensive, human-like tissue[6]. Engineered flat, tubular, and hollow organs have already been successfully implanted in patients, but in vitro formation of solid organs has not yet been achieved. Thus, a major goal of regenerative medicine is to bioengineer complex, solid organs for transplantation composed patient-specific cells[7].

Among the myriad of techniques attempted to engineer solid organs, 3D bioprinting today offers the best potential. Bioprinting is a powerful resource in tissue engineering and has a role to play in advancing the fabrication of solid, viable organs. 3D printing utilizes computer-controlled systems to deposit biomaterials (with or without cells) into precise geometries to create anatomically correct structures[8]. These devices can print cell aggregates, cells encapsulated in hydrogels, supported by cell-free polymer structures[9]. Bioprinting builds upon the reproducibility seen in mold casting techniques by improving the ability to layer and interweave constructs with improved control of the placement and specificity of bioink and cell distribution[10]. Cells used in constructs may be isolated and expanded from patient-specific biopsies, allowing for autologous implants[11]. 3D reconstruction images from MRI may also allow for patient-specific implants.

Even with significant advances in bioprinting machinery, engineers aspiring to fabricate solid organs face challenges. The cell and structural diversity within solid organs, coupled with a constant demand for nutrients and oxygen from perfusable vasculature, adds layers of complexity to organ engineering[12]. In this review, we address the challenges presented by whole organ bioprinting and opportunities for growth within the field. First, we will present an overview of organ anatomy by structural resolution: Macrostructure, Mesostructure, Microstructure, and Nanostructure. Next, we will review how tissue engineers seek to overcome the challenge of organ microstructure engineering by addressing: 1) Mesostructure: vascularity is crucial to organ integration, 2) Microstructure: advances in engineering organ-specific structures to enable organ function, and 3) Nanostructure: biomaterials promote cellular self-assembly and provide structural support. The review will conclude with a description of the most recent advances for rapid microstructural printing, detailed printing, post-printing organ maturation and assessment, manufacturing scale-up, and regulatory considerations.

2. Organ structure and classification

2.1 Organ anatomy by structural resolution

The great challenge in solid organ printing is the complexity of structural elements, ranging from macrostructural shape to nanostructural detail (See Figure 1). As an example, the kidney, macrostructurally (resolution >1cm), is a bean-shaped organ with three major tubular structures connecting to the body's vascular supply and renal network; the renal artery, the renal vein, and the ureter. Once dissected further, mesostructured elements (1mm-1cm) help transport key products to and from the functional kidney units: the renal pelvis as the collecting place for urea deposited by minor and major calyxes produced within renal pyramids of the renal medulla, with a clear separation from the renal cortex; interlobular and arcuate blood vessels stemming from and depositing into the renal artery and vein supply nutrients. On the microstructural level (1μm-1mm) are a network of complex structures which make up the nephron, composed of the proximal and distal convoluted tubules, the loop of Henle, and the collecting duct, the known functional unit of the kidney; and a complex capillary network composed of the glomerulus, afferent, and efferent arterioles[13, 14]. Their unique cellular composition can further categorize each of these

microstructural units. Finally, the kidney nanostructure (1nm -1μm), can be characterized, with its unique extracellular matrix (ECM) components, diffusion channels, and enzymes.

In embryonic development, the body takes a nano to a macro approach to organ formation[16]. From a single fertilized egg, the entire human body develops. Cells differentiate and use their inherent machinery to form the nanostructural organ scaffold. Capillary networks develop with angiogenesis providing essential nutrients and growth factors. Eventually, meso- and macrostructural anatomy can be recognized as the organ prepares to perform its intended function. Thus, human development takes a Nano to Macro approach to organ development.

Biomaterials that closely mimic organ nanostructure can be employed to replicate the Nano- to Macro- approach for human organ development[17]. Providing essential ques can help guide cellular assembly into the functional microstructural elements of human organs. However, proper biomaterial placement is necessary to direct cellular self-assembly[18]. Current bioprinting capabilities rely on the mechanical placement of cells that can produce low-resolution structures (>1cm) down to very high-resolution 20μm (LIFT)[19]. However, even the highest resolution printing methods are limited in replication of the microstructural anatomy with high fidelity. Bioprinters can replicate Macro- and Meso-structural resolution by utilizing the CAD/CAM coding from CT/MRI images to recreate normal anatomy. In essence, bioprinting takes a Macro to Micro approach to organ development. To fully realize the potential for whole organ bioprinting, a Macro to Micro (bioprinting) and a Nano to Meso (biomaterials/cell self-assembly) approach must work in harmony.

2.2 Macrostructural organ classification

There are four general levels of tissues and organ macrostructural complexity; flat tissue, such as the skin; tubular structures, such as blood vessels; hollow structures, such as the bladder; and solid organs, such as the kidney (See Figure 2). Tissue engineering complexity generally increases along this continuum as increased metabolic functions and structural requirements are needed for targeted for repair of the tissue or organ[20].

First, flat tissues are composed of cell sheets stacked in multiple layers. Skin is one example of flat tissue. Skin is the largest organ in the body, and provides an essential barrier to provide protection, both physically and immunologically from the outside world. Due to the relative structural simplicity of skin, it was one of the first tissue engineering targets using autologous cells from patients[21], demonstrating the feasibility for human cell isolation, culture, and re-implantation. Furthermore, flat structures are relatively thin, allowing for nutrient diffusion without complete vascularization. Nearly all the structural elements of the skin are reproducible through bioprinting, however further work must be done to replicate the delicate microstructures such as hair follicles and glands[22].

Second, tubular organs are composed of cell sheets formed into circular, bilayer tissues. Blood vessels are a natural example of tubular structures, with endothelial cells forming an inner layer and functional barrier; and smooth muscle and connective tissue form an outer layer to provide support[23]. Similar to flat tissues, the relatively thin wall thickness of tubular tissue enables nutrient diffusion and oxygen exchange. Thus, large diameter blood vessels

are relatively easy to manufacture, while microstructural arterioles, capillaries, and venules remain a challenge.

Third, hollow organs consist of epithelial cells forming the inner layer of surrounded by smooth muscle forming an outer layer of with or without connective tissue. The bladder is a clear example of a hollow organ. Compared with the flat and tubular structures, the bladder has higher metabolic requirements, functional parameters, and complex interactions with other organs. Even with an organ of this complexity, tissue engineers have regenerated bladder tissue using autologously derived urothelial and smooth muscle cells[24]. These and other studies have demonstrated that the macro- and meso-structural elements of hollow organs can be replicated. However, recreating organ microstructure, including glands and vascularity, remains a challenge.

Finally, solid organs such as the kidney, liver, heart, and pancreas are the most complex. The goal of fabricating solid organs presents major hurdles due to the developmental process and tissue complexity of these organs. Whole organs require mature vascular networks with extensive branching for cells to remain viable. Whole organs also require precise organization of multiple cell types. To this end, present endeavors focus on developing biomaterial-based approaches and the use of 3D printing methods[25, 26].

2.3. Critical opportunities for development: mesostructure, microstructure, nanostructure

As bioprinting technology has enabled macrostructural (>1cm) and mesostructural (1mm-1cm) mimicry with high fidelity, there are vital areas for further development. Tunable biomaterials that closely replicate the nanostructure ECM of native organs are required to replicate organ nanostructure and provide mechanical stability for maturing organs. Improvements in vascular network bioprinting will be crucial for the integration and delivery of oxygen and nutrients[27]. Finally, organ-specific microstructures essential for organ function must form by directing the inherent ability of cells to self-assemble with guidance from growth factors and biophysical cues.

3. Biomaterials promote cellular self-assembly and provide structural support

Biomaterials are crucial to achieving the ultimate goal of whole organ bioprinting (see table 1). Tunable biomaterials aim to replicate extracellular matrix properties and are designed to promote cell attachment, proliferation, and self-assembly into microstructures.

3.1. Naturally derived materials

There is an abundance of natural polymers available for use in biofabrication (see figure 3). These polymers may be utilized independently with their natural structure or may be chemically modified to achieve further tunable hydrogel characteristics. Furthermore, these materials can be combined to utilize the favorable elements inherent in each.

Alginate is a natural polymer from brown algae that has been used extensively for biomedical applications[57]. Alginate structures can gel through multiple crosslinking mechanisms, including ionic crosslinking, covalent crosslinking, and thermal gelation, with the most common activator being divalent cations such as Ca2+. A 7.5% alginate bioink was used to engineer cardiac tissue from human cardiac progenitor cells[35]. By using an extrusion-based bioprinting approach, they were able to distribute the cells throughout the construct homogeneously and saw increased expression of cardiac transcription factors (NKx2.5, Gata-4, and Mef-2c) and Troponin T after 3D culture. It is also common for alginate to be coupled with RGD to improve its mechanical properties. This form of alginate has been used to fabricate hypertrophic cartilage[58]. The RGD-Alginate printed with polycaprolactone fibers produced a 350-fold increase in the compressive modulus of the construct. When placed in vivo, the reinforced cartilaginous template allowed for vascularized bone containing trabecular-like endochondral bone to form. Another way to improve alginate hydrogel properties is to add other natural and synthetic polymers to form specialized composite hydrogels. Investigators used a composite gel of glycosylated alginate, collagen, and PVLA to develop liver microstructures. PVLA contains galactose chains that are known to increase ASGPR expression by hepatocytes, which in turn improves adhesion cell adhesion. However, since PVLA is a hydrophobic polymer, it could not be directly used with hydrophilic alginate hydrogel. Thus, galactosylate alginate was synthesized to control cell polarity and promote hepatocyte adhesion[59].

Collagen is the most common protein in the human body, and collagen-based biomaterials have been extensively studied and applied over the past decade[60]. It is biodegradable, biocompatible, and readily available. It makes up approximately 25% of the total dry weight of humans. Fibroblasts produce the majority of collagen in connective tissue with 29 different currently known forms. Type I collagen is the common form uses in tissue engineering and represents 90% of the total collagen content in the human body[61]. Collagen is commonly isolated in two primary forms. First, decellularized organs retain the collagen matrix with the original tissue shape, which may be used for direct cell seeding[62]. Alternatively, collagen can be extracted, purified, and polymerized to form functional scaffolds. The crosslinking mechanism for collagen relies on amine and carboxyl group modification of collagen molecules to allow for covalent bonds. This can be done through physical crosslinking (UV or thermal), or Chemical (aldehydes, carbodiimide, isocyanate) and enzymatic (transglutaminases) reactions. A collagen hydrogel was used to encapsulate bladder smooth muscle cells (SMC) for bioprinting[41]. The investigators found that encapsulated SMCs proliferated within the fabricated collagen building blocks, which were then assembled to create a SMC patch. The patch formed a 3D tissue-like construct over 50 day of culture, and was found to be histologically similar to native rat bladder. Another group formed a composite hydrogel of type I collagen, sodium hydroxide, and sodium bicarbonate, which they used to fabricate a functional vascularized thyroid gland[40]. First, thyroid, allantoic spheroids were generated, which were then encapsulated in collagen hydrogel and deposited in close association by a 3D bioprinter. During culture, spheroids placed near each other fused into a single structure, and endothelial cells from the allantoic spheroid vascularized the thyroid spheroid, while thyroid spheroid epithelial cells formed follicles. A capillary network formed around the follicular cells, similar to what is seen

during in utero thyroid development. The cultured bioprinter construct was functional *in vivo* after being grafted under the kidney capsule of hypothyroid mice, and were able to normalize body temperature and blood thyroxine levels.

Fibrinogen is a natural monomer that reacts with thrombin to form the biopolymer fibrin[63]. Fibrin is a crucial protein element of the blood coagulation cascade. In this form, fibrinogen is converted to fibrin by a thrombin mediated cleavage of fibrinopeptide-a, which causes a conformational change and exposure of polymerization sites. Fibrin monomers then self-associate to form insoluble fibrin. Further covalent bonding produces a stable fibrin network that is resistant to protease degradation. However, a commonly cited weakness of fibrin hydrogels is its relatively weak rheological properties[64]. Even so, fibrinogen has been used extensively for engineering adipose, cartilage, bone, cardiac, liver, nervous, ocular, and skin tissue engineering. Song and Millman created a microporous device of for β cell transplantation with polylactic acid to house stem cell-derived β cell clusters with a degradable fibrin gel[46, 65]. In order to load and secure SC-β cell clusters within the 3D-printed devices, SC-β cell clusters were suspended in a fibrinogen solution and inserted into the device. Thrombin solution was immediately added into the cellular suspension, which crosslinked rapidly. The devices with cell suspension were then implanted into immunocompromised mice. Following glucose injection, they found a significant increase in human insulin, indicating that the transplanted grafts were functional and glucose-responsive. Our group has utilized a composite fibrin hydrogel of fibrin, gelatin, HA, and glycerol. Kang et al. used this composite gel to demonstrate the capabilities of our integrated tissue organ printing (ITOP) platform by fabricating cartilage, complex models of the mandible and calvarial bone, and skeletal muscle[45]. The shape of the tissue constructs was made using clinical imaging data that was converted into a computer CAD/CAM model, which was then translated a code to control the printer nozzles pneumatic dispenses and motions to distribute the bioink in precise locations. They further utilized polycaprolactone (PCL) to confer mechanical strength to tissue constructs. The ITOP printer allowed for fabrication of micro channels composed of a porous lattice network design to facilitate diffusion of nutrients and oxygen. The bioprinted ear, bone, and muscle constructs showed evidence of vascularization without necrosis when implanted in vivo, and the muscle constructs formed neuromuscular junctions.

Gelatin is a natural polymer that is highly advantageous as a biomaterial for organ printing due to its off-the-shelf availability, low immunogenicity, cell-adhesive structure, biodegradability, and low cost[66]. It is manufactured by acid or alkaline hydrolysis of animal collagen, and is generally-regarded as Safe GRAS by the FDS. Gelatin molecules contain repeating sequences of Gly-X–Y, where X and Y are most often proline (Pro) and hydroxyproline (Hypro) amino acids[67]. Gelatin is often used in combination with other biomaterials to improve cell adhesion, spreading, and proliferation. Investigators have employed a gelatin/hyaluronic acid composite bioink to produce a cardiac patch[47]. In their design, human cardiac myoprogenitor cells were encapsulated in hyaluronic acid/ gelatin composite gel at a density of 30 × 106 cells/ml. There construct was made of six perpendicularly printed layers, with an overall thickness of 400 μm. The printed construct was transplanted in a mouse model of myocardial infarction. The applied patch resulted in improved cardiac performance, and reduced scarred remodeling on both MRI and

histology. The matrix-supported long-term survival and *in vivo* engraftment of the human cardiomyocytes, which continued to differentiate into cardiac and vascular structures over a 4-weeks.

Hyaluronic Acid is a glycosaminoglycan consisting of repeating units of D-glucuronic Aid and N-acetyl D-Glucosamine[68]. It is found in the ECM of all tissues but is highly concentrated in mechanically active tissues including the vocal folds, cartilage, and dermis. Hyaluronic acid is non-allergic and non-inflammatory; however, it is quickly degraded by reactive oxygen or nitrogen species and hyaluronidases[69]. Hyaluronan has been shown to promote cell invasiveness and epithelial-mesenchymal transition[70]. Its breakdown products have further been shown to stimulate angiogenesis, a crucial component of successful tissue-engineered organs[71]. It is highly viscous and has a strong ability to retain water. Due to readily available reactive functional groups, HA can be chemically modified to be biocompatible for use in tissue engineering. One common form of chemically modified hyaluronic acid is methacrylated hyaluronic acid (HAMA), which improves tissue formation and enhances printability. HAMA has be added to thermosensitive hydrogels composed of methacrylated poly [N-(2-hydroxypropyl)] methacrylamide mono/dilactate][72]. This was used on for cartilage engineering and demonstrated a dose-dependent effect of HAMA concentration on cartilage matrix synthesis by chondrocytes. The investigators also found that Glycosaminoglycan and type II collagen content increased with intermediate HAMA concentrations. They also found that relatively high HAMA concentration greater than 1% formed more fibrocartilage.

Silk is a macromolecular protein polymer found in nature that is synthesized by lepidopteran larvae using epithelial cells of specialized glands and ultimately spun into fibers[73]. The spun fiber is made of a central protein known as fibroin that is encased by a glue-like coating sericin. It has been shown that the bio-incompatibility of silk is due to the sericin glue and that sericin free fibroin fiber has excellent biocompatibility[74]. The copolymer organization of silk fibroin with hydrophobic and hydrophilic blocks combine to give a highly elastic and mechanically robust polymer. Furthermore, its degradation kinetics are tunable[75]. Silk has more recently been used in composite hydrogels, particularly in cartilage bioprinting. Investigators developed clinically relevant cartilage tissue by bioprinting human cartilage tissue-derived mesenchymal progenitor cells encapsulated in a silk fibroin-gelatin composite bioink[76]. The bioink gelation was induced by enzymatic crosslinking with mushroom tyrosinase and physical crosslinking by sonication. Optimization of the rheology of their bioink, resulted in maximum cell viability and ultimately lineage differentiation of the mesenchymal progenitor cells.

3.2. Synthetic polymers

Synthetic polymers are widely used in biofabrication applications (see figure 4). The significant advantage of synthetic polymers is their flexibility for chemical modification to allow for tunable hydrogel characteristics. Furthermore, these materials can be combined to utilize favorable elements inherent to each material.

Agarose is a biocompatible polysaccharide extracted from marine red algae, which contains repeating of agarobiose[77]. It is thermoreversible, gelling at 30–40c and can be easily

dissolved in hot water or DMSA, and the presence of oxygen and hydrogen supports its self-gelling behavior. Investigators have encapsulated human mesenchymal stem cells and MG-63 cells into agarose hydrogels supported in high-density fluorocarbon, and printed to form structures[30]. The fidelity of the printed constructs improved by performing the procedure in the fluorocarbon shape, while also adding stability during the procedure and maintaining cell viability. In subsequent work, agarose coupled with collagen and chitosan was used to determine if hydrogels stiffness impacted cell differentiation[28]. The human MSCs, encapsulated chitosan–agarose and type I collagen bioinks were differentiated toward osteoblasts and adipocytes. Osteogenic differentiation occurred more often in soft substrates that were collagen-rich, while adipogenic differentiation mostly occurred in stiff matrices that were agarose-rich.

Gelatin methacryloyl has been used extensively as result of its tunable physical properties and promising biological characteristics[78]. When printed in 3D, hydrogels strictly retain the naïve extracellular matrix with cells attaching and MMP peptide motifs. GelMA is crosslinked by photoinitiated radical polymerization under UV light exposure with photoinitiation. It improves upon its gelatin only counterpart, in that it has better solubility and less antigenicity. Hybrid forms of GelMA include GelMA with carbon nanotubes, graphene oxide, inorganic nanoparticles, and other biopolymers and synthetic polymers have been documented. A biphasic artificial vascularized bone construct with regional bioactive factors using a GelMA hydrogel was recently reported[79]. The construct was fabricated on a dual bioprinting platform comprised of both SLA 3D and FDM 3D bioprinter, with alternating deposition of biodegradable polylactide filament and cell-laden GelMa. To promote osteogenesis and angiogenesis, a p regional immobilization of bone morphogenetic protein 2 (BMP2) and vascular endothelial growth factor (VEGF) peptides was introduced. This resulted in a highly osteogenic bone construct with organized vascular networks. GelMA/HAMA composite hydrogel was used to generate a clinically translatable bioscaffold for cartilage repair. For improved clinical application, a handheld 3D printer called a “Biopen” was developed to allow for freeform biofabrication and scaffold delivery for chondral repair, with both high cell viability and structural stiffness[80]. The system was composed a co-axial hydrogel containing infrapatellar adipose-derived MSCs encapsulated in a GelMA-HAMA composite hydrogel. The outer shell component contained the same hydrogel along with a photoinitiator. Hardening the shell provided the structural support, allowing for cell preservation in relatively cell-friendly environment inside the core separated from the damaging effects of the ithium-acylphosphinate (LAP) photo-activated cross-linking. The LAP photo-initiator is generated by Dimethyl phenylphosphonite reaction with 2,4,6-trimethylbenzoyl chloride via a Michaelis-Arbuzov reaction[81]. The water-soluble LAP photo-initiator can generate crosslinked hydrogels with a high modulus value with short exposure time (10 seconds), increased polymerization rates, and absorbance above 400 nm[82].

Polyethylene glycol (PEG) is a hydrophilic synthetic polymer commonly used in bioprinting applications[83]. It is known for its biocompatibility, non-immunogenicity, and limited protein absorption. PEG is made up of linear and branched structures and is a diol with two tunable hydroxyl end groups. The key crosslinking mechanism includes radiation of branch PEG polymers, free radical polymerization, chemical reaction, and enzymatic. Most commonly

photopolymerization is used to convert liquid PEG macromers into stable hydrogels at physiological temperature and pH. One weakness of the highly bio-inert nature of PEG hydrogels is the low adhesion results and low viability when cells are added. Attempts have been made for tethering ECM derived bioactive molecules in order to enhance cell adhesion, proliferation, and viability. Investigators demonstrated the use of a PEG - alginate composite hydrogel for cartilage biofabrication[84]. The hydrogel relied two mechanisms: the reversible Ca2+ crosslinking of alginate dissipates mechanical energy, while the covalent crosslinking of PEG maintains elasticity under large deformations. Due to these crosslinking mechanisms the composite hydrogel could undergo both tension and compression stress, making it tougher than natural cartilage with a fracture toughness above 1500 J m^{-2}. The investigators printed the robust hydrogel into complicated 3D structures with encapsulated human MSCs with high viability maintained over seven days.

Polyurethane is a synthetic polymer with a unique segmented structure that allows for diverse, tunable properties. The range of physical and mechanical properties associated with polyurethane includes thermoplastic to thermosetting, stability, and biodegradability, and can be either hydrophobic or hydrophilic depending on the composition and synthesis procedure applied[85]. While polyurethane has been widely used for medical applications, more recent uses include the formulation of polyurethane-based hydrogels. Investigators described the formation of an elliptic hybrid hierarchical polyurethane encapsulated cell/hydrogel construct[86]. They used synthetic polyurethane to form an external scaffold material to provide mechanical support with hydrogel as the internal scaffold material for adipose-derived stem cell encapsulation. The 3D composite construct was able to be cultured in vitro and was stable enough to embed *in vivo*. More recently, a study demonstrated that a composite gel of graphene and polyurethane could be used for 3D printing and the differentiation of neural stem cells[87]. The polyurethane was synthesized to contained poly (ε-caprolactone) and (1.5 kDa) poly (D, L-lactide) chains. Graphene was then added for neural stem cell printing. The graphene significantly improved oxygen metabolism and ultimately increase neural differentiation of the neural stem cells.

3.3. Tissue-specificity from ECM-derived hydrogels

Scaffolds derived from a natural extracellular matrix (ECM) are under investigation for use in therapeutic applications[43]. Decellularized organs are known to provide an ideal transplantable scaffold since they contain all the necessary microstructure and extracellular cues for cell attachment and differentiation, vascularization, and function[88, 89]. Furthermore, biological ECM scaffolds are rapidly degraded and replaced in vivo, resulting in the generation of downstream bioactive molecules with bioreductive properties[90, 91].

Extensive studies have been published in the field of ECM biomaterials. Investigators demonstrated a method for producing ECM of porcine small intestinal submucosa (SIS) to form a resorbable tissue repair and remodeling scaffold. Their study demonstrated that the ECM scaffolds rapidly and extensively degraded when used as a bioscaffold for augmentation cystoplasty in the dog model; however, the scaffold positively impacted tissue repair[92]. In later studies, they found that the material induced angiogenesis when implanted in wounds. To further investigate this finding in vitro, the group administered ECM in

a fibrin gel-based angiogenesis assay. Human microvascular endothelial cells embedded in the fibrin gel formed vascular tubes comparable to those formed by constructs treated with VEGF. Furthermore, tube formation was blocked when an anti-VEGF neutralizing antibody was added, further demonstrating that VEGF is present in the decellularized extracellular matrix[93]. In later studies, investigators compared the utility of organ-specific ECM to improve tissue remodeling following injury. The ECM of each tissue type can have a direct effect on the host response due to its unique structure and composition. To test this hypothesis, muscle ECM was compared vs. to non-muscle ECM of the small intestine. It was clear that the muscle ECM contained basement membrane structural proteins, glycosaminoglycans, and growth factors that were unique from those present in small intestine. However, implantation of the scaffold into an abdominal wall injury model in a rat demonstrated comparable constructive remodeling in both the muscle and small intestine scaffold. The improved remodeling appears to have been related to degradation of the scaffold, followed by myogenesis in the implant area, suggesting that superior tissue remodeling is not universally dependent on ECM scaffolds derived from homologous tissues[94]. Another group addressed volumetric muscle loss by engineering muscle constructs composed of cell-laden dECM bioinks with a granule-based printing reservoir. The muscle constructs were prevascularized with a hierarchical architecture through coaxial nozzle printing with muscle and vascular dECM bioinks. The tissue-specific dECM bioinks appeared to offer organized microenvironmental cues for the differentiation cells and improved vascularization, innervation, and functional recovery[95].

At the cutting edge of biomaterials for 3D bioprinting has been the discovery that decellularized organ ECM materials can be solubilized to form hydrogels. Organ-specific hydrogels have been found to direct remodeling and influence cell behavior by mechanisms through structural and biological signals retained from the natural source tissue[96]. It is thought that these tissue-specific cues are relayed by bound growth factors or the exposure of bioactive motifs[97, 98]. The method for decellularization and formation of hydrogels has been described in detail in the literature[96, 97, 99]. Several factors must be considered in determining the most efficient agents for decellularization, including the tissue's thickness, density, cellularity, and lipid content. A full description of the various agents used is outside the scope of this review but can be referenced elsewhere[100]. Following decellularization and lyophilization of organ tissue, ECM derived hydrogel formation is performed through solubilization of the ECM material and temperature or pH-controlled neutralization to induce re-formation of the intramolecular bonds to form a gel.

Engineers have successfully produced decellularized ECM (dECM) hydrogels specific to nearly every organ in the body, including the brain, heart, liver, lung, and pancreas[96]. Investigators developed a composite consisting of biodegradable elastomeric fibers and dECM gel from porcine dermal tissue demonstrated that the ECM gel is biocompatible and bioactive. To overcome this, the ECM gel was supplemented with electrospun biodegradable poly (ester urethane) urea. Next, electrospinning method was employed to create fiber composites with high flexibility and strength. The composite constructs were then tested in vivo with implantation into a full-thickness abdominal wall defect in rats, with herniation or infection over 4 weeks[101]. Later, a hydrogel was fabricated using spinal cord and brain ECM. The investigators found clear rheological differences between ECM from the brain,

spinal cord, and urinary bladder, with the greatest rheologic modulus seen with the spinal cord-derived. Interestingly, all ECM types, including the bladder matrix, increased the number of cells expressing neurites and promoted neurite outgrowth, but only brain-derived ECM increased neurite length[102]. Recently, proteomic analysis of dECMs from four tissues was performed to determine the tissue-specific functionalities of unique dECM[103]. In the study, dECM bioinks were printed with encapsulated human bone marrow mesenchymal stem cells, which differentiated in association with variable matrisome proteins within each dECM. Furthermore, tissue-specific differentiation was evident depending on the multipotency of MSCs. These findings provide strong evidence of tissue-specific advantages of homologous dECM bioinks.

Another research team developed a method for printing cell-laden dECM bioink with microenvironment conducive to the growth of 3D structured tissue[43] (see figure 5). Derived stem cells or mesenchymal stem cells were encapsulated in dECM gel, there was an increased number of cells that differentiated towards chondrogenic lineage within cartilage dECM or adipogenic lineage within adipose-derived dECM. Myoblasts formed in constructs prepared with dECM from heart tissue, which ultimately organized into the myofibers and expressed slow myosin heavy chain. The myofibers then synchronized with native tissue, suggesting that myoblasts printed in heart dECM can be used for myocardial reconstruction. Other groups have also used dECM to print cardiac tissues[43, 104].

Our group has similarly formulated composite hydrogels composed of decellularized ECM-based solution incorporated into highly tunable combinations of PEG crosslinkers with varying molecular weights, geometries, and functional groups to manufacture bioinks for extrusion bioprinting[42]. We have found that the ECM-derived solutions contain complex combinations of collagens, glycosaminoglycans, elastin, and growth factors, which enhance cell viability and eventual tissue construct function. We found high cell viability in a liver-specific hydrogel when compared with the extremely poor viability of cells printed in the gelatin-based hydrogel. Furthermore, liver function assays demonstrated that the spheroids secreted albumin and urea, suggesting that tissue-specific hydrogel bioink allow the bioprinted liver constructs to remain viable and function properly. More recently, our team has developed a photo-cross-linkable kidney ECM-derived bioink with a kidney-specific microenvironment for renal tissue bioprinting. The bioink is formed by decellularizing whole porcine kidneys by perfusion, dissolving in an acid solution, and chemically modifying by methacrylation. Human kidney cells encapsulated in the in the bioink maintained high viability and matured to exhibit the functional and structural characteristics of renal tissue. This tissue-specific ECM-derived bioink enhances cellular maturation and could eventually improve tissue formation[105].

3.4. Media-based printing

While most bioprinting methods require the use of biomaterials for printing, other methods, including inkjet bioprinting, require the use of media-based liquid cell suspensions. In this technique, cells are suspended in media or PBS, and then carefully extruded into specific locations or small co-cultured spheroids[106]. Spheroids then form through microwell centrifugation, hanging drop, and other known methods. Once these spheroid cell aggregates

have formed, they can be placed by a bioprinter. This method has been used with a microvalve printer to form kidney microstructures[36]. The investigators utilized gradients of bio-ink, one with hESCs in medium and the other media only, and then flipped the culture dish to form hanging drop spheroids with high cell viability. It has also been shown that isolated cardiac cells can be extruded in media to form cardiac microstructures[39]. The microstructures then self-assembled into beating solid tissue blocks, with synchronous contraction and early signs of vascularization by endothelial cells. This method has also been implemented to form functional myotubes that responded synchronously to electrical stimulation[55].

Another media-based bioprinting technique uses cell spheroids that are formed, resuspended, and skewered onto a needle array. Closely aligned spheroids then self-aggregate to form larger structures that can be removed from the needle array as a fabricated tissue. The feasibility of this scaffold-free approach has been demonstrated for liver microstructure development[54]. The self-assembled tissue maintained the expression of several hepatic drug transporters and metabolic enzymes. Glucose production by the fabricated tissue was suppressed by insulin, and bile acid secretion was evident. Also, structural sinusoid-hepatocyte-bile duct routes formed. The use of needle array tissue fabrication has also been used to form cardiac patches[53]. After fabrication, the patches exhibited ventricular-liked action potential waveforms with uniform electrical conduction in a spontaneous beat through the patch. The patch also vascularized when implanted into native rat myocardium in vivo.

4. Vascularity is crucial for integration of bioprinted organs

Central to bioprinting whole organs is the need for vascularity to provide nutrients, oxygen, and waste removal[107]. These challenges are not as drastic in flat and tubular organs, as their wall thickness can remain below 300 μm[108]. However, in hallow and solid organs, the wall thickness may exceed 300 μm[109]. Attempts to promote the infiltration of blood vessels to form capillary networks within bioprinted constructs are relevant, but ultimately replication of the hierarchical vascular network is necessary for biofabrication of complex tissues at clinically appropriate sizes[110]. In this section, we will present the current state of the art of vascular bioprinting as it applies to whole organ engineering.

4.1 Vascular anatomy

Vascular tissue composition includes extracellular matrix and cells organized into concentric layers in a tubular structure composed of three layers; the endothelial tunica intima, the muscular tunica media, and epithelial tunica externa[111]. Arteries that extend to whole organs branch into an anatomically unique microvasculature composed of arterioles, capillaries, and venules. Arterioles have a diameter of 10–200μm with an average lumen of 30 μm, and retain the three tunica layers (intima, media, and externa)[14]. Arterioles then branch into capillaries, characterized by a narrow lumen diameter of around 5–10 μm. Capillaries retain the endothelial layer and a basement membrane. Pericytes act to stabilize the vessel and allow for diffusion of solutes into nearby cells and tissues. Capillary permeability results from their structure, which can be continuous, fenestrated, or sinusoid[112]. Continuous

capillaries are primarily found in skin, muscle, lung, and the central nervous system, and are typically distinguished by their “continuous” basement membrane. Fenestrated capillaries are in renal glomeruli, intestinal mucosa, and exocrine glands. Finally, sinusoidal capillaries have even larger intercellular gaps, and are present in the liver, spleen, and bone marrow. The capillaries reunite and empty into venules (8–100μm lumen), composed of the externa, a thin media layer, and endothelium. Multiple venules empty into much larger veins for blood to be transported back to the heart for pulmonary circulation[113].

The most vital organs that researchers currently engineer (i.e., heart, liver, lung, kidney, pancreas, and brain) are highly vascularized in vivo and require a vascular network with high fidelity and functionality. The vascular network must be present throughout the solid organ, with arterioles separated by a maximum distance of 300μm to ensure that the tissue diffusion limit is not exceeded[114]. In addition to the vital necessity for nutrient and oxygen exchange within structures greater than 300μm, there is evidence that vascular formation may govern tissue formation itself[115]. Furthermore, innervation regulated by mechanisms shared with blood vessel formation could promote the integration of engineered organs[116–118].

The first attempt to replicate vascular tissue includes synthetic vascular grafts[119]. However, these have only been effective in large (>8mm) and medium-large vessels. Success in synthetic grafting of crucial small vessels (<6mm), such as the coronary arteries, remains poor compared with autologous grafting of the internal thoracic and radial arteries[120]. Challenges typically arise in these applications due to a lack of endothelial cells, diameter, and compliance mismatch resulting in graft failure due to intimal hyperplasia, thrombosis, and graft site infections[121]. Consequently, the FDA has not approved synthetic small-caliber vascular grafts (<5mm). However, bioprinting with endothelial cells in lumens in the small caliber category has become an attractive alternative. Indeed, fabrication of small-diameter arteries and veins seem feasible, however, the central challenge of replicating the delicate anatomy of arterioles, capillaries, and venules remains a key limitation[122, 123]. To address the need for these smaller diameter vessels, tissue engineers have employed angiogenic remodeling and biofabrication strategies.

4.2. Angiogenic remodeling

Two main strategies for angiogenic remodeling of tissue-engineered organs are to provide growth factors that will cause rapid capillary formation inside implanted constructs, or by stimulating blood vessel infiltration by host vasculature. Agents including vascular endothelial growth factor (VEGF), fibroblast growth factor (FGF), platelet-derived growth factor (PDGF), and transforming growth factor (TGF), have been delivered alone or in combination. Researchers demonstrated the use of gelatin microparticles to prolong VEGF activity in 3D bioprinted scaffolds[52]. Matrigel encapsulated endothelial progenitor cells along with VEGF encased in gelatin nanoparticles have been used. Implantation of the scaffolds in nude mice showed significantly higher vessel formation in the sustained-release group. In another study, a vertical organization of hallow channels was designed to replicate the liver vascular network using a gelatin/alginate/fibrinogen gel[124]. Hepatocytes combined with gelatin/alginate and chitosan provided structural support around the vascular network. The group was able to induce stromal cells to differentiate into endothelial cells

and form a vascular network by administering EGF. Others printed hematopoietic stem cells encapsulated in hydrogels cross-linked on-demand in patterns with liquid media. Differentiation into multiple lineages then occurred[125]. Other methods include promoting the recruitment of circulating stem cells through specific antibodies.

4.3. Direct printing of vascular constructs

In direct printing of vascular constructs, a pre-designed three-dimensional structure forms through one of several bioprinting methods (i.e., Extrusion, inkjet, LIFT) by depositing cell-laden hydrogels or media[126]. Within this context, one method of vessel printing is through vertically stacking circles or pores within the Z-Plane in concentric layers. In one study, a multi-nozzle extrusion-based technique allowed for the vertical fabrication of alginate-based tubular constructs. The design incorporated a large outer circular structure (12mm diameter) of alginate followed by an inner circle (8mm diameter) of deposited crosslinker (CaCl2) stacked to 15mm vertically[127]. However, one limitation of the vertical printing design was shrinkage occurring during the crosslinking process. Vertical channels can be implemented into larger tissue constructs to overcome this challenge. Other researchers demonstrated this idea using a drop-on-demand modified HP Deskjet 500 and showed that a bioink composed of human microvascular endothelial cells in fibrin could fabricate micron-sized channels. Cell viability improved by implementing an aqueous printing process. Following depositing, structures were cross-linked with thrombin to provide structural stability. Cells within printed channels proliferated and aligned to form confluent 3D tubular structures. Thus, combining cell and scaffold printing promotes cell proliferation and formation of microvasculature[128].

The challenge of vertical shrinkage has also been addressed by printing vessels horizontally. In one study, a horizontal printing strategy with a four-armed polyethylene glycol derivative to improve hydrogel rheological stiffness and allow higher density cell suspensions. NIH 3T3 cells were encapsulated in PEG gel and then printed in sausage-like hydrogel microfilaments using a layer-by-layer deposition[50]. This method was later used to produce tubular constructs with a core and structural halo. Encapsulated cells gradually remodeled the synthetic environment into a tissue-like extracellular matrix[129]. While horizontally printing vascular constructs can reduce some of the physical demands on fabricated vessels, the stability of the lateral walls must remain in consideration in terms of compensation shrinkage. Consequently, groups recognized this need and optimized a tubular printing technique by accounting for concavity deformation by compensating and adopting a non-circular printing trajectory, resulting in a nearly circular product[130].

In whole organs, vascular networks have complex vascular trees. To replicate branched tubular structures, Norette et al. used a combination of cell spheroids and extrusion bioprinting. In their design, HUVMCS, fibroblasts, and SMCs were printed as small multicellular cylindrical rods, and rounded into spheroids. Printed agarose rods formed horizontal bifurcations, followed by dispensing spheroids into the mold. The spheroids fused in the mold and matured, and a vascular network developed after removing the agarose mold[38]. However, in vivo vascular branching is not limited to a horizontal plane. Thus, fabricated fibroblast-based vertical conduits with zig-zag overhangs can be formed

using a specialized platform-assisted 3D inkjet bioprinting system[131]. This technology was later improved with an inkjet printing approach with a liquid support-based of calcium chloride solution. The solution was multi-modal, acting as both the support material and as a cross-linking agent. This enabled freeform printing of overhanging features by providing a buoyant force. Vascular-like channels with both vertical and horizon bifurcations, as well as overhangs, were successfully printed[132].

Further attempts to improve the structural integrity of bioprinted vasculature have also utilized support baths to provide physical support during tissue development. Feinberg et al. modified a MakerBot Replicator for syringe-based extrusion deposition of bioink solutions, termed freeform reversible embedding of suspended hydrogels (FRESH). Bioink solutions printed within the gelatin support that served as a temporary, thermoreversible, and biocompatible support[133]. Using a similar approach, Blaeser et al. used liquid fluorocarbon as liquid support. The high buoyant density of the fluorocarbon allowed their soft hydrogels to float, allowing for freeform printing thin-walled hydrogel cylinders[29].

While direct printing of porous structures method has proved successful, the ultimate goal would be to print vessels with patent lumens in a single step[134]. Coaxial nozzle printing is a significant step in this effort. In coaxial printing, a nozzle is prepared with an inner and outer tube, and a connected feed nozzle (See Figure 6). The feed nozzle is filled with a bioink crosslinker that is distributed through the inner tube, while the outer tube contains the desired matrix bioink with encapsulated cells. During printing, the outer and inner tubes dispense simultaneously, resulting in an outer tube with a matrix bioink and an inner cylinder with the crosslinker. The crosslinking mechanism occurs instantaneously from the luminal center outward, maintaining patency during printing.

Zhang et al. demonstrated the use of coaxial nozzle blood vessel bioprinting, wherein alginate hydrogel flowed through the feed tube while a crosslinking solution of CaCl2 flowed through the central tube, creating a patent lumen. The investigators printed microfluidic channels embedded within a bulk hydrogel to test functionality. Cells within the construct maintained high viability, suggesting that vascular networks could be produced using a coaxial nozzle[135]. Subsequent work has improved the structural stability of printed coaxial vascular conduits through reinforcement with carbon nanotubes (CNTs). Conduits were printed with encapsulated human coronary artery smooth muscle cells. The multi-walled carbon nano-tube reinforcement increased the tensile strength and allowed the conduits to be printed at a lumen diameter of less than 1mm[136].

Recently, Gao et al. combined bioprinting with coaxial vascular conduits to create microchannels for nutrient delivery (See Figure 7). The scaffolds were printed using L929 mouse fibroblasts encapsulated in sodium alginate and CaCl2 to partially crosslink filaments as they were laid within a CaCl2 bath[137]. It was easier to form high-strength structures when a higher concentration sodium alginate solution is used, and the distance between adjacent hollow filaments was smaller. In subsequent work, the investigators encapsulated endothelial progenitor cells with the proangiogenic drug atorvastatin in vascular tissue derived decellularized ECM and alginate composite hydrogel. Vascular conduits were then fabricated from this bioink using their coaxial method. Bioprinted vessels were then

ligated onto the venous area of an ischemic model in mice. A functional blood vessel graft developed, resulting in recovery from ischemic injury[138]. Most recently, this coaxial printing technique was implemented for the direct printing of an in vitro vascular model. Upon endothelialization, the vessels exhibited representative vascular function, including selective permeability, antiplatelets/leukocyte adhesion, and self-remodeling in response to physiological shear stress and directional proangiogenic signals[134].

One cutting edge technology, SLATE (stereolithography apparatus for tissue engineering) has been developed by Miller et al. to generate biologically compatible complex multi vascular networks with functional intravascular topologies[139]. The photopolymerizable hydrogels can be used to establish intravascular and multi vascular design with great freedom with projection stereolithography. In a recent study, researchers demonstrated that monolithic transparent hydrogels comprising functional bicuspid valves and intravascular fluid mixers and could be formed. Interwoven vascular networks were generated with space-filling topologies to test oxygenation and flow of human red blood cells during tidal ventilation and distension of a proximate airway[140] (see figure 8).

4.4. Indirect printing with sacrificial material

In addition to direct printing of vascular networks, luminal support made of sacrificial materials (i.e., gelatin or agarose) can maintain a patent internal lumen during vessel formation using a method termed indirect printing. Wust et al. described this process in-depth to determine the effects of material, orientation, geometry, and cell embedding on the indirect printing of vascular channels. For their experiment, an alginate-based bioink was used to embed human MSCs while a central tube of gelatin served to stabilize the luminal center. The gelatin was then leached from the center with tissue maturation, leaving a hollow channel[141]. Other indirect printing methods used to form microchannel networks include the use of agarose gel fibers were bioprinted with a highly controlled 3d architecture followed by casting cell-laden GelMA hydrogel over agarose gel fibers and photopolymerization. The agarose cylinders were then removed from the photo crosslinked cast, forming perfusable microchannels[142]. The vascular networks improved cellular viability, differentiation, and mass transport in the tissue constructs, and endothelial monolayers formed in the channels.

Dai et al. designed their own novel indirect bioprinting method. First, a layer of collagen hydrogel was printed in a flow chamber, followed by a single strand of human umbilical vein endothelial cells (HUVECs) embedded in gelatin. Collagen was then cast around the gelatin strand, and the construct was incubated at 37c. A flow of media was then sent through the open channel, which removed the thermoresponsive gelatin, leaving HUVECs attached to the remaining collagen matrix. A confluent endothelial channel formed, which was able to maintain cell viability up to 5mm from the channel under physiological flow conditions[143]. To build on this method, two cylindrical tubes were printed, separated by a fibrin support center imbedded with endothelial cells and fibroblasts. Under physiological flow conditions, a microvascular bed formed within the fibrin support center, connecting the two parallel fluidic vessels[123].

Lewis et al. have reported embedded three-dimensional bioprinting to functionalize tissue segments with patient-specific induced pluripotent stem cell-derived organoids, in an attempt

to achieve tissues high cellular density and function (See Figure 9). The organoid matrices exhibited self-healing behaviors and had clear viscoplastic properties required for sacrificial writing into functional tissues. To further demonstrate the functionality of the printed constructs, the group created perfusable microarchitectural cardiac tissue fragments that fused and beat synchronously over a 7-day period[144].

5. Advances in engineering organ-specific structures to enable organ function

Organ-specific microstructures are crucial for bioprinted whole organs to function properly. Microstructures are often highly complex, with intricate and delicate structural elements arranged in complex patterns and composed of multiple cell types. Attempts to engineer microstructures have proven successful in less complex organs, such as skin. Christiano et al. described a method for engineering hair follicle spheroids, which formed primitive hair follicles when embedded in a biomimetic skin structure then implanted on mice. The 3D structure of the spheroids increased hair follicle specific genetic markers[145]. To further improve this method, the group implemented a casting method in which hair follicle columns were engineered with high-density FDPC cells at the base, followed by a column of keratinocytes. These structures matured into hair follicles-like structures that were evident on H/E. When implanted on full-thickness skin wounds in mice, the engineered hair follicles formed hair[146]. In like manner, the complex microstructures of whole organs will need to be formed using both mechanical and cellular ques, while also maintaining the macro and mesostructural elements necessary for organ function. For some organs, technology has advanced to the point where organ bioprinting, or bioprinting of critical organ structure, is currently being developed. For more complex organs, such as the lungs and kidney, alternative methods such as organoid formation are providing preliminary efficacy and organ-like function which may serve as the building blocks toward the goal of complete organ engineering. For this reason, we have included studies that describe the spectrum of organ bioprinting development.

5.1. The heart

Cardiovascular tissue is composed of fully differentiated cells, which are organized to constitute the various anatomical elements of the heart. Cardiovascular diseases, including acute coronary syndrome, arrhythmias, hypertension, and congenital heart disease account for over 17 million deaths per year, with a predicted increase to over 23 million by 2030[147–149]. Adult cardiovascular tissue exhibits a very limited ability to self-renew after injury, thus later stage cardiovascular disease, extensive intervention may be required, such as artificial mechanical replacements[150]. Mechanical valves have been used with great success for several decades; however, these treatments have limited efficacy in pediatric patients, as the growing size of their heart necessitates multiple procedures to implant larger valves[151]. Ventricular Assist devices have become a standard of care for patients on the transplant waitlist[152]. Further development and implementation of the total artificial heart has proved successful. However, this is very costly. Ultimately, functional replacement with transplantation is the main therapy that can provide a permanent resolution for heart failure patients[153]. As with other organs, donor’s hearts are difficult to acquire. Thus, the demand

for tissue-engineered human hearts would be great. Engineered hearts have traditionally had limited success due to their onerous load requirements, a constant flow of blood through the organ, and the complex network of vessels necessary for the delivery of oxygen and nutrients.

Heart valves are one of the most delicate structures in the heart and are necessary to control against the backflow of blood in the heart and for creating a pressurized chamber for blood to be pumped throughout the body[154]. Thus, valves, while incredibly thin, must withstand incredible amounts of mechanical pressure[155]. Deficiencies of traditional bio-prosthetic and mechanical valves, such as durability of the device, the need for anticoagulation, implant anti-immunogenicity, and the capacity for growth, may be improved through tissue engineering. Our lab has specifically addressed this challenge through an in situ healing approach[156]. Specifically, donor heart valves were decellularized and seeded with CD144 antibody to allow for the capture of circulating endothelial progenitor cells. Once implanted in the tricuspid position, the valves remodeled to form physiologically normal heart valves that grew with the growing lamb[157]. However, 3D bioprinting can further help to fabricate specific valve constructs that can be fitted specifically into patients with their personalized anatomy. Other printing strategies involve both scaffolds and cells. In one study, 3D printing of an aortic valve scaffold was performed by incorporating alginate and poly (ethylene glycol)-diacrylate (PEG-DA) hydrogels aortic valve interstitial cells[158]. Micro-CT was used to compare native aortic valve geometries with the printed construct, demonstrating high fidelity printing. Additionally, the aortic heart valves were capable of encapsulating aortic root sinus smooth muscle cells and aortic valve interstitial cells for the leaflets. Methacrylated hyaluronic acid gelatin methacrylate bioink encapsulating human aortic valvular interstitial cells were also developed by extrusion bioprinting[34, 49]. By using 3D printing technology, the group was able to optimize cell distribution and viability. Additionally, the use of variable bioink components resulted in high cellular ECM deposition of collagen, glycosaminoglycan, and muscle actin. Still, these technologies and studies do not adequately answer the questions of longevity and mechanical performance that will be required of these bioprinted valves. The complex biomechanical requirements of these valves are outside of the scope of this review, but have been addressed in detail in other reviews[159].

Bioprinting the complex cardiac vascular network is the crucial next challenge faced by cardiac tissue engineers. 3D bioprinted vessels can replicate the anatomical structure and physiological characteristics of vessels, especially for small diameter vessels less than 6mm in diameter[160]. Perfusable vasculature relies on an endothelial lining for biomechanical support[161]. Multiple methods have been described in printing vascularized tissue, including 1) the use of sacrificial templates and indirect bioprinting to form open channels in solid constructs, 2) printing channels directly into a construct in an interconnected network, and 3), direct printing tubular blood vessels in a vasculature network[162]. However, thus far, these preliminary methods are inadequate for the generation of clinically relevant tissues[163], particularly for complex, and hierarchically scaled structures complete with cells and relevant physiology[164] (see section 4 for more details).

Ultimately the goal of the coronary vasculature is to allow for perfusion of blood and delivery of nutrients to the myocardium to allow for synchronous contraction. In place of fully engineered vasculature, some groups have chosen to forgo “over-engineering” in favor of cellular self-assembly. In a study by Forcas et al., cardiac tissues were bioengineered using a self-assembly approach, allowing for multicellular spheroids to fuse and form a beating patch. The solid tissue blocks demonstrated synchronous beating, and endothelial cells organized into primitive vessels[39]. More recently, a novel biomaterial-free method was developed to deliver stem cells using printed cardiac patches[53]. Similar to the Forcas method, cells were aggregated to create mixed cardiac spheroids with pluripotent stem cell cardiomyocytes, fibroblasts, and endothelial cells, and then assembled into a cardiac patch. The beating printed constructs exhibited action potential waveforms and uniform electrical conduction similar to those seen in the native ventricle. The patch successfully vascularized when engrafted into rat myocardium[53]. However, long term follow up and functional analysis was not reported. The short culture of the cardiac patches and cellular immaturity resulted in weak mechanical properties. Future studies of cardiac patches should include additional characteristics, including modulation with electrical and mechanical stimulation with a bioreactor, and implantation into more translatable myocardial injury are more likely to yield viable therapeutics.

Laser-Induced-Forward-Transfer (LIFT) and extrusion bioprinting can also be used in combination to form cardiac patches with angiogenesis at the edge of myocardial infarction, which have been shown to preserve cardiac function after acute MI[56]. A cardiac patch was printed using a decellularized heart ECM derived bioink. The constructs contained cardiac progenitor cells and stem cells, and the native ECM derive bioink created a suitable biochemical and biophysical microenvironment for cell differentiation and functionality. When implanted in vivo, the printed cardiac patch demonstrated enhanced cardiac function with minimal infarct complications and promoted robust vascularization within the engineered tissue matrix[104]. Implantation of constructs with primary human derived cardiomyocyte progenitor cells into a mouse MI model demonstrated that transplanted cells were able to survive for up to one month and improved cardiac function, demonstrating the capacity for autologous myocardial printing[47].

Our group has fabricated contractile myocardial tissue through 3D bioprinting[165]. The cardiac tissue constructs contained primary cardiomyocytes isolated from infant rat hearts and suspended fibrin-based bioink, a sacrificial hydrogel, and a supporting polycaprolactone frame. Like other bioprinted cardiac tissue, ours demonstrated spontaneous synchronous contraction in vitro. Immunostaining for α-actinin and connexin 43 confirmed that the cardiac tissues electromechanically coupled, dense, and aligned cardiomyocytes. The constructs demonstrated a physiologic responses cardio inductive drugs with contraction forces and beating frequency similar to the expected response in native tissue[165].

Dvir and colleagues 3D-bioprinted a heart-like model using decellularized ECM hydrogel, demonstrating that human cardiomyocytes and endothelial cells could be integrated into their printing design[166]. In their method, an omental tissue biopsy was excised from the patient. Cells isolated from the tissue were reprogrammed towards stem cells, and ultimately differentiated into endothelial cells and cardiomyocytes. Simultaneously, a personalized

hydrogel was processed from a patient-specific extracellular matrix. The two reprogrammed cell types were then encapsulated to form hydrogel bioinks that were printed to generate the parenchymal cardiac tissue and blood vessels. To prove this concept, cellularized miniature hearts were printed, and although not functional, demonstrated the potential for the approach to engineer functional and personalized hearts[166].

Feinberg et al. utilized freeform reversible embedding of suspended hydrogels (FRESH) technique to generate a large-scale and complex, 3D construct of the heart[133]. The technique utilizes a support bed of a thermally reversible, viscous gelatin slurry that offers somewhat flexible support for the printing nozzle[133]. The gelatin slurry allows the nozzle to easily penetrate the support bed without resistance while still holding the printed hydrogel structure in place without collapse. After printing, the hydrogel is released by heating to 37°C, which melts the support gelatin. Using their model, they bioprinted a heart construct for 5-day-old chick embryo, using a gelatin microparticle slurry supported by a fibrinogen collagen Matrigel bioink with myoblasts (See Figure 10). Their method was the first to bioprint the complex trabecular structures unique to cardiac anatomy by utilizing CAD modeling, and their low-viscosity collagen bioinks were printed in the gelatin slurry[133]. Most recently, The FRESH technique was used to rebuild elements native to the human heart, ranging from small capillaries to the full organ. PH-driven gelation allowed for unprecedented filament resolution (20-micrometer). This allowed them to print porous microstructure to enable rapid microvascularization and cell infiltration. The gelatin microparticle slurry supported the relatively weak, low viscosity collagen hydrogel, which was printed with physiological cell numbers of 300 million cells/mL. Micro-computed tomography confirmed that the FRESH bioprinted heart reproduce patient-specific anatomical structure. Furthermore, the ventricles printed with human cardiomyocytes contracted synchronously with directional action potential propagation, and wall thickening at peak systole. Finally, the group combined all elements of their printing process to print a neonatal sized heart model, and although not functional, microCT confirmed the shape fidelity of the construct[167]. Even so, significant challenges remain before bioprinting hearts of adult human scale is realized, including generating the billions of cells required for bioprinting large tissues, scaling up the manufacturing, and creating a standardized regulatory process for translation to the clinic. Furthermore, engineered cardiac tissue studies published to date lack long term follow-up, biomechanical and functional analysis, and in most cases do not include *in vivo* implantation. In order to address the critical need for transplantable organs, addressing the biomechanical requirements and longevity of the engineered organ is paramount. Future studies should aim for this standard of translation.

5.2. The liver

The liver accounts for 2–5% of body weight, making it the largest solid organ in the body, and is responsible for performing over 500 functions, including metabolic, immunologic, and detoxification processes[168]. Native hepatic tissue is primarily of hepatocytes, stromal cells, Kupffer cells, and blood vessel associated cells. These cells are arranged into tissue structures with cells tunneled through with bile ducts and blood vessels. This complex network, known as the hepatic acinus, is responsible for filtering toxins from the blood

and producing bile that is used in digestion. The liver has a unique ability to regenerate and restore mass and function after greater than two-thirds damage[169, 170]. Treatment options for severe liver disease include cell transplantation and extracorporeal devices; however, orthotopic whole or partial liver transplantation remains the gold standard for liver failure[171]. The benefits of transplantation are strained due to health care expenses and the risk of immune rejection[172]. Furthermore, attempts to produce an autologous artificial liver have been thwarted by an inability to culture primary hepatocytes for an extended time[31].

Hepatocytes comprise 60% of the liver volume and have a high proliferation capacity in vivo; however, these cells can lose their specific function with *in vitro* culture. It has been shown that the function and viability of these cells enhance when they are in the form of aggregations[173]. Recently, Bhatia et. al described this phenomenon in a study that used *in situ* expansion of engineered liver[174]. They fabricated structurally organized tissue units composed of human hepatocyte and fibroblast aggregates engineered with endothelial cords. The tissues expanded in after implantation into a mouse model of liver injury. These findings were in part the result of the degradable fibrinogen hydrogel they used. Ultimately, the graft expanded over 50 times through the course of the 3 month study and produced multiple liver proteins.

In other studies, investigators used a hepatocyte seeded biodegradable poly-lactic co-glycolic acid with a three-dimensional synthetic scaffold to improve cellular transplantation[175]. They found that the persistence of hepatocyte survival and phenotype expression were dependent on the implantation site, with improvement demonstrated in transplanted hepatocytes bathed in hepatotropic factors were the gut drains into the portal vein[176]. To address the need for branched vascular channels, the group micromachined complete vascular systems on silicon and Pyrex surfaces with the potential for integration into engineered tissue before implantation. Specifically, trench patterns with branched vascular and capillary network architecture were etched using photolithography. Endothelial cells and hepatocytes were cultured as monolayers on the molds and both cell types were maintained, and hepatocytes maintained albumin production.

Later studies demonstrated that hepatocellular function can be maintained in bioprintable hydrogels, including photo-cross-linkable polyethylene glycol (PEG)[177]. Bhatia et al. fabricated hepatic tissue constructs with photopatterning platform for embedding cells in hydrogels with multi-layered, complex architecture[178]. Later termed human ectopic artificial livers (HEALs), their constructs stabilized primary human hepatocyte by paracrine and juxtacrine and paracrine signals in the scaffold. Transplantation of the HEALs into mice exhibited humanized liver function persistent, including synthesis of human proteins, human drug metabolism, drug-drug interaction, and drug-induced liver injury[179]. The group later utilized inVERT molding (Intaglio-Void/Embed-Relief Topographic molding) to direct microscale organization of induced pluripotent stem cells with compartmental placement of cells and compartment microstructure to modulate hepatic functions (see figure 11)[180].

Other groups have demonstrated that human embryonic stem cells or human induced pluripotent stem cells can be used to generate hepatocyte-like cells. In one study, a bioprinting model used a valve-based inkjet printer to fabricate mini livers, which

demonstrated both nuclear factor 4 alpha and albumin secretion[32]. The printed cellular alginate hydrogel matrix reached peak albumin secretion after differentiation for three weeks, the longest in vitro culture published at the time. It also demonstrated that valve-based printing did not damage human pluripotent stem cells, and helped maintain their pluripotency, followed by directed differentiation into specific lineages of patient-specific hepatic cells. More recently, primary rat hepatocytes, HUVECs, and human lung fibroblasts were printed with an extrusion bioprinter. In the design, polycaprolactone formed a framework, while collagen bioink containing the cells was infused into the support structure. The resulting 3D co-culture environment induced capillary network formation, which facilitated hepatic cell growth. The hepatocytes demonstrated the ability to secrete albumin and synthesize urea, suggesting that the heterotypic interaction among hepatocytes and the newly formed vascular network increased the survival and function of hepatocytes in collagen hydrogel[65]. While these findings are promising, the complexity of the liver microvascular network and anastomosis with the bile duct, portal vein, and hepatic artery have yet to be realized. These elements will be essential to the scale-up of current tissue-engineered liver models into clinically relevant liver tissue.

5.3. The lungs

Many patients suffer from end-stage lung diseases that ultimately requires transplantation. However, these procedures require highly specialized expert surgeons, and the risk of rejection and donor scarcity continue to be major challenges. Engineers have made several attempts to regenerate *in vitro* lung tissue[181–183]. However, a functional 3D alveolar model has still not been successfully fabricated. The native lung has an intricate diverging network of airway, with alveolar sacs that are 200micrometeres in diameter. This branching network an incredible surface area to volume ratio with a up to $100m^2$ [184]. The delicate blood-air interface within these sacs is formed as branching vascular networks divide into capillaries adjacent to the thin respiratory membrane outlining the alveolar sacs. The respiratory membrane is perhaps the most remarkable human tissues, with an average thickness of only 0.5 microns, which facilitates the oxygen and carbon exchange for 5 L/min of blood in the pulmonary capillaries[184]. Thus the anatomical complexity of the lung has made a reproduction of this tissue a challenge.

One method to address the complex microanatomy of the lung is to approach it from the angle of microfabrication. Mockros et al. described the feasibility of developing microchannel artificial lungs. The method theorized blood-side channels, up to hundreds of millions of parallel vascular channels, short blood paths, low-pressure drops, and low blood primes. They compared small circular or rectangular channels, broad open channels, or rectangular channels with gas-permeable screen-filled walls. Each was tested with a theorized drop in pressure of 10 mm Hg while eliminating the possibility of shear-induced blood trauma, and determining the acceptable channel length for oxygenating at least 4 L/min of blood. One theorized method to achieve this would require 140 million, 12 μm circular channels fabricated with gas-permeable materials[185]. One of the significant challenges of fabricating such a device is the requirement for uniform microchannel formations and seamless connections. To address this need, the group used microscale screens to provide uniform support and stability for the microchannels. The prototype

devices were formed with one single 3 or 6 mm long and 69 mm wide channel, and blood oxygenation was tested. They demonstrated fluxes in oxygen up to 9×10^{-7} moles/(min × cm^2), demonstrating that their device reached the theoretical membrane limit[186]. Similarly, Federspiel et al. utilized soft lithography to create three-dimensional blood microchannel and gas pathway arrays in PDMS (poly-dimethylsiloxane) to prototype gas permeance and cell culture testing. In their novel design, the blood microchannels were lined with endothelial cells to reduce the risk of thrombosis in the system. The gas permeance had maximum values of 9.16×10^{-6} and 3.55×10^{-5} mL/s/cm^2/cmHg, for O_2 and CO_2 respectively, and confluent and viable endothelial cell monolayers were maintained with perfusion[187].

Similar technology was developed by a lung assist device to bridge the gap to transplant for patients suffering from failing lungs. The device incorporated a branched network of vascular channels with a contiguous gas chamber, separated by a gas-permeable membrane. Three gas-permeable membranes were used to test the exchange of oxygen and carbon dioxide. They found a linear increase in Oxygen and carbon dioxide transfer up to 8.0 mL/min blood flow[188].

Alternatively, several groups have explored the use of the decellularization approach, followed by cell seeding as a method for maintaining the complex microstructural network of the native lung. Investigators explored if lung tissue can be regenerated in vitro by removing the cellular components of rat lung while preserving and ECM scaffold to maintain the innate branching structures of lung airways and vasculature. The decellularized organs seeded with pulmonary epithelium and vascular endothelium in a bioreactor. They found the epithelium did in fact display hierarchical organization, and the endothelium repopulated the vasculature. Mechanical characterization of the *in vitro* engineered lungs demonstrated values similar to native lung tissue. Furthermore, the engineered lungs participated in gas exchange when implanted into rats. While these findings only demonstrate an initial step in generating functional lungs *in vitro*, these results suggest that cellular repopulation of the lung ECM is a possible strategy[189]. Panoskaltsis-Mortari also developed a lung matrix bioreactor to regenerate lung tissue seeded with cells. Their decellularized mouse lung matrix was connected to a ventilator to simulate breathing-induced stretch while submerged in a growth medium, which allowed them to show that the pulmonary matrix remained intact over time. Key structural components, including the basement membrane, alveoli, vessels, and airways, were preserved with remarkable maintenance orientation. They ultimately seeded the matrix with fetal alveolar type II cells, which demonstrated pro-Sp-C, cytokeratin 18, and 4', 6-diamidino-2-phenylindole-positive cells lining alveolar areas of the decellularized matrix[190]. Finally, the method of decellularized lungs by detergent perfusion was also implemented to yield acellular vasculature scaffolds with intact airways and alveolar ECM[182] (see figure 12). Their seeded scaffolds contained epithelial and endothelial cells, maintained in a perfused and ventilated in a bioreactor. Within one week, the constructs were capable of blood perfusion at physiologic pressures comparable to isolated native lungs.

Alternatively, groups have applied organoid designs for forming organ-level lung function on a chip. Investigators designed a micro physiological organoid with a functional alveolar-

capillary interface mimicking the human lung and compared it with observations in a mouse lung. When bacteria and inflammatory cytokines were introduced into the alveolar space, the system mounted a biomimetic response. Furthermore, the application of a cyclic mechanical strain while exposing the system to silica nanoparticles accentuated the toxic and inflammatory response of the cells. The mechanical stimulation also enhanced epithelial and endothelial uptake of nanoparticulates, stimulating the transport of the nanoparticles into microvascular channels[181]. More recently, an in vitro human lung basement membrane model was fabricated using inkjet bioprinting. The tissue implemented endothelial cells and type II alveolar epithelial cells separated by a thin layer of Matrigel™ to act as a basement membrane. They found that manually seeded cells formed patchy, layered clusters with thick ECM between the cells that hindered communication between the cells. Alternatively, cells that were printed spread out uniformly over the surface of the membrane, allowing for thin mono-layers to form. Thus the bioprinted monolayer cell cultures demonstrated enhanced barrier quality than the manually formed samples[51]. Ultimately, advances in these technologies, when coupled with vascularization technologies such as the SLATE printing technique described by the Miller lab[139] (see section 4.3, figure 8) and optimized cell culture, could be scaled up to translatable lung tissue for transplantation.

5.4. The pancreas

The pancreas is a complex and fragile organ that is responsible for producing enzymes that are released into the small intestine to aid in digestion. It is also responsible for producing the hormones insulin and glucagon which regulate blood sugar and uptake. This key function is carried out by cell clusters called the islets, composed of α-cells (glucagon), β-cells (insulin), and δ-cells (somatostatin). Destruction or loss of function of any of these cell types can result in serious diseases for patients. For example, diabetes mellitus (DM) results from loss of sensitivity or destruction of beta cells. The disease is characterized by extreme hyperglycemia resulting from failed glucose metabolism. This can result in major long-term organ complications nephropathy, neuropathy, retinopathy, and vasculopathy[191, 192]. It is estimated that 8.5% of the world population (422 million people) suffers from diabetes, and these numbers are predicted to increase to over 590 million by the year 2040[193]. About 10% of patients with diabetes have Type 1 diabetes mellitus (T1DM)[191], which occurs most often as a result of autoimmune destruction of the insulin-producing β cells, resulting in absolute insulin deficiency[194].

Pancreas transplantation has been shown to be an effective and curative treatment for T1DM. However, there is a significant risk of mortality with the procedure, so it is reserved for patients receiving kidney transplants as a result of T1D induced end-stage kidney disease[195]. Pancreatic islet transplantation has been developed to address the need for minimally invasive pancreatic implantation. The approach utilizes purified allogeneic donor islets which are infused percutaneously into the recipient’s liver via the portal vein[196, 197]. However, the high glucose, low oxygen, and increased toxin levels in the liver are suboptimal for the integration of fragile pancreatic islets[198]. Thus, alternative delivery methods and locations are being investigated[192].

One attempt at overcoming the hypoxia associated with pancreatic islet transplantation involves is to seed islets onto degradable 3D scaffolds[199]. Scaffolds can be made of that mimic the microenvironment of the pancreas and increase the surface area and porous channels for vascular ingrowth to increase oxygen and nutrient supply[200]. As the scaffold degrades, the ECM proteins are deposited into surrounding tissues while the islets are engrafted gradually[201]. Investigators have aimed to identify a more optimal site for islet transplantation for implanting a biodegradable scaffold construct. The scaffolds were seeded with islets and transplanted into the epididymal fat pad of diabetic mice. All animals with islets embedded in a scaffold or implanted in the kidney became normoglycemic. Islets transplanted without scaffolds took much longer to become normoglycemia, and less than 45% of mice survived. All grafts were removed after 100 days post-transplantation, at which point animals became hyperglycemic. Ultimately, this study demonstrated the benefit of embedding islets in scaffolds to restore normoglycemic levels, and that the effect is similar to islets transplanted underneath the kidney capsule[200]. Similarly, extrahepatic transplantation of islets was performed using a synthetic biodegradable polymer scaffold. The polymer scaffold was fabricated from copolymers of lactide and glycolide (PLGA) and formed with micropores to improve nutrient diffusion and vascular ingrowth from host tissues. The islet seeded scaffold was then transplanted into onto intraperitoneal fat of diabetic recipients and compared with islets implanted without a scaffold. Bioluminescence imaging of the engraftment site demonstrated that islets transplanted onto the polymer scaffold remained in the transplant location with prolonged survival. Furthermore, these islets maintained the native islet architecture and vascularized. Islets that were implanted onto the scaffold demonstrated improved function compared to those without. This was true in terms of diabetes reversal, the average time necessary to achieve euglycemia, intraperitoneal glucose tolerance, and weight gain. These findings indicate that the synthetic polymer scaffold provided a delivery vehicle for islet transplantation while enhancing the function of the extrahepatic transplantation of islets[202]. Finally, the omental pouch has been tested as an alternative site for islet implantation in a nonhuman primate model of diabetes. They found that omental pouch recipients had delayed engraftment, but with similar protein production compared to hepatic transplantation, suggesting that extrahepatic transplantation could be used as an alternative site for some patients[203]. Furthermore, since rejection by the immune system remains a major hurdle, the co-encapsulation of islets with regulatory T-cells (Tregs) could be of great benefit. Wallace et al. described how this could be achieved via 3D bioprinting using a co-axial bioprinter, to generate a scaffold containing a core of islets surrounded by a shell of Tregs, providing localized immune protection[204]. When murine pancreatic isolated are printed with human Tregs, the Tregs protect the islets from xeno response associated with xenogeneic mononuclear cells, demonstrating that co-encapsulation of Tregs by co-axial 3D bioprinting can provide local immune protection.

A vital characteristic of all extrahepatic islet cell transplants is the requirement for mechanically stable porous scaffolds that will allow for vascularization when implanted in vivo. Bioplotting has been used to fabricate a 3D alginate-based porous scaffold with an improved surface to volume ratio, to allow for increased nutrient and oxygen transport. The morphology and viability of β-cells and islets were not altered during the embedding process, and the method prevented cell aggregation. The 3D plotted scaffold confines islets

in one location which allowed for blood vessel growth into the pores of the construct[33]. Alternatively, investigators have developed a multifaceted transplantation strategy combining 3D bioprinting and differentiation of stem cell-derived β cells. Their microporous device composed of polylactic acid filled with stem cell β cell clusters embedded in a fibrin gel. Cell cluster sizes were then identified using finite element modeling to design a scaffold for optimal oxygen consumption and diffusion for culture at physiological levels of oxygen. When transplanted into mice, their β cell-embedded bioprint device improved islet cell function and maintained their structural integrity[46].

Similarly, Shea et al. investigated using a porous, biodegradable scaffold to deliver islets to extrahepatic sites. The scaffold architecture was optimized for cells, allowing for revascularization of the islets with increasing the inflammatory response. Islets were seeded on the scaffolds and implanted into epididymal fat on pigs, which restored normoglycemia in less than two days. This was achieved by increasing the islet seeding density. The group also found that transplanting the constructs into the porcine omentum improved engraftment compared with gastric submucosa[205]. These investigators have since explored the use of microporous scaffolds to promote engraftment of pancreatic progenitors derived from stem cells. They found that the microporous scaffolds supported cell engraftment which matured into insulin producing units. They added a sustained release of exendin-4, which led to significantly increased C-peptide production, with increased concentrations monohormonal insulin-producing cells[206]. Most recently, Shea et al. engineered scaffold with microporous biomaterials to guide pancreatic progenitor assembly into clusters, allowing differentiation of hPSC-derived pancreatic progenitors. They found that modulating the scaffold pore sizes augmented insulin expression and secretion in response to glucose compared to cells cultured in suspension[207].

Bioprinting also enables the co-transplantation of islets with supporting which has been shown to improve islet survival[210]. One study showed that a bioprinted heterogeneous tissue strand of insulinoma beta TC3 and dermal fibroblasts exhibited rapid fusion with high viability, and consistent cylindricity to allow for precise fabrication, while maintaining cell-specific functional markers[211]. This process can be improved through the use of co-axial extrusion, allowing co-printing of islets with supporting cell[192]. This allows for the delicate core islets to be surrounded by a protective biomaterial shell layer[208]. This was achieved by printing a novel microcapsule with core-shell structures using a two-fluid co-axial electro-jetting. This single-step method confined the islets to the core region, resulting in improved encapsulation and diabetes correction. Most recently, Wallace et al. used a coaxial based printing system and an alginate/gelatin-based bioink formulation for islet cell encapsulation. They found that pancreatic islet structure was well maintained during the 3D printing process, and that co-axially printed endothelial progenitor cells and islets had improved function and viability, enabling survival of clinically relevant doses of islets (see figure 13)[212].

An additional component of pancreatic cell printing is the ECM microenvironment. Investigators have studied the effect of matrix-integrins on beta-cell function and viability following isolation. One group found that immediately after islets isolation, the peri-insular basement membrane was absent, and over six days, they saw a decline in islet attachment to

the collagen matrix. Furthermore, arginine-glycine-aspartate synthetic peptide was shown to block the attachment of islets, suggesting that the process was integrin-mediated. This was confirmed as expression of alpha3, alpha5, and alphaV diminished during the culture period. This change was correlated with functional changes, including decreased proinsulin gene expression, islet insulin content, and stimulated insulin release, and resulted in increased β-cell death from apoptosis. These adverse events could be reversed by exposure of islets to matrix proteins[201]. Odorico et al. have also demonstrated that ECM plays an essential role in development by regulating cell behavior through biochemical and structural stimulation. To utilize this concept, their group developed a novel decellularization method to produce an acellular, 3D biological pancreatic scaffold and hydrogel (see figure 14). They found that including a homogenization step during the decellularization process significantly improved lipid removal, resulting in improved gelation capacity of the resulting ECM at body temperature[209]. Most recently, the decellularization process was used to produce ECM isolated from the pancreas to provide a tissue-specific microenvironment for islet cells printing. This process yielded in vitro culture of Human islets with greater than 60% viability, with an associated increase in insulin secretion by islets printed in the ECM bioink. This process was further enhanced by the additional of endothelial cells and a layered, printed, 3D construct. The construct demonstrated advanced pancreatic functions including regulation of insulin secretion and maturation of insulin-producing cells from stem cell progenitors[213].

To address the need for viable β cells, Melton et al. developed a scalable differentiation protocol to generate millions of glucose-responsive β cells from hPSC. The stem-cell-derived β cells (SC-β) were found to be phenotypically and functionally, similar to native β cells. Specifically, the in SC-β cells expressed markers found in mature β cells, fluxed calcium in response to glucose, packaged insulin into secretory granules, and secrete insulin. Furthermore, the cells secreted human insulin into the serum in a glucose-responsive manner and ameliorated hyperglycemia when implanted into diabetic mice[189]. Next, human SC-β cells were used for long-term glycemic correction, a diabetic, immunocompetent animal. The SC-β cells were encapsulated with alginate derivatives and implanted into the intraperitoneal space of streptozotocin treated mice. Glycemic correction occurred following implantation without immunosuppression until removal at day 174 post-implantation. The grafts produced human C-peptide, and in vivo, glucose responsiveness was controlled to confirm the function of the implanted cells. Finally, implants removed after 174 days in vivo contained viable insulin-producing cells[214]. Most recently, they reported an approach to generate SC-β cells from type 1 diabetic patients. The produced cells responded to different forms of β-cell stress in vitro and maintained normal β-cell function. They concluded that no major differences were present in SC-β cells derived from type 1 diabetic patients compared with SC-β cells derived from non-diabetic patients, suggesting that SC-β cells derived from type 1 diabetic patients could be used to treat the patient’s diabetes in an autologous manner[215]. By combing functional engineered pancreatic units such as insulin-producing organoids, encapsulated β-cells, and differentiated stem cells with bioprinting technologies that enable large scale deposition and organization of these building blocks, there is potential for pancreatic engineering and replacement to be realized.

5.5. The kidney

Kidney failure is a global challenge facing countless patients, the only available therapeutic options are dialysis and renal transplantation, however limited donor organs, risk of tissue rejection, coast, and other complications remain a concern[216]. For tissue engineers, the kidney is one of the most complex organs due to the unique developmental cues and micro-scale spatial organization. The kidney contains more than 30 different cell types, with intricately patterned epithelial tubes named nephrons[217]. Each nephron is further segmented into unique regions, including Bowman's capsule that surrounds the glomerulus, followed by the renal tubule. Each segment of the kidney is responsible for its own unique physiological roles, and thus has different micro-anatomical features[218]. Thus, the complexity of kidney cannot be reproduced by traditional tissue engineering methodologies. Rather, each element of the kidney macro and microstructure must be engineering logically, including specific cell types required by each element, microtubular structure, vascularization, and kidney-specific biomaterials.

The (Re)Building a Kidney consortium aims to combine many of these approaches to improve the isolation, expansion, and differentiation of kidney cell types that can be integrated into complex biomimetic kidney replicates. This will allow for the development of in vitro engineering of replacement kidney tissue, as well as develop strategies to stimulate regeneration of nephrons in situ[219]. Within the group, Little et al. identified developmental mechanisms that regulate differentiation of progenitors to form the kidney mesenchyme versus the collecting duct. These factors were used to generate kidney organoids containing nephrons connected to an organized collecting duct network encapsulated in renal interstitium and endothelial cells. This delicate structure included single nephrons, with markers specific to the proximal and distal tubules, which ultimately for loops of Henle, and glomeruli containing podocyte foot processes. The transcription profiles of kidney organoids were highly correlated with developing human kidneys in the first trimester. Finally, the proximal tubules endocytose dextran and react appropriately to cisplatin, a nephrotoxin (see figure 15). These kidney organoids represent powerful models for future applications, including disease modeling and nephrotoxicity screening[220]. Furthermore, kidney organoids and other tissue equivalents may be applicable as building blocks for whole organ engineering.

Finding reliable cell sources and appropriate biomaterial supporting the cell growth and functionality is the essential factor to achieve successful tissue formation[221]. Our group demonstrated the ability to create a functional renal unit using a renal device fabricated from polycaprolactone polymer[222]. The structure was then seeded with renal cells isolated from the mouse kidney. The fabricated structure formed functional renal like structures upon in vivo implantation. Recent progress in stem cell-based methodologies is allowing for even more specified kidney engineering strategies. First, the ability to replicate essential developmental cues *in vitro* can allow human pluripotent stem cells to be differentiated towards renal cell types that are lost in kidney disease, including tubular cells and podocytes[217]. It has been shown that iPSC-derived podocytes are morphologically analogous to cultured human podocytes, including mRNA expression and protein localization of the podocyte markers synaptopodin, nephrin, and Wilm's tumor protein (WT1). The system

can be further tuned to allow the cells to maintain proliferative capacity. Finally, the iPSC-derived podocytes integrate into re-aggregated metanephric kidney explants and developed into glomeruli[223]. More recently, iPSC-derived podocyte-like cells were used to generate a morphology and expression typical of podocytes, including synaptopodin, podocin, nephrin, and WT-1. They further demonstrated the upregulation of the podocyte marker synaptopodin with a correlating downregulation of pluripotency markers Oct4 and Sox-2, further confirming cell differentiation. The cultured podocytes were capable of endocytotic uptake of albumin[224]. Finally, investigators showed that hPSCs first can be induced to primitive streak-like cells by activating canonical Wnt signaling. The cells processed from mesoderm precursors to nephron progenitors, and ultimately matured into podocytes that adopted podocyte morphology, expressed appropriate markers and phenotypes, including albumin[225].

With the development of methods for generation of glomerulus specific cells in hand, the technology can be implemented into more complex approaches such as the use of tissue spheroids and chip platforms as building blocks for fabricating microtissues such as vascular networks and macrotissues[226]. This concept was tested by co-culturing differentiated hiPS cells derived podocytes, with human glomerular endothelial cells in a microfluidic device. A biomimetic glomerulus formed with glomerular basement membrane collagen, which had the ability for clearance of insulin and albumin. Furthermore, their glomerulus-on-a-chip mimicked albuminuria and podocyte injury when exposed to Adriamycin[227, 228]. Protocols are also established for differential induction of each lineage of the uteric bud from mouse and human PSCs[229]. Similarly, 3D human glomeruli have been formed from induced pluripotent stem cell-derived kidney organoids combined with podocyte cell lines. The 3D co-cultures were able to maintain *in vitro* protein localization, and improve the glomerular basement membrane. The investigators went on to form a glomerular organoid using cells from a patient with congenital nephrotic syndrome. The disease modeling organoid demonstrated reduced protein levels of both nephrin and podocin[230]. Ultimately, the usefulness of kidney organoids will be limited by their developmental accuracy, and may ultimately provide insight into nephrogenesis[231].

Similarly, the formation of either isolation of cells specific to the renal proximal tubule or differentiation of these cells from progenitor precursors is required to continue the engineering of a functional nephron. A protocol was developed for the differentiation of hESCs into renal epithelial cells that expressed renal proximal tubular cell markers. The differentiated stem cells were morphologically and functionally similar to renal proximal tubular cells and generated tubular structures in vitro. When implanted in vivo, the cells formed a simple epithelium in the kidney cortex[232]. 3D bioprinting was used to print primary renal proximal tubule epithelial cells, fibroblasts, and endothelial cells into an in vitro model of the proximal tubule interstitial interface. The bioprinted construct formed microvascular networks, supported by cellular ECM deposition. Tight junctions were formed in the 3D proximal tubule tissues and had the expression of renal efflux and uptake transporters. The tissues demonstrated a fibrotic response to TGFβ, with both excess extracellular matrix deposition and increased gene expression associated with human fibrosis. Furthermore, when the group treated the proximal tubule with cisplatin, they found

a biomimetic reduction viability. Cimetidine reversed these effects, confirming the presence and action of OCT2 transporters in cisplatin-induced nephrotoxicity[233].

More recent advances by Lewis et al. have developed more complex three-dimensional models of kidney tissue that recapitulate human. In the model, a 3D human renal proximal tubule with convoluted tubular architecture with an open lumen was printed into an extracellular matrix and formed into a microfluidic chip. The tube is then actively perfused with proximal tubule epithelial cells, resulting in enhanced epithelial morphology and functional properties. Furthermore, when the nephrotoxin Cyclosporine A was perfused in the system, the epithelial barrier is disrupted in a dose-dependent manner[44]. The investigators have since added adjacent conduits lined with confluent epithelium and endothelium with independently closed-loop perfusion. This system demonstrated active reabsorption via the tubular-vascular exchange of solutes, as well as both albumin uptake and glucose reabsorption (see figure 16). Finally, when induced with hyperglycemia, a human-like diseased state is formed, which can be rescued by administering a glucose transport inhibitor[234]. Most recently, Cho et al. utilized coaxial printing to fabricate hollow microfluidic tubes to engineer renal parenchyma composed of endothelial cells and renal tubular epithelial[235]. Their system was aided by a functional hybrid bioink that improved the microenvironment to allow for vascularization. This method yielded both functional renal proximal tubule on a chip as well as implantable constructs. The hollow tubes demonstrated long-term graft survival *in vivo* with therapeutic capability in a renal disease model. Thus, the combination of bioactive biomaterials, along with microfabrication of the renal tubules can produce functional kidney units. As these technologies are scaled up they can be used as building blocks, combined with larger scale vasculature, to bioprint function kidney tissue for clinical translation.

5.6. The brain and nervous system

Treatment of central nervous system disorders is one of the most challenging for physicians due to the lack of regenerative capability in neural tissues[236]. Currently available treatments for central nervous system diseases rely on correcting the physical manifestations of the syndrome, and cell therapies have shown some efficacy[237]. 3D bioprinting aims to do more to treat nervous tissue disease through engineering neural constructs. Bioprinting brain tissue possesses many challenges for engineers, including a complex vascular network, challenging cell isolation and culture, and incredibly complex neural networks[171]. The bioprinting technique best suited to address these challenges is micro extrusion bioprinting. This technique enables engineers to create a multicellular structure as using neural cells for building neural networks and vascular cells to enhance vascularity in the printed construct[238]. It has been speculated that the co-culture of both neuronal and endothelial cell types enhances cellular proliferation and the formation of neural tissue networks.

Cellular spheroids have been implied as a method to improve cellular integration and enhance cellular communications. The advantage of using co spheroid system for construction mini-brain is to enhance neurovascular network formation, moreover using spheroid based bioink maintains the cellular viability during printing by protecting the cells from the applied shear stress[239]. A 3D tissue construct was engineered with a

neuronal network capable of transplantation onto brain tissue *in vivo*. The neuro spheroid were generated in a polydimethylsiloxane microchamber, which allowed for sprouting and connection neuronal. The neuro spheroid maintained the neuronal network after transfer onto the cortical surface of a brain. After transfer the network was active for over one week. Imaging demonstrated that the network had extended axons into the host cortical tissue, establishing synaptic connections with host neurons[240]. Later, the investigators established a millimeter-sized neural building block to form a 3D heterogeneous neural component. In conjunction with this technology, they established a method to observe the spatiotemporal changes of a single neuron to visualize in real-time the axonal extension and dendritic branching[241]. Similarly, collagen fiber orientation and polydimethylsiloxane microchambers were used to develop a 3D reconstructed neuronal tissue to mimic the cerebral cortex, allowing for specific positioning of somata and directionality of neurite elongation. The investigators detected interlayer synchronous firings with interlayer propagation by chemical synaptic transmission[242]. Finally, spheroids with cortical cells were generated that formed neurons and glia with laminin-containing 3D networks. Furthermore, the neurons formed excitatory and inhibitory synaptic circuitry[243]. A method was also developed to form large multicellular organoids with layers of neuronal cells expressing human midbrain markers (see figure 17). The investigators found mature and electrically active neurons capable of dopamine production, as well as neuromelanin-like granules, similar to human substantia nigra tissues[244].

One method used by researchers to functionalize tissue organoids is through the use of microfluidics. Lee et al. developed a microfluidic chip to provide a constant flow of fluid to neuro spheroids. Neuro spheroids that were cultured under flow conditions formed more robust and complex neural networks and were larger than spheroids held in standard culture conditions. This is likely due to the supply of continuous nutrient, oxygen, and cytokine transport and removal of metabolic wastes as a result of constant flow. When Amyloid-β was introduced into the flow system, the viability of neuro spheroids was reduced, destroying neural networks[245]. Similarly, a microfluidic model of a simplified 3D neural circuit was formed. The microfluidic device was filled with Matrigel with continuous flow administered during gelation, resulting in the alignment of the ECM components along the flow direction. Neurites of primary cortical neurons were then grown into the Matrigel to form axon bundles approximately 1500 μm in length. By day 14, neural networks formed from presynaptic to postsynaptic neurons, and aligned 3D neural circuits were established that expressed PSD-95 and synaptophysin[246]. Recently, our group has developed a 3D tissue equivalent model of the blood brain barrier will all six major human brain cell types (neurons, endothelial cells, astrocytes, microglia, and oligodendrocytes). The organoids closely mimic normal brain tissue, with expression of cell specific markers, tight junctions, and adherens junctions. Furthermore, the organoids demonstrate charge selectivity through the blood-brain barrier and alteration of functional protein distribution under hypoxic conditions[247].

The idea of printing neural tissue is not new; however, due to the complexity of neural networks, progress has been slow. Investigators described a method of fabricating cellular patterns and structures with primary embryonic hippocampal and cortical neurons using automated and direct inkjet printing. After printing, the neurons maintained healthy neuronal

phenotypes and electrophysiological characteristics. The printing process allowed for sheets of neural cells to be layered in fibrin gels[248]. Later, direct cell printing was used to pattern neural cells in a multilayered collagen gel. The construct included embryonic neurons and astrocytes printed on top of a collagen base layer and gelled by adding aerosolized sodium bicarbonate. This process was repeated with multiple layers to form a cell-hydrogel composite[249]. Similar technology was utilized to fabricate biological nerve grafts, that improved compound action potential critical for motor function when implanted into a rat model of sciatic nerve injury. This ultimately improved the arterial blood pressure by electrically eliciting the pressor reflex[37].

Inkjet printing was used to investigate the deposition of retinal ganglion cells and glia. Both cell types were successfully printed using a piezoelectric printer with no evidence of destruction or distortion of the cells during jet ejection and drop formation. The investigators did, however, find a reduced cell population due to sedimentation during printing. Most importantly, cell viability was not affected by the printing process. To confirm these findings, the group tested printed and non-printed RGC/glial cells in culture and found no significant difference in cell survival or neurite outgrowth. Finally, glial substrate increased neurite outgrowth[250]. In another study, 3D brain-like structures with distinct layers composed of primary neural cells encapsulated in a gellan gum-RGD hydrogel were bioprinted. The investigators found that peptide modification of the gellan gum hydrogel had a positive impact on cell proliferation and the formation of a supportive neural network formation[48]. Later, a piezoelectric-inkjet-printer was used to distribute Schwann cells and neuronal analog NG108-15 cells. The neuronal and glial cell viabilities were both maintained above 85% immediately after printing, and the printed neuronal cells quickly produced neurites[251]. Others have sought to use other complex methods to functionalize neuronal tissue. Kaplan et al. reported a method in which modular 3D compartmentalized architectures were formed with a silk protein-based porous scaffolds. A complex cutting process was developed to fabricate modular structures to allow for a puzzle-like assembly. The silk protein scaffolds were highly versatile, allowing the modules to fit into self-supporting structures without additional reinforcements. By doing so, the group could target complex architectural features of the brain, including six-layered laminar cortex and white matter tracts with microcircuitry. Ultimately, primary cortical neurons on the scaffold demonstrated electrophysiological function. When injured, the scaffolds responded in a biomimetic manner, electrophysiologically and biochemically, confirming that this modular brain-like tissue is capable of real-time nondestructive assessments including an injury-induced surge of excitatory neurotransmitters and transient seizure activities post-TBI[252].

Finally, the implementation of stem cells in bioprinted neuronal tissue provides a platform for generating functional implants without requiring primary neuronal biopsies. Neural stem cells have been embedded in a range of thermoresponsive and biodegradable polyurethane dispersion and bioprinted them. Investigators found that a 25–30% polyurethane hydrogel had both excellent cell proliferation and differentiation compared with all other groups. When acellular polyurethane hydrogel was injected into a model of neural injury in zebrafish, the impaired nervous system was repaired. Surprisingly, the neural stem cell-laden polyurethane-only group showed a minor repair effect in the zebrafish model. However,

traumatic brain injury in the adult was rescued by implantation of a 3D-printed neural construct[253]. More recently, other investigators printed human neural stem cells embedded in a polysaccharide-based bioink comprising alginate, carboxymethyl-chitosan, and agarose deposited by direct-write printing (see figure 18). The bioink gels rapidly with stable cross-linking and forms a porous 3D scaffold, which allows encapsulated stem cells to expand and differentiate. The neural tissue constructs differentiated in situ and formed synaptic contacts and established neural networks that were spontaneously active. Furthermore, the constructs expressed gamma-aminobutyric acid and showed a bicuculline-induced increase in calcium response[254]. These promising results suggest that functional neural units can be engineered. However, consistent fabrication of site-specific neuronal building blocks of more complex and critical brain structures are far from being realized. Current efforts to map and understand the complexity of neuronal networks and the functions of each brain structure will inform engineering in the future. In the meantime, neural tissue engineers can continue to make advances towards clinically translatable tissue implants of the peripheral nervous system.

6. Outlook and future directions for the field

3D bioprinting has revolutionized the field of organ engineering[255]. Early implementation of the technology has shown that the three-dimensional macrostructure (>1cm) of organs can be recapitulated with high fidelity and resolution. Further advances in the field have enabled the development of mesostructural elements (1mm-1cm), including small-diameter blood vessels to allow organ engineering with perfusion. At the other end of the spectrum, biomaterial advances have produced tunable bioinks that replicate nanostructural organ components (<1μm) such as the ECM that is essential to promote cellular attachment, proliferation, and growth. The full potential for cells to self-assemble into functional organ microstructures will require all these elements, with bioprinting enabling Macro to Micro organization and biomaterials promoting Nano to Micro self-assembly.

While significant efforts have been made to enhance bioprinting techniques, biofabrication methods to date are often siloed within the camps of extrusion, inkjet, and laser-assisted bioprinters[256]. A combination of these and other forms of 3D fabrication will need to be incorporated into one multi-functional machine in order to meet all the demands of high-fidelity organ fabrication[257]. Combination bioprinters are not without precedent, and several groups have shown the added value of utilizing the strengths of complementary fabrication methods, allowing enhanced structural stability by high viscosity hydrogels with mass deposition by extrusion techniques[258, 259]. Coaxial extrusion printing technology could then be implemented to fabricate vascularity and other tubular constructs necessary within the construct. Furthermore, LIFT or inkjet methods may be used to fabricate high-resolution microstructures. Also, organ-specific printers could be developed to meet the needs of different organ types. Combination bioprinters can then be enhanced by the use of a combination of biomaterials. Composite bioinks already present in the literature, ranging from mixed natural polymers, mixed synthetic polymers, and natural-synthetic combinations, have demonstrated their ability to improve the mechanical and biological properties of printed organs[260–262]. Furthermore, the implementation of organ-specific ECM bioinks or solutions supplements within composite bioinks could enhance cell attachment,

proliferation, biological performance, and self-assembly into organ-specific microstructures for organ function.

6.1. Cutting edge technologies

At the cutting edge of whole organ bioprinting, new printing technologies, including SLATE (described in section 3), FRESH (described in section 5), and SWIFT, have been implemented to printing microscale complexity of native tissues[263]. The SWIFT method uses sacrificial biomaterials in combination with functional tissue utilize cellular organoids with autologous induced pluripotent stem cell organoids. These are formed into matrices with high cellular density, after which perfusable vascular channels are printed by embedding. The organ like constructs exhibited perfusable cardiac tissue that beats synchronously over one week. Thus this 3D biomanufacturing method may enable the rapid assembly of perfusable tissues at therapeutic scales[144].

Additionally, the use of microfluidic technology is recently entering the arena of bioprinting as a method for developing complex and tunable characteristics of printed constructs. Khademhosseini et al. developed a stereolithography-based bioprinting platform that incorporates microfluidics for multi-material fabrication (see figure 19). The method uses a digital micro-mirror, incorporated into a moving stage, along with a microfluidic system containing four pneumatic switch valves for dynamic patterning of 3D constructs. The multivalve device is capable of fast switching between hydrogel bioinks, allowing for layer-by-layer multi-material bioprinting with a high spatial resolution with faster print times than conventional stereolithographic printers. Their group tested a variety of hydrogel constructs ranging from including poly (ethylene glycol) diacrylate and gelatin methacryloyl[264].

Most recently, investigators described an improved method for rapid voxelated matter printing. Inkjet-based three-dimensional (3D) printing is widely adopted as a method for creating 3D voxelated materials with high precision. However, this method requires low-viscosity inks to ensure successful printing. Extrusion-based printing has been developed to enable a broader range of materials; however, the use of extrusion printing has been limited to extrusion of filaments that are aligned and then layered. To combined the strengths of these methods, investigators developed a multi-material multi-nozzle 3D (MM3D) printing method in which voxelated soft matter composition, function, and structure can be programmed at the voxel scale (see figure 20). Their MM3D print heads exploit a diode-like behavior as a result of multiple viscoelastic materials converging at a common junction, enabling high-frequency switching between up to eight bioinks. This results in the formation of voxels (approximately the size of the nozzle diameter cubed), allowing manufacturing of intricate motifs, while also increasing the speed at which the structures can be fabricated[265].

6.2. Manufacturing scale-up of biofabricated organs

Scaling and commercialization of bioprinted tissues present significant hurdles for the translation of cutting edge technologies. Cell sourcing, fabrication logistics, and tissue designs are highly personalized to each patient and to the organ type being fabricated. Thus, the current costs associated with these technologies present a practical challenge. Simplifying the manufacturing processes and materials used could substantially improve the

outlook for tissue-engineered products in this space. For example, investments in this area should develop universal components to reduce the costs associated with original materials and designs. Furthermore, upfront costs of 3D bioprinted or tissue-engineered structures must be seen in the light of the alternative of costly life-long treatments and the associated morbidities (i.e., dialysis, management of chronic disease, immunosuppression for transplant recipient). For many conditions, a cost analysis could demonstrate that a single, curative intervention is economically preferred to life-long, non-curative treatments[266].

Furthermore, the use of automated design and fabrication can be used to improve reproducibility and regulation of personalizing tissue designs. While the complexity of anatomical designs designed requires certain engineering leeway, clear design parameters can be utilized by implementing modeling software for structures personalize to the patient and their unique injury in an automated manner[267]. This concept is complicated by biomaterial and cellular self-assembly, along with the integration of the bioprinted construct by host cells. Further knowledge is required to predict the outcomes of such complex prints properly and requires thorough analysis of the in vitro and in vivo interactions over time[268].

Finally, the logistical demands of living cells and tissues are especially challenging. Manufacturing autologous patient-specific tissues is particularly complex, since most hospitals and clinics do not have clinical-grade cell processing or 3D-printing capabilities. Thus, a new shipping system will be required to provide stability and documented compliance. Furthermore, the number of facilities with the technology, resources, and expertise for fabricating organs and tissue for transplantation is limited. Strategically located biofabrication hubs, could be implemented, where patient-derived cells would be sent to the hub, the biofabricated organ produced, and then shipped back to the care provider for implantation. This could be done in concert with ongoing programs, such as UNOS, that have optimized methods for organ procurement, multi-site coordination, preservation and transportation, and include centers of excellence for implantation.

6.3. Regulation and standardization of engineered organs

The promise of 3D-bioprinted tissues and organs as a curative treatment for human disease will follow a steep regulatory path. Despite advances in the reproducibility of bioprinting, the FDA continues to assess 3D-printed medical devices under the same guidelines as conventionally manufacture products. The 21st Century Cures Act has provided a first step in simplifying the pathway by providing an alternative approval pathway for therapies designated as a ‘regenerative medicine advanced therapy’ (RMAT)[269]. The FDA also released detailed guidance for manufacturers of 3D printers to guide their efforts towards translatable clinical products[270]. At their core, these guidelines are in place to protect patients and ensure consistent therapy. This, of course, also applies to bioprinted constructs that contain bioactive materials and cells.

Regenerative medicine technologies are fundamentally distinct from other clinical products and rely on incredibly complex mechanisms, with unknown effects in humans. However, it should be recognized that molding or casting has already been used for approved tissue-engineered products for many years. In the simplest form, bioprinting builds upon the reproducibility of mold casting techniques by tightly controlling the deposition of

biomaterials. Bioprinting also has the potential to reduce human interaction and human error while manufacturing engineered tissues. These improvements in biomaterial deposition by bioprinters need to be recognized by regulators as a benefit of the technology in terms of safety and reproducibility.

There are no standards for 3D bioprinting technology, biomaterials, or the bioprinting process despite current standard (ISO/DIS 17296-1) and guidance documents[270]. For this technology to expand to clinical relevance, increased levels of standardization are necessary. Standardizing bioprinting materials, similar to standardized cell expansion media, would improve product-development time and clinical translation of bioprinted constructs. Additional quality-control systems including a data throughout the manufacturing process will be require to ensure reproducibility and safety of regenerative-medicine product manufacturing[271].

6.4. Outlook

Clinically relevant bioprinted organs will need to demonstrate functionality and efficacy, with biomechanical properties that closely mimic the native organ, complete with vascular networks. While the scale of 3D-printed tissue constructs continue to improve, bioprinting complex tissues with high physiological demands continues to be a challenge, that will require advances in primary cell and stem cell isolation and expansion, specialized biomaterial development, and combined bioprinting technologies. Furthermore, as these technologies develop, validation of the function and longevity of engineered organs will need to be established. For clinical translation, these parameters will need to be realistic, safe, and provide a real and understandable benefit to the patients consenting to these treatments. Each of the enabling technologies discussed herein provides great hope for the future of our field, and the promise of printing solid organs for clinical translation. In this pursuit, it is essential to the translation of whole organ bioprinting is the preclinical testing of bioprinted whole organs. This in vivo data is crucial to defining the level of in vitro maturation vs. post-implantation remodeling and integration by the host. Thus, early pre-clinical in vivo models are crucial to clarify the direction of future studies further. Finally, the driving force behind all the innovations in solid organ engineering is to meet the unmet clinical need for transplantable organs among suffering patients. It has been theorized that by replacing all current supply constraints, organ replacement could prevent >30% of all deaths in the United States[4]. Solid-organ bioprinting is at the cusp of this endeavor, with the promise of whole organ engineering on the horizon.

Acknowledgements

The authors declare no competing financial interest. Thank you to S.J. Lee and M. Ali for providing editing and feedback for this manuscript. Thank you to E. Gregg for helping prepare figures 1 and 2. The graphical abstract was created with BioRender.com.

Funding Information

Funding for this work was provided in part by NIH/NIAMS 1 F30 AR074866-01A1 (A.M.J).

Author Biographies

Adam M. Jorgensen

Adam is an MD/PhD Candidate and NIH/NIAMS F30 NRSA Fellow working in the Atala lab at the Wake Forest Institute for Regenerative Medicine. His research focuses on 3D bioprinting skin for full-thickness wound healing. His other research pursuits include the generation of a novel spherical skin organoid for in vitro drug testing and dermatologic disease modeling, the use of both cellular and acellular hydrogels and scaffolds for wound healing applications, and biofabrication of hair follicles. He is an NIH/NIAMS F30 NRSA Fellowship recipient for his thesis research on “Integration and remodeling of bioprinted skin in full-thickness wound healing.” His findings to date have resulted in two first-author publications, including one featured as the current cover of Tissue Engineering, Part A; eleven peer-reviewed abstracts with associated presentations at local, national, and international conferences; and eight research awards, including the 2019 Tissue Engineering and Regenerative Medicine International Society-AM Mary Ann Liebert, Inc. Outstanding Student Award and an invited participant at the 2020 Society for Investigative Dermatology Future Leaders Post-Doctoral Retreat, all within the first year of this NIAMS F30 NRSA fellowship.

James J. Yoo, MD, PhD

Dr. Yoo is Professor and Associate Director of the Wake Forest Institute for Regenerative Medicine (WFIRM), with a cross-appointment to the Departments of Urology, Physiology and Pharmacology, and the Virginia Tech-Wake Forest School of Biomedical Engineering and Sciences. Dr. Yoo’s research efforts have been directed toward the clinical translation of tissue engineering technologies and cell-based therapies. Dr. Yoo’s background in cell biology and medicine has facilitated the transfer of several cell-based technologies from the bench-top to the bedside. Dr. Yoo has been a lead scientist in the bioprinting program at WFIRM and has been instrumental in developing skin bioprinting and integrated tissue and organ printing (ITOP) systems for preclinical and clinical applications. He has authored more than 300 scientific publications, over 50 patent registrations/applications, 1000 scientific presentations, 260 invited lectures and mentored over 290 trainees, ranging from undergraduate students to practicing physicians.

Anthony Atala, M.D.

Dr. Atala is the G. Link Professor and Director of the Wake Forest Institute for Regenerative Medicine, and the W. Boyce Professor and Chair of Urology. Dr. Atala is a practicing surgeon and a researcher in the area of regenerative medicine. Fifteen applications of technologies developed in Dr. Atala’s laboratory have been used clinically. He is Editor of 25 books and 3 journals. Dr. Atala has published over 600 journal articles, and has received over 250 national and international patents. Dr. Atala was elected to the Institute of Medicine of the National Academies of Sciences, to the National Academy of Inventors as a Charter Fellow, and to the American Institute for Medical and Biological Engineering. Dr. Atala is a recipient of the US Congress funded Christopher Columbus Foundation Award, bestowed on a living American who is currently working on a discovery that

will significantly affect society; the World Technology Award in Health and Medicine, for achieving significant and lasting progress; the Edison Science/Medical Award for innovation, the R&D Innovator of the Year Award, and the Smithsonian Ingenuity Award for Bioprinting Tissue and Organs. Dr. Atala's work was listed twice as Time Magazine's Top 10 medical breakthroughs of the year, and once as one of 5 discoveries that will change the future of organ transplants. He was named by Scientific American as one of the world's most influential people in biotechnology, by U.S. News & World Report as one of 14 Pioneers of Medical Progress in the 21st Century, by Life Sciences Intellectual Property Review as one of the top key influencers in the life sciences intellectual property arena, and by Nature Biotechnology as one of the top 10 translational researchers in the world. Dr. Atala has led or served several national professional and government committees, including the National Institutes of Health working group on Cells and Developmental Biology, the National Institutes of Health Bioengineering Consortium, and the National Cancer Institute's Advisory Board. He is a founding member of the Tissue Engineering Society, Regenerative Medicine Foundation, Regenerative Medicine Manufacturing Innovation Consortium, Regenerative Medicine Development Organization, and Regenerative Medicine Manufacturing Society.

References

1. OPTN/SRTR 2018 annual data report: preface. Am J Transplant2020, 20Suppl s1, 1–10.
2. OPTN/SRTR 2018 annual data report: introduction. Am J Transplant2020, 20Suppl s1, 11–19. [PubMed: 31898409]
3. Israni AK; Zaun D; Hadley N; Rosendale JD; Schaffhausen C; McKinney W; Snyder JJ; Kasiske BL, OPTN/SRTR 2018 annual data report: deceased organ donation. Am J Transplant2020, 20Suppl s1, 509–541. [PubMed: 31898414]
4. Giwa S; Lewis JK; Alvarez L; Langer R; Roth AE; Church GM; Markmann JF; Sachs DH; Chandraker A; Wertheim JA; Rothblatt M; Boyden ES; Eidbo E; Lee WPA; Pomahac B; Brandacher G; Weinstock DM; Elliott G; Nelson D; Acker JP; Uygun K; Schmalz B; Weegman BP; Tocchio A; Fahy GM; Storey KB; Rubinsky B; Bischof J; Elliott JAW; Woodruff TK; Morris GJ; Demirci U; Brockbank KGM; Woods EJ; Ben RN; Baust JG; Gao D; Fuller B; Rabin Y; Kravitz DC; Taylor MJ; Toner M, The promise of organ and tissue preservation to transform medicine. Nat Biotechnol2017, 35, 530–542. [PubMed: 28591112]
5. Alliance for Regenerative Medicine: 2018 annual report. https://alliancerm.org/publication/2018-annual-report/ (accessed7/30).
6. Murphy SV; Atala A, 3D bioprinting of tissues and organs. Nat Biotechnol2014, 32, 773–85. [PubMed: 25093879]
7. Atala A; Kasper FK; Mikos AG, Engineering complex tissues. Sci Transl Med2012, 4, 160rv12.
8. Schubert C; van Langeveld MC; Donoso LA, Innovations in 3D printing: a 3D overview from optics to organs. Br J Ophthalmol2014, 98, 159–61. [PubMed: 24288392]
9. Mandrycky C; Wang Z; Kim K; Kim DH, 3D bioprinting for engineering complex tissues. Biotechnol Adv2016, 34, 422–434. [PubMed: 26724184]
10. Vijayavenkataraman S; Yan WC; Lu WF; Wang CH; Fuh JYH, 3D bioprinting of tissues and organs for regenerative medicine. Adv Drug Deliv Rev2018, 132, 296–332. [PubMed: 29990578]
11. Albanna M; Binder KW; Murphy SV; Kim J; Qasem SA; Zhao W; Tan J; El-Amin IB; Dice DD; Marco J; Green J; Xu T; Skardal A; Holmes JH; Jackson JD; Atala A; Yoo JJ, In situ bioprinting of autologous skin cells accelerates wound healing of extensive excisional full-thickness wounds. Sci Rep2019, 9, 1856. [PubMed: 30755653]

12. Kolesky DB; Truby RL; Gladman AS; Busbee TA; Homan KA; Lewis JA, 3D bioprinting of vascularized, heterogeneous cell-laden tissue constructs. Adv Mater2014, 26, 3124–30. [PubMed: 24550124]
13. J R, Anatomy of kidney tubules. *In*International review of cytology1958, *Vol.* 7, *pp.* 485–534.
14. Rhodin JA, The ultrastructure of mammalian arterioles and precapillary sphincters. J Ultrastruct Res1967, 18, 181–223. [PubMed: 5337871]
15. Conti S; Perico N; Novelli R; Carrara C; Benigni A; Remuzzi G, Early and late scanning electron microscopy findings in diabetic kidney disease. Sci Rep2018, 8, 4909. [PubMed: 29559657]
16. Kirkegaard K; Hindkjaer JJ; Ingerslev HJ, Human embryonic development after blastomere removal: a time-lapse analysis. Hum Reprod2012, 27, 97–105. [PubMed: 22081251]
17. AS R, Biomaterial biotechnology using self-assembled lipid microstructures. Journal of cellular biochemistry1994, 56(2), 183–187. [PubMed: 7829578]
18. Stupp SI, Self-assembly and biomaterials. Nano Lett2010, 10, 4783–6. [PubMed: 21028843]
19. Wang Z; Abdulla R; Parker B; Samanipour R; Ghosh S; Kim K, A simple and high-resolution stereolithography-based 3D bioprinting system using visible light crosslinkable bioinks. Biofabrication2015, 7, 045009. [PubMed: 26696527]
20. Mikos AG; Herring SW; Ochareon P; Elisseeff J; Lu HH; Kandel R; Schoen FJ; Toner M; Mooney D; Atala A; Van Dyke ME; Kaplan D; Vunjak-Novakovic G, Engineering complex tissues. Tissue Eng2006, 12, 3307–39. [PubMed: 17518671]
21. Grafting of burns with cultured epithelium prepared from autologous epidermal cells. Lancet1981, 1, 75–8. [PubMed: 6109123]
22. Jorgensen AM; Varkey M; Gorkun A; Clouse C; Xu L; Chou Z; Murphy SV; Molnar J; Lee SJ; Yoo JJ; Soker S; Atala A, Bioprinted skin recapitulates normal collagen remodeling in full-thickness wounds. Tissue Eng Part A2020, 26, 512–526. [PubMed: 31861970]
23. Folkman J; D'Amore PA, Blood vessel formation: what is its molecular basis?Cell1996, 87, 1153–5. [PubMed: 8980221]
24. Atala A; Bauer SB; Soker S; Yoo JJ; Retik AB, Tissue-engineered autologous bladders for patients needing cystoplasty. Lancet2006, 367, 1241–6. [PubMed: 16631879]
25. Pashuck ET; Stevens MM, Designing regenerative biomaterial therapies for the clinic. Sci Transl Med2012, 4, 160sr4. [PubMed: 23152328]
26. Derby B, Printing and prototyping of tissues and scaffolds. Science2012, 338, 921–6. [PubMed: 23161993]
27. Jia W; Gungor-Ozkerim PS; Zhang YS; Yue K; Zhu K; Liu W; Pi Q; Byambaa B; Dokmeci MR; Shin SR; Khademhosseini A, Direct 3D bioprinting of perfusable vascular constructs using a blend bioink. Biomaterials2016, 106, 58–68. [PubMed: 27552316]
28. Duarte Campos DF; Blaeser A; Korsten A; Neuss S; Jakel J; Vogt M; Fischer H, The stiffness and structure of three-dimensional printed hydrogels direct the differentiation of mesenchymal stromal cells toward adipogenic and osteogenic lineages. Tissue Eng Part A2015, 21, 740–56. [PubMed: 25236338]
29. Blaeser A; Duarte Campos DF; Weber M; Neuss S; Theek B; Fischer H; Jahnen-Dechent W, Biofabrication under fluorocarbon: a novel freeform fabrication technique to generate high aspect ratio tissue-engineered constructs. Biores Open Access2013, 2, 374–84. [PubMed: 24083093]
30. Duarte Campos DF; Blaeser A; Weber M; Jakel J; Neuss S; Jahnen-Dechent W; Fischer H, Three-dimensional printing of stem cell-laden hydrogels submerged in a hydrophobic high-density fluid. Biofabrication2013, 5, 015003. [PubMed: 23172592]
31. Kim Y; Kang K; Jeong J; Paik SS; Kim JS; Park SA; Kim WD; Park J; Choi D, Three-dimensional (3D) printing of mouse primary hepatocytes to generate 3D hepatic structure. Ann Surg Treat Res2017, 92, 67–72. [PubMed: 28203553]
32. Faulkner-Jones A; Fyfe C; Cornelissen D-J; Gardner J; King J; Courtney A; Shu W, Bioprinting of human pluripotent stem cells and their directed differentiation into hepatocyte-like cells for the generation of mini-livers in 3D. Biofabrication2015, 7, 044102. [PubMed: 26486521]
33. Marchioli G; van Gurp L; van Krieken PP; Stamatialis D; Engelse M; van Blitterswijk CA; Karperien MB; de Koning E; Alblas J; Moroni L; van Apeldoorn AA, Fabrication

of three-dimensional bioplotted hydrogel scaffolds for islets of Langerhans transplantation. Biofabrication2015, 7, 025009. [PubMed: 26019140]

34. Duan B; Hockaday LA; Kang KH; Butcher JT, 3D bioprinting of heterogeneous aortic valve conduits with alginate/gelatin hydrogels. J Biomed Mater Res A2013, 101, 1255–64. [PubMed: 23015540]
35. Gaetani R; Doevendans PA; Metz CH; Alblas J; Messina E; Giacomello A; Sluijter JP, Cardiac tissue engineering using tissue printing technology and human cardiac progenitor cells. Biomaterials2012, 33, 1782–90. [PubMed: 22136718]
36. Faulkner-Jones A; Greenhough S; King JA; Gardner J; Courtney A; Shu W, Development of a valve-based cell printer for the formation of human embryonic stem cell spheroid aggregates. Biofabrication2013, 5, 015013. [PubMed: 23380571]
37. Owens CM; Marga F; Forgacs G; Heesch CM, Biofabrication and testing of a fully cellular nerve graft. Biofabrication2013, 5, 045007. [PubMed: 24192236]
38. Norotte C; Marga FS; Niklason LE; Forgacs G, Scaffold-free vascular tissue engineering using bioprinting. Biomaterials2009, 30, 5910–7. [PubMed: 19664819]
39. Jakab K; Norotte C; Damon B; Marga F; Neagu A; Besch-Williford CL; Kachurin A; Church KH; Park H; Mironov V; Markwald R; Vunjak-Novakovic G; Forgacs G, Tissue engineering by self-assembly of cells printed into topologically defined structures. Tissue Eng Part A2008, 14, 413–21. [PubMed: 18333793]
40. Bulanova EA; Koudan EV; Degosserie J; Heymans C; Pereira FD; Parfenov VA; Sun Y; Wang Q; Akhmedova SA; Sviridova IK; Sergeeva NS; Frank GA; Khesuani YD; Pierreux CE; Mironov VA, Bioprinting of a functional vascularized mouse thyroid gland construct. Biofabrication2017, 9, 034105. [PubMed: 28707625]
41. Xu F; Moon SJ; Emre AE; Turali ES; Song YS; Hacking SA; Nagatomi J; Demirci U, A droplet-based building block approach for bladder smooth muscle cell (SMC) proliferation. Biofabrication2010, 2, 014105. [PubMed: 20811120]
42. Skardal A; Devarasetty M; Kang HW; Mead I; Bishop C; Shupe T; Lee SJ; Jackson J; Yoo J; Soker S; Atala A, A hydrogel bioink toolkit for mimicking native tissue biochemical and mechanical properties in bioprinted tissue constructs. Acta Biomater2015, 25, 24–34. [PubMed: 26210285]
43. Pati F; Jang J; Ha DH; Won Kim S; Rhie JW; Shim JH; Kim DH; Cho DW, Printing three-dimensional tissue analogues with decellularized extracellular matrix bioink. Nat Commun2014, 5, 3935. [PubMed: 24887553]
44. Homan KA; Kolesky DB; Skylar-Scott MA; Herrmann J; Obuobi H; Moisan A; Lewis JA, Bioprinting of 3D convoluted renal proximal tubules on perfusable chips. Sci Rep2016, 6, 34845. [PubMed: 27725720]
45. Kang HW; Lee SJ; Ko IK; Kengla C; Yoo JJ; Atala A, A 3D bioprinting system to produce human-scale tissue constructs with structural integrity. Nat Biotechnol2016, 34, 312–9. [PubMed: 26878319]
46. Song J; Millman JR, Economic 3D-printing approach for transplantation of human stem cell-derived beta-like cells. Biofabrication2016, 9, 015002. [PubMed: 27906687]
47. Gaetani R; Feyen DA; Verhage V; Slaats R; Messina E; Christman KL; Giacomello A; Doevendans PA; Sluijter JP, Epicardial application of cardiac progenitor cells in a 3D-printed gelatin/hyaluronic acid patch preserves cardiac function after myocardial infarction. Biomaterials2015, 61, 339–48. [PubMed: 26043062]
48. Lozano R; Stevens L; Thompson BC; Gilmore KJ; Gorkin R 3rd; Stewart EM; in het Panhuis M; Romero-Ortega M; Wallace GG, 3D printing of layered brain-like structures using peptide modified gellan gum substrates. Biomaterials2015, 67, 264–73. [PubMed: 26231917]
49. Duan B; Kapetanovic E; Hockaday LA; Butcher JT, Three-dimensional printed trileaflet valve conduits using biological hydrogels and human valve interstitial cells. Acta Biomater2014, 10, 1836–46. [PubMed: 24334142]
50. Skardal A; Zhang J; Prestwich GD, Bioprinting vessel-like constructs using hyaluronan hydrogels crosslinked with tetrahedral polyethylene glycol tetracrylates. Biomaterials2010, 31, 6173–81. [PubMed: 20546891]

51. Horvath L; Umehara Y; Jud C; Blank F; Petri-Fink A; Rothen-Rutishauser B, Engineering an in vitro air-blood barrier by 3D bioprinting. Sci Rep2015, 5, 7974. [PubMed: 25609567]
52. Poldervaart MT; Gremmels H; van Deventer K; Fledderus JO; Oner FC; Verhaar MC; Dhert WJ; Alblas J, Prolonged presence of VEGF promotes vascularization in 3D bioprinted scaffolds with defined architecture. J Control Release2014, 184, 58–66. [PubMed: 24727077]
53. Ong CS; Fukunishi T; Zhang H; Huang CY; Nashed A; Blazeski A; DiSilvestre D; Vricella L; Conte J; Tung L; Tomaselli GF; Hibino N, Biomaterial-free three-dimensional bioprinting of cardiac tissue using human induced pluripotent stem cell derived cardiomyocytes. Sci Rep2017, 7, 4566. [PubMed: 28676704]
54. Kizawa H; Nagao E; Shimamura M; Zhang G; Torii H, Scaffold-free 3D bio-printed human liver tissue stably maintains metabolic functions useful for drug discovery. Biochem Biophys Rep2017, 10, 186–191. [PubMed: 28955746]
55. Cui X; Gao G; Qiu Y, Accelerated myotube formation using bioprinting technology for biosensor applications. Biotechnol Lett2013, 35, 315–21. [PubMed: 23160742]
56. Gaebel R; Ma N; Liu J; Guan J; Koch L; Klopsch C; Gruene M; Toelk A; Wang W; Mark P; Wang F; Chichkov B; Li W; Steinhoff G, Patterning human stem cells and endothelial cells with laser printing for cardiac regeneration. Biomaterials2011, 32, 9218–30. [PubMed: 21911255]
57. Lee KY; Mooney DJ, Alginate: properties and biomedical applications. Prog Polym Sci2012, 37, 106–126. [PubMed: 22125349]
58. Daly AC; Cunniffe GM; Sathy BN; Jeon O; Alsberg E; Kelly DJ, 3D Bioprinting of developmentally inspired templates for whole bone organ engineering. Adv Healthc Mater2016, 5, 2353–62. [PubMed: 27281607]
59. Arai K; Yoshida T; Okabe M; Goto M; Mir TA; Soko C; Tsukamoto Y; Akaike T; Nikaido T; Zhou K; Nakamura M, Fabrication of 3D-culture platform with sandwich architecture for preserving liver-specific functions of hepatocytes using 3D bioprinter. J Biomed Mater Res A2017, 105, 1583–1592. [PubMed: 27643636]
60. Parenteau-Bareil R, Gauvin R, & Berthod F, Collagen-based biomaterials for tissue engineering applications. Materials 2010, 3(3), 1863–1887.
61. Cen L; Liu W; Cui L; Zhang W; Cao Y, Collagen tissue engineering: development of novel biomaterials and applications. Pediatr Res2008, 63, 492–6. [PubMed: 18427293]
62. Lu Q; Ganesan K; Simionescu DT; Vyavahare NR, Novel porous aortic elastin and collagen scaffolds for tissue engineering. Biomaterials2004, 25, 5227–37. [PubMed: 15110474]
63. Ahmed TA; Dare EV; Hincke M, Fibrin: a versatile scaffold for tissue engineering applications. Tissue Eng Part B Rev2008, 14, 199–215. [PubMed: 18544016]
64. Hoffman AS, Hydrogels for biomedical applications. Advanced drug delivery reviews2012, 64, 18–23.
65. Lee JW; Choi YJ; Yong WJ; Pati F; Shim JH; Kang KS; Kang IH; Park J; Cho DW, Development of a 3D cell printed construct considering angiogenesis for liver tissue engineering. Biofabrication2016, 8, 015007. [PubMed: 26756962]
66. Su K; Wang C, Recent advances in the use of gelatin in biomedical research. Biotechnol Lett2015, 37, 2139–45. [PubMed: 26160110]
67. Duan H; Umar S; Xiong R; Chen J, New strategy for expression of recombinant hydroxylated human-derived gelatin in Pichia pastoris KM71. J Agric Food Chem2011, 59, 7127–34. [PubMed: 21604758]
68. Walimbe T; Panitch A; Sivasankar PM, A Review of Hyaluronic Acid and Hyaluronic Acid-based Hydrogels for Vocal Fold Tissue Engineering. J Voice2017, 31, 416–423. [PubMed: 28262503]
69. Hemshekhar M; Thushara RM; Chandranayaka S; Sherman LS; Kemparaju K; Girish KS, Emerging roles of hyaluronic acid bioscaffolds in tissue engineering and regenerative medicine. Int J Biol Macromol2016, 86, 917–28. [PubMed: 26893053]
70. Toole BP, Hyaluronan: from extracellular glue to pericellular cue. Nat Rev Cancer2004, 4, 528–39. [PubMed: 15229478]
71. West DC; Kumar S, Hyaluronan and angiogenesis. Ciba Found Symp1989, 143, 187–201; discussion 201–7, 281–5. [PubMed: 2478344]

72. Mouser VH; Abbadessa A; Levato R; Hennink WE; Vermonden T; Gawlitta D; Malda J, Development of a thermosensitive HAMA-containing bio-ink for the fabrication of composite cartilage repair constructs. Biofabrication2017, 9, 015026. [PubMed: 28229956]

73. Kasoju N; Bora U, Silk fibroin based biomimetic artificial extracellular matrix for hepatic tissue engineering applications. Biomed Mater2012, 7, 045004. [PubMed: 22556184]

74. Cao Y; Wang B, Biodegradation of silk biomaterials. Int J Mol Sci2009, 10, 1514–24. [PubMed: 19468322]

75. Partlow BP; Hanna CW; Rnjak-Kovacina J; Moreau JE; Applegate MB; Burke KA; Marelli B; Mitropoulos AN; Omenetto FG; Kaplan DL, Highly tunable elastomeric silk biomaterials. Adv Funct Mater2014, 24, 4615–4624. [PubMed: 25395921]

76. Das S; Pati F; Choi YJ; Rijal G; Shim JH; Kim SW; Ray AR; Cho DW; Ghosh S, Bioprintable, cell-laden silk fibroin-gelatin hydrogel supporting multilineage differentiation of stem cells for fabrication of three-dimensional tissue constructs. Acta Biomater2015, 11, 233–46. [PubMed: 25242654]

77. Zarrintaj P; Manouchehri S; Ahmadi Z; Saeb MR; Urbanska AM; Kaplan DL; Mozafari M, Agarose-based biomaterials for tissue engineering. Carbohydr Polym2018, 187, 66–84. [PubMed: 29486846]

78. Yue K; Trujillo-de Santiago G; Alvarez MM; Tamayol A; Annabi N; Khademhosseini A, Synthesis, properties, and biomedical applications of gelatin methacryloyl (GelMA) hydrogels. Biomaterials2015, 73, 254–71. [PubMed: 26414409]

79. Cui H; Zhu W; Nowicki M; Zhou X; Khademhosseini A; Zhang LG, Hierarchical Fabrication of engineered vascularized bone biphasic constructs via dual 3D bioprinting: Integrating Regional Bioactive Factors into Architectural Design. Adv Healthc Mater2016, 5, 2174–81. [PubMed: 27383032]

80. Duchi S; Onofrillo C; O'Connell CD; Blanchard R; Augustine C; Quigley AF; Kapsa RMI; Pivonka P; Wallace G; Di Bella C; Choong PFM, Handheld co-axial bioprinting: application to in situ surgical cartilage repair. Sci Rep2017, 7, 5837. [PubMed: 28724980]

81. Majima T; Schnabel W; Weber W, Phenyl-2, 4, 6-trimethylbenzoylphosphinates as water-soluble photoinitiators. Generation and reactivity of O Ṗ (C6H5)(O−) radical anions. Die Makromolekulare Chemie: Macromolecular Chemistry and Physics1991, 192, 2307–2315.

82. Fairbanks BD; Schwartz MP; Bowman CN; Anseth KS, Photoinitiated polymerization of PEG-diacrylate with lithium phenyl-2, 4, 6-trimethylbenzoylphosphinate: polymerization rate and cytocompatibility. Biomaterials2009, 30, 6702–6707. [PubMed: 19783300]

83. Zhu J, Bioactive modification of poly(ethylene glycol) hydrogels for tissue engineering. Biomaterials2010, 31, 4639–56. [PubMed: 20303169]

84. Hong S; Sycks D; Chan HF; Lin S; Lopez GP; Guilak F; Leong KW; Zhao X, 3D printing of highly stretchable and tough hydrogels into complex, cellularized structures. Adv Mater2015, 27, 4035–40. [PubMed: 26033288]

85. Janik H; Marzec M, A review: fabrication of porous polyurethane scaffolds. Mater Sci Eng C Mater Biol Appl2015, 48, 586–91. [PubMed: 25579961]

86. Huang Y; He K; Wang X, Rapid prototyping of a hybrid hierarchical polyurethane-cell/hydrogel construct for regenerative medicine. Mater Sci Eng C Mater Biol Appl2013, 33, 3220–9. [PubMed: 23706204]

87. Huang CT; Kumar Shrestha L; Ariga K; Hsu SH, A graphene-polyurethane composite hydrogel as a potential bioink for 3D bioprinting and differentiation of neural stem cells. J Mater Chem B2017, 5, 8854–8864. [PubMed: 32264279]

88. Song JJ; Ott HC, Organ engineering based on decellularized matrix scaffolds. Trends Mol Med2011, 17, 424–32. [PubMed: 21514224]

89. Jorgensen AC. Z; Gillispie G; Lee SJ; Yoo JJ; Soker S; Atala Adecellularized skin extracellular matrix (dsECM) improves the physical and biological properties of fibrinogen hydrogel for skin bioprinting applications. Nanomaterials2020, 10, 1484.

90. Badylak SF, The extracellular matrix as a biologic scaffold material. Biomaterials2007, 28, 3587–93. [PubMed: 17524477]

91. Faulk DM; Johnson SA; Zhang L; Badylak SF, Role of the extracellular matrix in whole organ engineering. J Cell Physiol2014, 229, 984–9. [PubMed: 24347365]
92. Badylak SF; Kropp B; McPherson T; Liang H; Snyder PW, Small intestinal submucosa: a rapidly resorbed bioscaffold for augmentation cystoplasty in a dog model. Tissue Eng1998, 4, 379–87. [PubMed: 9916170]
93. Hodde JP; Record RD; Liang HA; Badylak SF, Vascular endothelial growth factor in porcine-derived extracellular matrix. Endothelium2001, 8, 11–24. [PubMed: 11409848]
94. Wolf MT; Daly KA; Reing JE; Badylak SF, Biologic scaffold composed of skeletal muscle extracellular matrix. Biomaterials2012, 33, 2916–25. [PubMed: 22264525]
95. Choi YJ; Jun YJ; Kim DY; Yi HG; Chae SH; Kang J; Lee J; Gao G; Kong JS; Jang J; Chung WK; Rhie JW; Cho DW, A 3D cell printed muscle construct with tissue-derived bioink for the treatment of volumetric muscle loss. Biomaterials2019, 206, 160–169. [PubMed: 30939408]
96. Saldin LT; Cramer MC; Velankar SS; White LJ; Badylak SF, Extracellular matrix hydrogels from decellularized tissues: Structure and function. Acta Biomater2017, 49, 1–15. [PubMed: 27915024]
97. Badylak SF, The extracellular matrix as a scaffold for tissue reconstruction. Semin Cell Dev Biol2002, 13, 377–83. [PubMed: 12324220]
98. Reing JE; Zhang L; Myers-Irvin J; Cordero KE; Freytes DO; Heber-Katz E; Bedelbaeva K; McIntosh D; Dewilde A; Braunhut SJ; Badylak SF, Degradation products of extracellular matrix affect cell migration and proliferation. Tissue Eng Part A2009, 15, 605–14. [PubMed: 18652541]
99. Keane TJ; Swinehart IT; Badylak SF, Methods of tissue decellularization used for preparation of biologic scaffolds and in vivo relevance. Methods2015, 84, 25–34. [PubMed: 25791470]
100. Crapo PM; Gilbert TW; Badylak SF, An overview of tissue and whole organ decellularization processes. Biomaterials2011, 32, 3233–43. [PubMed: 21296410]
101. Hong Y; Huber A; Takanari K; Amoroso NJ; Hashizume R; Badylak SF; Wagner WR, Mechanical properties and in vivo behavior of a biodegradable synthetic polymer microfiber-extracellular matrix hydrogel biohybrid scaffold. Biomaterials2011, 32, 3387–94. [PubMed: 21303718]
102. Medberry CJ; Crapo PM; Siu BF; Carruthers CA; Wolf MT; Nagarkar SP; Agrawal V; Jones KE; Kelly J; Johnson SA; Velankar SS; Watkins SC; Modo M; Badylak SF, Hydrogels derived from central nervous system extracellular matrix. Biomaterials2013, 34, 1033–40. [PubMed: 23158935]
103. Han W; Singh NK; Kim JJ; Kim H; Kim BS; Park JY; Jang J; Cho DW, Directed differential behaviors of multipotent adult stem cells from decellularized tissue/organ extracellular matrix bioinks. Biomaterials2019, 224, 119496. [PubMed: 31557592]
104. Jang J; Park HJ; Kim SW; Kim H; Park JY; Na SJ; Kim HJ; Park MN; Choi SH; Park SH; Kim SW; Kwon SM; Kim PJ; Cho DW, 3D printed complex tissue construct using stem cell-laden decellularized extracellular matrix bioinks for cardiac repair. Biomaterials2017, 112, 264–274. [PubMed: 27770630]
105. Ali M; Pr AK; Yoo JJ; Zahran F; Atala A; Lee SJ, A photo-crosslinkable kidney ECM-derived bioink accelerates renal tissue formation. Adv Healthc Mater2019, 8, e1800992. [PubMed: 30725520]
106. Phillippi JA; Miller E; Weiss L; Huard J; Waggoner A; Campbell P, Microenvironments engineered by inkjet bioprinting spatially direct adult stem cells toward muscle- and bone-like subpopulations. Stem Cells2008, 26, 127–34. [PubMed: 17901398]
107. Kolesky DB; Homan KA; Skylar-Scott MA; Lewis JA, Three-dimensional bioprinting of thick vascularized tissues. Proc Natl Acad Sci U S A2016, 113, 3179–84. [PubMed: 26951646]
108. Williams SJ; Huang HH; Kover K; Moore W; Berkland C; Singh M; Smirnova IV; MacGregor R; Stehno-Bittel L, Reduction of diffusion barriers in isolated rat islets improves survival, but not insulin secretion or transplantation outcome. Organogenesis2010, 6, 115–24. [PubMed: 20885858]
109. Hwang CM; Sant S; Masaeli M; Kachouie NN; Zamanian B; Lee SH; Khademhosseini A, Fabrication of three-dimensional porous cell-laden hydrogel for tissue engineering. Biofabrication2010, 2, 035003. [PubMed: 20823504]

110. Leong MF; Toh JK; Du C; Narayanan K; Lu HF; Lim TC; Wan AC; Ying JY, Patterned prevascularised tissue constructs by assembly of polyelectrolyte hydrogel fibres. Nat Commun2013, 4, 2353. [PubMed: 23955534]
111. Stegemann JP; Kaszuba SN; Rowe SL, Review: advances in vascular tissue engineering using protein-based biomaterials. Tissue Eng2007, 13, 2601–13. [PubMed: 17961004]
112. Bennett HS; Luft JH; Hampton JC, Morphological classifications of vertebrate blood capillaries. Am J Physiol1959, 196, 381–90. [PubMed: 13627187]
113. Datta P; Ayan B; Ozbolat IT, Bioprinting for vascular and vascularized tissue biofabrication. Acta Biomater2017, 51, 1–20. [PubMed: 28087487]
114. Rouwkema J; Rivron NC; van Blitterswijk CA, Vascularization in tissue engineering. Trends Biotechnol2008, 26, 434–41. [PubMed: 18585808]
115. Zhang X; Xie Y; Koh CG; James Lee L, A novel 3-D model for cell culture and tissue engineering. Biomed Microdevices2009, 11, 795–9. [PubMed: 19288199]
116. Hatch J; Mukouyama YS, Spatiotemporal mapping of vascularization and innervation in the fetal murine intestine. Dev Dyn2015, 244, 56–68. [PubMed: 25138596]
117. Galvez-Monton C; Fernandez-Figueras MT; Marti M; Soler-Botija C; Roura S; Perea-Gil I; Prat-Vidal C; Llucia-Valldeperas A; Raya A; Bayes-Genis A, Neoinnervation and neovascularization of acellular pericardial-derived scaffolds in myocardial infarcts. Stem Cell Res Ther2015, 6, 108. [PubMed: 26205795]
118. Criswell TL; Corona BT; Wang Z; Zhou Y; Niu G; Xu Y; Christ GJ; Soker S, The role of endothelial cells in myofiber differentiation and the vascularization and innervation of bioengineered muscle tissue in vivo. Biomaterials2013, 34, 140–9. [PubMed: 23059002]
119. TV, H. U.SPatent No.4,552,707. Washington, DC: U.S. Patent and Trademark Office. 1985.
120. Wilson WR; Bower TC; Creager MA; Amin-Hanjani S; O'Gara PT; Lockhart PB; Darouiche RO; Ramlawi B; Derdeyn CP; Bolger AF; Levison ME; Taubert KA; Baltimore RS; Baddour LM; American Heart Association Committee on Rheumatic Fever, E.; Kawasaki Disease of the Council on Cardiovascular Disease in the, Y.; Council on, C.; Stroke N; Council on Cardiovascular, R.; Intervention; Council on Cardiovascular, S.; Anesthesia; Council on Peripheral Vascular, D.; Stroke C, Vascular graft infections, mycotic aneurysms, and endovascular infections: a scientific statement from the american heart association. Circulation2016, 134, e412–e460. [PubMed: 27737955]
121. Lorentzen JE; Nielsen OM; Arendrup H; Kimose HH; Bille S; Andersen J; Jensen CH; Jacobsen F; Roder OC, Vascular graft infection: an analysis of sixty-two graft infections in 2411 consecutively implanted synthetic vascular grafts. Surgery1985, 98, 81–6. [PubMed: 4012610]
122. Ozbolat IT, Bioprinting scale-up tissue and organ constructs for transplantation. Trends Biotechnol2015, 33, 395–400. [PubMed: 25978871]
123. Lee VK; Lanzi AM; Haygan N; Yoo SS; Vincent PA; Dai G, generation of multi-scale vascular network system within 3D hydrogel using 3D bio-printing technology. Cell Mol Bioeng2014, 7, 460–472. [PubMed: 25484989]
124. Li S; Xiong Z; Wang X; Yan Y; Liu H; Zhang R, Direct fabrication of a hybrid cell/hydrogel construct by a double-nozzle assembling technology. Journal of bioactive and compatible polymers2009, 24, 249–265.
125. Kesari P, Xu T, & Boland T, Layer-by-layer printing of cells and its application to tissue engineering. MRS Online Proceedings Library Archive 2004, 845.
126. Zhu W; Qu X; Zhu J; Ma X; Patel S; Liu J; Wang P; Lai CS; Gou M; Xu Y; Zhang K; Chen S, Direct 3D bioprinting of prevascularized tissue constructs with complex microarchitecture. Biomaterials2017, 124, 106–115. [PubMed: 28192772]
127. Tan EYS, & Yeong WY, Concentric bioprinting of alginate-based tubular constructs using multi-nozzle extrusion-based technique. . International Journal of Bioprinting 2015, 1(1).
128. Cui X; Boland T, Human microvasculature fabrication using thermal inkjet printing technology. Biomaterials2009, 30, 6221–7. [PubMed: 19695697]
129. Skardal A; Zhang J; McCoard L; Xu X; Oottamasathien S; Prestwich GD, Photocrosslinkable hyaluronan-gelatin hydrogels for two-step bioprinting. Tissue Eng Part A2010, 16, 2675–85. [PubMed: 20387987]

130. Xu C, Christensen K, Zhang Z, Huang Y, Fu J, & Markwald RR, Predictive compensation-enabled horizontal inkjet printing of alginate tubular constructs. . Manufacturing letters 2013, 1(1), 28–32.

131. Xu C; Chai W; Huang Y; Markwald RR, Scaffold-free inkjet printing of three-dimensional zigzag cellular tubes. Biotechnol Bioeng2012, 109, 3152–60. [PubMed: 22767299]

132. Christensen K; Xu C; Chai W; Zhang Z; Fu J; Huang Y, Freeform inkjet printing of cellular structures with bifurcations. Biotechnol Bioeng2015, 112, 1047–55. [PubMed: 25421556]

133. Hinton TJ; Jallerat Q; Palchesko RN; Park JH; Grodzicki MS; Shue HJ; Ramadan MH; Hudson AR; Feinberg AW, Three-dimensional printing of complex biological structures by freeform reversible embedding of suspended hydrogels. Sci Adv2015, 1, e1500758. [PubMed: 26601312]

134. Gao G; Park JY; Kim BS; Jang J; Cho DW, Coaxial cell printing of freestanding, perfusable, and functional in vitro vascular models for recapitulation of native vascular eEndothelium pathophysiology. Adv Healthc Mater2018, 7, e1801102. [PubMed: 30370670]

135. Zhang Y, Yu Y, & Ozbolat IT, Direct bioprinting of vessel-like tubular microfluidic channels. Journal of nanotechnology in engineering and medicine 2013, 4(2).

136. Dolati F; Yu Y; Zhang Y; De Jesus AM; Sander EA; Ozbolat IT, In vitro evaluation of carbon-nanotube-reinforced bioprintable vascular conduits. Nanotechnology2014, 25, 145101. [PubMed: 24632802]

137. Gao Q; He Y; Fu JZ; Liu A; Ma L, Coaxial nozzle-assisted 3D bioprinting with built-in microchannels for nutrients delivery. Biomaterials2015, 61, 203–15. [PubMed: 26004235]

138. Gao G, Lee JH, Jang J, Lee DH, Kong JS, Kim BS, … & Cho DW, Tissue engineered bio-blood-vessels constructed using a tissue-specific bioink and 3D coaxial cell printing technique: a novel therapy for ischemic disease. Advanced functional materials 2017, 27(33), 1700798.

139. Miller JS; Stevens KR; Yang MT; Baker BM; Nguyen DH; Cohen DM; Toro E; Chen AA; Galie PA; Yu X; Chaturvedi R; Bhatia SN; Chen CS, Rapid casting of patterned vascular networks for perfusable engineered three-dimensional tissues. Nat Mater2012, 11, 768–74. [PubMed: 22751181]

140. Grigoryan B; Paulsen SJ; Corbett DC; Sazer DW; Fortin CL; Zaita AJ; Greenfield PT; Calafat NJ; Gounley JP; Ta AH; Johansson F; Randles A; Rosenkrantz JE; Louis-Rosenberg JD; Galie PA; Stevens KR; Miller JS, Multivascular networks and functional intravascular topologies within biocompatible hydrogels. Science2019, 364, 458–464. [PubMed: 31048486]

141. Wust S; Muller R; Hofmann S, 3D Bioprinting of complex channels-Effects of material, orientation, geometry, and cell embedding. J Biomed Mater Res A2015, 103, 2558–70. [PubMed: 25524726]

142. Bertassoni LE; Cecconi M; Manoharan V; Nikkhah M; Hjortnaes J; Cristino AL; Barabaschi G; Demarchi D; Dokmeci MR; Yang Y; Khademhosseini A, Hydrogel bioprinted microchannel networks for vascularization of tissue engineering constructs. Lab Chip2014, 14, 2202–11. [PubMed: 24860845]

143. Lee VK, Kim DY, Ngo H, Lee Y, Seo L, Yoo SS, … & Dai G, Creating perfused functional vascular channels using 3D bio-printing technology. Biomaterials 2014, 35(28), 8092–8102. [PubMed: 24965886]

144. Skylar-Scott MA; Uzel SGM; Nam LL; Ahrens JH; Truby RL; Damaraju S; Lewis JA, Biomanufacturing of organ-specific tissues with high cellular density and embedded vascular channels. Sci Adv2019, 5, eaaw2459. [PubMed: 31523707]

145. Higgins CA; Chen JC; Cerise JE; Jahoda CA; Christiano AM, Microenvironmental reprogramming by three-dimensional culture enables dermal papilla cells to induce de novo human hair-follicle growth. Proc Natl Acad Sci U S A2013, 110, 19679–88. [PubMed: 24145441]

146. Abaci HE; Coffman A; Doucet Y; Chen J; Jackow J; Wang E; Guo Z; Shin JU; Jahoda CA; Christiano AM, Tissue engineering of human hair follicles using a biomimetic developmental approach. Nat Commun2018, 9, 5301. [PubMed: 30546011]

147. Simon-Yarza T; Bataille I; Letourneur D, Cardiovascular bio-engineering: current state of the art. J Cardiovasc Transl Res2017, 10, 180–193. [PubMed: 28265882]

148. Mathur A; Ma Z; Loskill P; Jeeawoody S; Healy KE, In vitro cardiac tissue models: Current status and future prospects. Adv Drug Deliv Rev2016, 96, 203–13. [PubMed: 26428618]

149. Go AS; Mozaffarian D; Roger VL; Benjamin EJ; Berry JD; Blaha MJ; Dai S; Ford ES; Fox CS; Franco S; Fullerton HJ; Gillespie C; Hailpern SM; Heit JA; Howard VJ; Huffman MD; Judd SE; Kissela BM; Kittner SJ; Lackland DT; Lichtman JH; Lisabeth LD; Mackey RH; Magid DJ; Marcus GM; Marelli A; Matchar DB; McGuire DK; Mohler ER 3rd; Moy CS; Mussolino ME; Neumar RW; Nichol G; Pandey DK; Paynter NP; Reeves MJ; Sorlie PD; Stein J; Towfighi A; Turan TN; Virani SS; Wong ND; Woo D; Turner MB; American Heart Association Statistics, C.; Stroke Statistics, S., Executive summary: heart disease and stroke statistics--2014 update: a report from the American Heart Association. Circulation2014, 129, 399–410. [PubMed: 24446411]

150. Parmacek MS; Epstein JA, Cardiomyocyte renewal. N Engl J Med2009, 361, 86–8. [PubMed: 19571289]

151. Oxenham H; Bloomfield P; Wheatley DJ; Lee RJ; Cunningham J; Prescott RJ; Miller HC, Twenty year comparison of a Bjork-Shiley mechanical heart valve with porcine bioprostheses. Heart2003, 89, 715–21. [PubMed: 12807838]

152. Slaughter MS; Rogers JG; Milano CA; Russell SD; Conte JV; Feldman D; Sun B; Tatooles AJ; Delgado RM 3rd; Long JW; Wozniak TC; Ghumman W; Farrar DJ; Frazier OH; HeartMate, I. I. I., Advanced heart failure treated with continuous-flow left ventricular assist device. N Engl J Med2009, 361, 2241–51. [PubMed: 19920051]

153. Nishimura RA; Otto CM; Bonow RO; Carabello BA; Erwin JP 3rd; Fleisher LA; Jneid H; Mack MJ; McLeod CJ; O'Gara PT; Rigolin VH; Sundt TM 3rd; Thompson A, 2017 AHA/ACC focused update of the 2014 AHA/ACC guideline for the management of patients with valvular heart disease: a report of the American College of Cardiology/American Heart Association task force on clinical practice guidelines. J Am Coll Cardiol2017, 70, 252–289. [PubMed: 28315732]

154. Christie GW, Anatomy of aortic heart valve leaflets: the influence of glutaraldehyde fixation on function. Eur J Cardiothorac Surg1992, 6Suppl 1, S25–32; discussion S33. [PubMed: 1389275]

155. Vesely I; Lozon A, Natural preload of aortic valve leaflet components during glutaraldehyde fixation: effects on tissue mechanics. J Biomech1993, 26, 121–31. [PubMed: 8429055]

156. Lee DJ; Steen J; Jordan JE; Kincaid EH; Kon ND; Atala A; Berry J; Yoo JJ, Endothelialization of heart valve matrix using a computer-assisted pulsatile bioreactor. Tissue Eng Part A2009, 15, 807–14. [PubMed: 19320610]

157. Jordan JE; Williams JK; Lee SJ; Raghavan D; Atala A; Yoo JJ, Bioengineered self-seeding heart valves. J Thorac Cardiovasc Surg2012, 143, 201–8. [PubMed: 22047685]

158. Hockaday LA; Kang KH; Colangelo NW; Cheung PY; Duan B; Malone E; Wu J; Girardi LN; Bonassar LJ; Lipson H; Chu CC; Butcher JT, Rapid 3D printing of anatomically accurate and mechanically heterogeneous aortic valve hydrogel scaffolds. Biofabrication2012, 4, 035005. [PubMed: 22914604]

159. Sacks MS YA, Heart valve function: a biomechanical perspectivePhilos Trans R Soc Lond B Biol Sci. 2007, 362(1484), 1369–1391. [PubMed: 17588873]

160. Park JH; Jang J; Lee JS; Cho DW, Three-dimensional printing of tissue/organ analogues containing living cells. Ann Biomed Eng2017, 45, 180–194. [PubMed: 27080374]

161. Visconti RP; Kasyanov V; Gentile C; Zhang J; Markwald RR; Mironov V, Towards organ printing: engineering an intra-organ branched vascular tree. Expert Opin Biol Ther2010, 10, 409–20. [PubMed: 20132061]

162. Cui H; Nowicki M; Fisher JP; Zhang LG, 3D bioprinting for organ regeneration. Adv Healthc Mater2017, 6.

163. Mosadegh B; Xiong G; Dunham S; Min JK, Current progress in 3D printing for cardiovascular tissue engineering. Biomed Mater2015, 10, 034002. [PubMed: 25775166]

164. Cui H; Miao S; Esworthy T; Zhou X; Lee SJ; Liu C; Yu ZX; Fisher JP; Mohiuddin M; Zhang LG, 3D bioprinting for cardiovascular regeneration and pharmacology. Adv Drug Deliv Rev2018, 132, 252–269. [PubMed: 30053441]

165. Wang Z; Lee SJ; Cheng HJ; Yoo JJ; Atala A, 3D bioprinted functional and contractile cardiac tissue constructs. Acta Biomater2018, 70, 48–56. [PubMed: 29452273]

166. Noor N; Shapira A; Edri R; Gal I; Wertheim L; Dvir T, 3D Printing of Personalized Thick and Perfusable Cardiac Patches and Hearts. Adv Sci (Weinh)2019, 6, 1900344. [PubMed: 31179230]

167. Lee A; Hudson AR; Shiwarski DJ; Tashman JW; Hinton TJ; Yerneni S; Bliley JM; Campbell PG; Feinberg AW, 3D bioprinting of collagen to rebuild components of the human heart. Science2019, 365, 482–487. [PubMed: 31371612]

168. Bhatia SN; Underhill GH; Zaret KS; Fox IJ, Cell and tissue engineering for liver disease. Sci Transl Med2014, 6, 245sr2. [PubMed: 25031271]

169. Taub R, Liver regeneration: from myth to mechanism. Nat Rev Mol Cell Biol2004, 5, 836–47. [PubMed: 15459664]

170. Michalopoulos GK; DeFrances MC, Liver regeneration. Science1997, 276, 60–6. [PubMed: 9082986]

171. Matai I; Kaur G; Seyedsalehi A; McClinton A; Laurencin CT, Progress in 3D bioprinting technology for tissue/organ regenerative engineering. Biomaterials2020, 226, 119536. [PubMed: 31648135]

172. Kholodenko IV; Yarygin KN, Cellular mechanisms of liver regeneration and cell-based therapies of liver diseases. Biomed Res Int2017, 2017, 8910821. [PubMed: 28210629]

173. Ma X, Qu X, Zhu W, et al., Deterministically patterned biomimetic human iPSC-derived hepatic model via rapid 3D bioprinting. Proc Natl Acad Sci U S A2016, 113, 2206. [PubMed: 26858399]

174. Stevens KR, S. M, Ramanan V, et al., In situ expansion of engineered human liver tissue in a mouse model of chronic liver disease. . Sci Transl Med. 2017, 9(399), eaah5505. [PubMed: 28724577]

175. Kim SS; Utsunomiya H; Koski JA; Wu BM; Cima MJ; Sohn J; Mukai K; Griffith LG; Vacanti JP, Survival and function of hepatocytes on a novel three-dimensional synthetic biodegradable polymer scaffold with an intrinsic network of channels. Ann Surg1998, 228, 8–13. [PubMed: 9671060]

176. Kim SS; Kaihara S; Benvenuto MS; Kim BS; Mooney DJ; Vacanti JP, Small intestinal submucosa as a small-caliber venous graft: a novel model for hepatocyte transplantation on synthetic biodegradable polymer scaffolds with direct access to the portal venous system. J Pediatr Surg1999, 34, 124–8. [PubMed: 10022156]

177. Underhill GH; Chen AA; Albrecht DR; Bhatia SN, Assessment of hepatocellular function within PEG hydrogels. Biomaterials2007, 28, 256–70. [PubMed: 16979755]

178. Liu Tsang V; Chen AA; Cho LM; Jadin KD; Sah RL; DeLong S; West JL; Bhatia SN, Fabrication of 3D hepatic tissues by additive photopatterning of cellular hydrogels. FASEB J2007, 21, 790–801. [PubMed: 17197384]

179. Chen AA; Thomas DK; Ong LL; Schwartz RE; Golub TR; Bhatia SN, Humanized mice with ectopic artificial liver tissues. Proc Natl Acad Sci U S A2011, 108, 11842–7. [PubMed: 21746904]

180. Stevens KR; Ungrin MD; Schwartz RE; Ng S; Carvalho B; Christine KS; Chaturvedi RR; Li CY; Zandstra PW; Chen CS; Bhatia SN, InVERT molding for scalable control of tissue microarchitecture. Nat Commun2013, 4, 1847. [PubMed: 23673632]

181. Huh D; Matthews BD; Mammoto A; Montoya-Zavala M; Hsin HY; Ingber DE, Reconstituting organ-level lung functions on a chip. Science2010, 328, 1662–8. [PubMed: 20576885]

182. Ott HC; Clippinger B; Conrad C; Schuetz C; Pomerantseva I; Ikonomou L; Kotton D; Vacanti JP, Regeneration and orthotopic transplantation of a bioartificial lung. Nat Med2010, 16, 927–33. [PubMed: 20628374]

183. Petersen TH; Calle EA; Zhao L; Lee EJ; Gui L; Raredon MB; Gavrilov K; Yi T; Zhuang ZW; Breuer C; Herzog E; Niklason LE, Tissue-engineered lungs for in vivo implantation. Science2010, 329, 538–41. [PubMed: 20576850]

184. Hoganson DM; Bassett EK; Vacanti JP, Lung tissue engineering. Front Biosci (Landmark Ed)2014, 19, 1227–39. [PubMed: 24896347]

185. Lee JK; Kung HH; Mockros LF, Microchannel technologies for artificial lungs: (1) theory. ASAIO J2008, 54, 372–82. [PubMed: 18645354]

186. Kung MC; Lee JK; Kung HH; Mockros LF, Microchannel technologies for artificial lungs: (2) screen-filled wide rectangular channels. ASAIO J2008, 54, 383–9. [PubMed: 18645355]

187. Burgess KA; Hu HH; Wagner WR; Federspiel WJ, Towards microfabricated biohybrid artificial lung modules for chronic respiratory support. Biomed Microdevices2009, 11, 117–27. [PubMed: 18696229]

188. Hoganson DM; Anderson JL; Weinberg EF; Swart E; Orrick BK; Borenstein JT; Vacanti JP, Branched vascular network architecture: a new approach to lung assist device technology. J Thorac Cardiovasc Surg2010, 140, 990–5. [PubMed: 20591445]

189. Pagliuca FW; Millman JR; Gurtler M; Segel M; Van Dervort A; Ryu JH; Peterson QP; Greiner D; Melton DA, Generation of functional human pancreatic beta cells in vitro. Cell2014, 159, 428–39. [PubMed: 25303535]

190. Price AP; England KA; Matson AM; Blazar BR; Panoskaltsis-Mortari A, Development of a decellularized lung bioreactor system for bioengineering the lung: the matrix reloaded. Tissue Eng Part A2010, 16, 2581–91. [PubMed: 20297903]

191. American Diabetes A, Diagnosis and classification of diabetes mellitus. Diabetes Care2014, 37Suppl 1, S81–90. [PubMed: 24357215]

192. Kim J; Kang K; Drogemuller CJ; Wallace GG; Coates PT, Bioprinting an artificial pancreas for type 1 diabetes. Curr Diab Rep2019, 19, 53. [PubMed: 31273530]

193. Forouhi NG, & Wareham NJ, Epidemiology of diabetes. Medicine, 38(11), 602–606. 2010.

194. Pathiraja V; Kuehlich JP; Campbell PD; Krishnamurthy B; Loudovaris T; Coates PT; Brodnicki TC; O'Connell PJ; Kedzierska K; Rodda C; Bergman P; Hill E; Purcell AW; Dudek NL; Thomas HE; Kay TW; Mannering SI, Proinsulin-specific HLA-DQ8, and HLA-DQ8-transdimer-restricted CD4+ T cells infiltrate islets in type 1 diabetes. Diabetes2015, 64, 172–82. [PubMed: 25157096]

195. Troppmann C, Complications after pancreas transplantation. Curr Opin Organ Transplant2010, 15, 112–8. [PubMed: 20009931]

196. Vardanyan M; Parkin E; Gruessner C; Rodriguez Rilo HL, Pancreas vs. islet transplantation: a call on the future. Curr Opin Organ Transplant2010, 15, 124–30. [PubMed: 20009930]

197. Robertson RP, Islet transplantation as a treatment for diabetes - a work in progress. N Engl J Med2004, 350, 694–705. [PubMed: 14960745]

198. Carlsson PO; Palm F; Andersson A; Liss P, Markedly decreased oxygen tension in transplanted rat pancreatic islets irrespective of the implantation site. Diabetes2001, 50, 489–95. [PubMed: 11246867]

199. De Vos P, Hillebrands JL, De Haan BJ, Strubbe JH, & Van Schilfgaarde R, Efficacy of a prevascularized expanded polytetrafluoroethylene solid support system as a transplantation site for pancreatic islets1. Transplantation 1997, 63(6), 824–830. [PubMed: 9089221]

200. Dufour JM; Rajotte RV; Zimmerman M; Rezania A; Kin T; Dixon DE; Korbutt GS, Development of an ectopic site for islet transplantation, using biodegradable scaffolds. Tissue Eng2005, 11, 1323–31. [PubMed: 16259588]

201. Wang RN; Rosenberg L, Maintenance of beta-cell function and survival following islet isolation requires re-establishment of the islet-matrix relationship. J Endocrinol1999, 163, 181–90. [PubMed: 10556766]

202. Blomeier H; Zhang X; Rives C; Brissova M; Hughes E; Baker M; Powers AC; Kaufman DB; Shea LD; Lowe WL Jr., Polymer scaffolds as synthetic microenvironments for extrahepatic islet transplantation. Transplantation2006, 82, 452–9. [PubMed: 16926587]

203. Berman DM; O'Neil JJ; Coffey LC; Chaffanjon PC; Kenyon NM; Ruiz P Jr.; Pileggi A; Ricordi C; Kenyon NS, Long-term survival of nonhuman primate islets implanted in an omental pouch on a biodegradable scaffold. Am J Transplant2009, 9, 91–104. [PubMed: 19133931]

204. Carroll Robert P.Barry Simon C.Wallace Gordon G.Coates Patrick Toby, K. JH. CMG. NP. GBS. SOY. ZL. XA. AUK. FDP. DD. CJ, Encapsulation of human natural and induced regulatory T-cells in IL-2 and CCL1 supplemented alginate-GelMA hydrogel for 3D bioprinting. Advanced Function Materials2020, Volume30, Issue15.

205. Gibly RF; Zhang X; Graham ML; Hering BJ; Kaufman DB; Lowe WL Jr.; Shea LD, Extrahepatic islet transplantation with microporous polymer scaffolds in syngeneic mouse and allogeneic porcine models. Biomaterials2011, 32, 9677–84. [PubMed: 21959005]

206. Kasputis T; Clough D; Noto F; Rychel K; Dye B; Shea LD, microporous polymer scaffolds for the transplantation of embryonic stem cell derived pancreatic progenitors to a clinically translatable site for the treatment of type I diabetes. ACS Biomater Sci Eng2018, 4, 1770–1778. [PubMed: 30345348]

207. Youngblood RL; Sampson JP; Lebioda KR; Shea LD, Microporous scaffolds support assembly and differentiation of pancreatic progenitors into beta-cell clusters. Acta Biomater2019, 96, 111–122. [PubMed: 31247380]

208. Ma M; Chiu A; Sahay G; Doloff JC; Dholakia N; Thakrar R; Cohen J; Vegas A; Chen D; Bratlie KM; Dang T; York RL; Hollister-Lock J; Weir GC; Anderson DG, Core-shell hydrogel microcapsules for improved islets encapsulation. Adv Healthc Mater2013, 2, 667–72. [PubMed: 23208618]

209. Sackett SD; Tremmel DM; Ma F; Feeney AK; Maguire RM; Brown ME; Zhou Y; Li X; O'Brien C; Li L; Burlingham WJ; Odorico JS, Extracellular matrix scaffold and hydrogel derived from decellularized and delipidized human pancreas. Sci Rep2018, 8, 10452. [PubMed: 29993013]

210. Penko D; Mohanasundaram D; Sen S; Drogemuller C; Mee C; Bonder CS; Coates PT; Jessup CF, Incorporation of endothelial progenitor cells into mosaic pseudoislets. Islets2011, 3, 73–9. [PubMed: 21478677]

211. Akkouch A; Yu Y; Ozbolat IT, Microfabrication of scaffold-free tissue strands for three-dimensional tissue engineering. Biofabrication2015, 7, 031002. [PubMed: 26373778]

212. Liu X; Carter SD; Renes MJ; Kim J; Rojas-Canales DM; Penko D; Angus C; Beirne S; Drogemuller CJ; Yue Z; Coates PT; Wallace GG, Development of a coaxial 3D printing platform for biofabrication of implantable islet-containing constructs. Adv Healthc Mater2019, 8, e1801181. [PubMed: 30633852]

213. Kim J; Shim IK; Hwang DG; Lee YN; Kim M; Kim H; Kim SW; Lee S; Kim SC; Cho DW; Jang J, 3D cell printing of islet-laden pancreatic tissue-derived extracellular matrix bioink constructs for enhancing pancreatic functions. J Mater Chem B2019, 7, 1773–1781. [PubMed: 32254919]

214. Vegas AJ; Veiseh O; Gurtler M; Millman JR; Pagliuca FW; Bader AR; Doloff JC; Li J; Chen M; Olejnik K; Tam HH; Jhunjhunwala S; Langan E; Aresta-Dasilva S; Gandham S; McGarrigle JJ; Bochenek MA; Hollister-Lock J; Oberholzer J; Greiner DL; Weir GC; Melton DA; Langer R; Anderson DG, Long-term glycemic control using polymer-encapsulated human stem cell-derived beta cells in immune-competent mice. Nat Med2016, 22, 306–11. [PubMed: 26808346]

215. Millman JR; Xie C; Van Dervort A; Gurtler M; Pagliuca FW; Melton DA, Generation of stem cell-derived beta-cells from patients with type 1 diabetes. Nat Commun2016, 7, 11463. [PubMed: 27163171]

216. Tangri N; Stevens LA; Griffith J; Tighiouart H; Djurdjev O; Naimark D; Levin A; Levey AS, A predictive model for progression of chronic kidney disease to kidney failure. JAMA2011, 305, 1553–9. [PubMed: 21482743]

217. Montserrat N; Garreta E; Izpisua Belmonte JC, Regenerative strategies for kidney engineering. FEBS J2016, 283, 3303–24. [PubMed: 26938311]

218. Begum S, Engineering renal epithelial cells: programming and directed differentiation towards glomerular podocyte's progenitor and mature podocyte. Am J Transl Res2019, 11, 1102–1115. [PubMed: 30899410]

219. Oxburgh L; Carroll TJ; Cleaver O; Gossett DR; Hoshizaki DK; Hubbell JA; Humphreys BD; Jain S; Jensen J; Kaplan DL; Kesselman C; Ketchum CJ; Little MH; McMahon AP; Shankland SJ; Spence JR; Valerius MT; Wertheim JA; Wessely O; Zheng Y; Drummond IA, (Re)building a kidney. J Am Soc Nephrol2017, 28, 1370–1378. [PubMed: 28096308]

220. Takasato M; Er PX; Chiu HS; Maier B; Baillie GJ; Ferguson C; Parton RG; Wolvetang EJ; Roost MS; Chuva de Sousa Lopes SM; Little MH, Kidney organoids from human iPS cells contain multiple lineages and model human nephrogenesis. Nature2015, 526, 564–8. [PubMed: 26444236]

221. Atala A, Regenerative medicine strategies. J Pediatr Surg2012, 47, 17–28. [PubMed: 22244387]

222. Yoo JI, Ashkar S, & Atala A, Creation of functional kidney structures with excretion of urine-like fluid in vivo. . British Journal of Urology 1997, 80(SUPPL. 2).

223. Song B; Smink AM; Jones CV; Callaghan JM; Firth SD; Bernard CA; Laslett AL; Kerr PG; Ricardo SD, The directed differentiation of human iPS cells into kidney podocytes. PLoS One2012, 7, e46453. [PubMed: 23029522]

224. Rauch C; Feifel E; Kern G; Murphy C; Meier F; Parson W; Beilmann M; Jennings P; Gstraunthaler G; Wilmes A, Differentiation of human iPSCs into functional podocytes. PLoS One2018, 13, e0203869. [PubMed: 30222766]

225. Qian T; Hernday SE; Bao X; Olson WR; Panzer SE; Shusta EV; Palecek SP, Directed differentiation of human pluripotent stem cells to podocytes under defined conditions. Sci Rep2019, 9, 2765. [PubMed: 30808965]

226. Mironov V; Visconti RP; Kasyanov V; Forgacs G; Drake CJ; Markwald RR, Organ printing: tissue spheroids as building blocks. Biomaterials2009, 30, 2164–74. [PubMed: 19176247]

227. Musah S; Mammoto A; Ferrante TC; Jeanty SSF; Hirano-Kobayashi M; Mammoto T; Roberts K; Chung S; Novak R; Ingram M; Fatanat-Didar T; Koshy S; Weaver JC; Church GM; Ingber DE, Mature induced-pluripotent-stem-cell-derived human podocytes reconstitute kidney glomerular-capillary-wall function on a chip. Nat Biomed Eng2017, 1.

228. Musah S; Dimitrakakis N; Camacho DM; Church GM; Ingber DE, Directed differentiation of human induced pluripotent stem cells into mature kidney podocytes and establishment of a Glomerulus Chip. Nat Protoc2018, 13, 1662–1685. [PubMed: 29995874]

229. Taguchi A; Nishinakamura R, Higher-order kidney organogenesis from pluripotent stem cells. Cell Stem Cell2017, 21, 730–746 e6. [PubMed: 29129523]

230. Hale LJ; Howden SE; Phipson B; Lonsdale A; Er PX; Ghobrial I; Hosawi S; Wilson S; Lawlor KT; Khan S; Oshlack A; Quinlan C; Lennon R; Little MH, 3D organoid-derived human glomeruli for personalised podocyte disease modelling and drug screening. Nat Commun2018, 9, 5167. [PubMed: 30514835]

231. Little MH; Combes AN, Kidney organoids: accurate models or fortunate accidents. Genes Dev2019, 33, 1319–1345. [PubMed: 31575677]

232. Narayanan K; Schumacher KM; Tasnim F; Kandasamy K; Schumacher A; Ni M; Gao S; Gopalan B; Zink D; Ying JY, Human embryonic stem cells differentiate into functional renal proximal tubular-like cells. Kidney Int2013, 83, 593–603. [PubMed: 23389418]

233. King SM; Higgins JW; Nino CR; Smith TR; Paffenroth EH; Fairbairn CE; Docuyanan A; Shah VD; Chen AE; Presnell SC; Nguyen DG, 3D proximal tubule tissues recapitulate key aspects of renal physiology to enable nephrotoxicity testing. Front Physiol2017, 8, 123. [PubMed: 28337147]

234. Lin NYC; Homan KA; Robinson SS; Kolesky DB; Duarte N; Moisan A; Lewis JA, Renal reabsorption in 3D vascularized proximal tubule models. Proc Natl Acad Sci U S A2019, 116, 5399–5404. [PubMed: 30833403]

235. Singh NK; Han W; Nam SA; Kim JW; Kim JY; Kim YK; Cho DW, Three-dimensional cell-printing of advanced renal tubular tissue analogue. Biomaterials2020, 232, 119734. [PubMed: 31918226]

236. Demopoulos HB; Flamm ES; Pietronigro DD; Seligman ML, The free radical pathology and the microcirculation in the major central nervous system disorders. Acta Physiol Scand Suppl1980, 492, 91–119. [PubMed: 6939309]

237. Bjorklund A; Lindvall O, Cell replacement therapies for central nervous system disorders. Nat Neurosci2000, 3, 537–44. [PubMed: 10816308]

238. Zhuang P; Sun AX; An J; Chua CK; Chew SY, 3D neural tissue models: From spheroids to bioprinting. Biomaterials2018, 154, 113–133. [PubMed: 29120815]

239. Urich E; Patsch C; Aigner S; Graf M; Iacone R; Freskgard PO, Multicellular self-assembled spheroidal model of the blood brain barrier. Sci Rep2013, 3, 1500. [PubMed: 23511305]

240. Kato-Negishi M; Tsuda Y; Onoe H; Takeuchi S, A neurospheroid network-stamping method for neural transplantation to the brain. Biomaterials2010, 31, 8939–45. [PubMed: 20850180]

241. Kato-Negishi M; Morimoto Y; Onoe H; Takeuchi S, Millimeter-sized neural building blocks for 3D heterogeneous neural network assembly. Adv Healthc Mater2013, 2, 1564–70. [PubMed: 23828857]

242. Odawara A, Gotoh M, & Suzuki I, A three-dimensional neuronal culture technique that controls the direction of neurite elongation and the position of soma to mimic the layered structure of the brain. . RSC advances 2013, 3(45), 23620–23630.

243. Jeong GS; Chang JY; Park JS; Lee SA; Park D; Woo J; An H; Lee CJ; Lee SH, Networked neural spheroid by neuro-bundle mimicking nervous system created by topology effect. Mol Brain2015, 8, 17. [PubMed: 25888468]

244. Jo J; Xiao Y; Sun AX; Cukuroglu E; Tran HD; Goke J; Tan ZY; Saw TY; Tan CP; Lokman H; Lee Y; Kim D; Ko HS; Kim SO; Park JH; Cho NJ; Hyde TM; Kleinman JE; Shin JH; Weinberger DR; Tan EK; Je HS; Ng HH, Midbrain-like organoids from human pluripotent stem cells contain functional dopaminergic and neuromelanin-producing neurons. Cell Stem Cell2016, 19, 248–257. [PubMed: 27476966]

245. Park J; Lee BK; Jeong GS; Hyun JK; Lee CJ; Lee SH, Three-dimensional brain-on-a-chip with an interstitial level of flow and its application as an in vitro model of Alzheimer's disease. Lab Chip2015, 15, 141–50. [PubMed: 25317977]

246. Bang S; Na S; Jang JM; Kim J; Jeon NL, Engineering-aligned 3D neural circuit in microfluidic device. Adv Healthc Mater2016, 5, 159–66. [PubMed: 26332914]

247. Nzou G; Wicks RT; Wicks EE; Seale SA; Sane CH; Chen A; Murphy SV; Jackson JD; Atala AJ, Human cortex spheroid with a functional blood brain barrier for high-throughput neurotoxicity screening and disease modeling. Sci Rep2018, 8, 7413. [PubMed: 29743549]

248. Xu T; Gregory CA; Molnar P; Cui X; Jalota S; Bhaduri SB; Boland T, Viability and electrophysiology of neural cell structures generated by the inkjet printing method. Biomaterials2006, 27, 3580–8. [PubMed: 16516288]

249. Lee W; Pinckney J; Lee V; Lee JH; Fischer K; Polio S; Park JK; Yoo SS, Three-dimensional bioprinting of rat embryonic neural cells. Neuroreport2009, 20, 798–803. [PubMed: 19369905]

250. Lorber B; Hsiao WK; Hutchings IM; Martin KR, Adult rat retinal ganglion cells and glia can be printed by piezoelectric inkjet printing. Biofabrication2014, 6, 015001. [PubMed: 24345926]

251. Tse C; Whiteley R; Yu T; Stringer J; MacNeil S; Haycock JW; Smith PJ, Inkjet printing Schwann cells and neuronal analogue NG108–15 cells. Biofabrication2016, 8, 015017. [PubMed: 26930268]

252. Tang-Schomer MD; White JD; Tien LW; Schmitt LI; Valentin TM; Graziano DJ; Hopkins AM; Omenetto FG; Haydon PG; Kaplan DL, Bioengineered functional brain-like cortical tissue. Proc Natl Acad Sci U S A2014, 111, 13811–6. [PubMed: 25114234]

253. Hsieh FY; Lin HH; Hsu SH, 3D bioprinting of neural stem cell-laden thermoresponsive biodegradable polyurethane hydrogel and potential in central nervous system repair. Biomaterials2015, 71, 48–57. [PubMed: 26318816]

254. Gu Q; Tomaskovic-Crook E; Lozano R; Chen Y; Kapsa RM; Zhou Q; Wallace GG; Crook JM, Functional 3D neural mini-tissues from printed gel-based bioink and human neural stem cells. Adv Healthc Mater2016, 5, 1429–38. [PubMed: 27028356]

255. Mironov V; Reis N; Derby B, Review: bioprinting: a beginning. Tissue Eng2006, 12, 631–4. [PubMed: 16674278]

256. Ozbolat IT; Yu Y, Bioprinting toward organ fabrication: challenges and future trends. IEEE Trans Biomed Eng2013, 60, 691–9. [PubMed: 23372076]

257. Ravi P, Shiakolas PS, Welch T, Saini T, Guleserian K, & Batra AK, On the capabilities of a multi-modality 3D bioprinter for customized biomedical devices. . American Society of Mechanical Engineers Digital Collection 2015, ASME 2015 International Mechanical Engineering Congress and Exposition.

258. Ravi P, Shiakolas PS, Oberg JC, Faizee S, & Batra AK, On the development of a modular 3D bioprinter for research in biomedical device fabrication. American Society of Mechanical Engineers Digital Collection 2015, International Mechanical Engineering Congress and Exposition.

259. Kim BS; Lee JS; Gao G; Cho DW, Direct 3D cell-printing of human skin with functional transwell system. Biofabrication2017, 9, 025034. [PubMed: 28586316]

260. Gao T; Gillispie GJ; Copus JS; Pr AK; Seol YJ; Atala A; Yoo JJ; Lee SJ, Optimization of gelatin-alginate composite bioink printability using rheological parameters: a systematic approach. Biofabrication2018, 10, 034106. [PubMed: 29923501]

261. Huang C-T; Shrestha LK; Ariga K; Hsu S. h., A graphene–polyurethane composite hydrogel as a potential bioink for 3D bioprinting and differentiation of neural stem cells. Journal of Materials Chemistry B2017, 5, 8854–8864. [PubMed: 32264279]

262. Kim W; Kim G, Collagen/bioceramic-based composite bioink to fabricate a porous 3D hASCs-laden structure for bone tissue regeneration. Biofabrication2019, 12, 015007. [PubMed: 31509811]

263. Dasgupta Q; Black LD 3rd, A FRESH SLATE for 3D bioprinting. Science2019, 365, 446–447. [PubMed: 31371600]

264. Miri AK; Nieto D; Iglesias L; Goodarzi Hosseinabadi H; Maharjan S; Ruiz-Esparza GU; Khoshakhlagh P; Manbachi A; Dokmeci MR; Chen S; Shin SR; Zhang YS; Khademhosseini A, Microfluidics-Enabled Multimaterial Maskless Stereolithographic Bioprinting. Adv Mater2018, 30, e1800242. [PubMed: 29737048]

265. Skylar-Scott MA; Mueller J; Visser CW; Lewis JA, Voxelated soft matter via multimaterial multinozzle 3D printing. Nature2019, 575, 330–335. [PubMed: 31723289]

266. Murphy SV; De Coppi P; Atala A, Opportunities and challenges of translational 3D bioprinting. Nat Biomed Eng2020, 4, 370–380. [PubMed: 31695178]

267. Kengla C, Renteria E, Wivell C, Atala A, Yoo JJ, & Lee SJ, Clinically relevant bioprinting workflow and imaging process for tissue construct design and validation. 3D Printing and Additive Manufacturing 2017, 4(4), 239–247.

268. Tibbits S, Design to Self-Assembly. Architectural Design2012, 82(2), 68–73.

269. Bonamici SH, R.34 – 21st century cures act. Senate Report. 114–146 (United States Congress). 2016.

270. FDA, Technical considerations for additive mManufactured medical devices - Guidance for Industry and Food and Drug Administration Staff. 2017.

271. Hunsberger JG, Goel S, Allickson J, & Atala A, Five critical areas that combat high costs and prolonged development times for regenerative medicine manufacturing. Current Stem Cell Reports 2017, 3(2), 77–82.

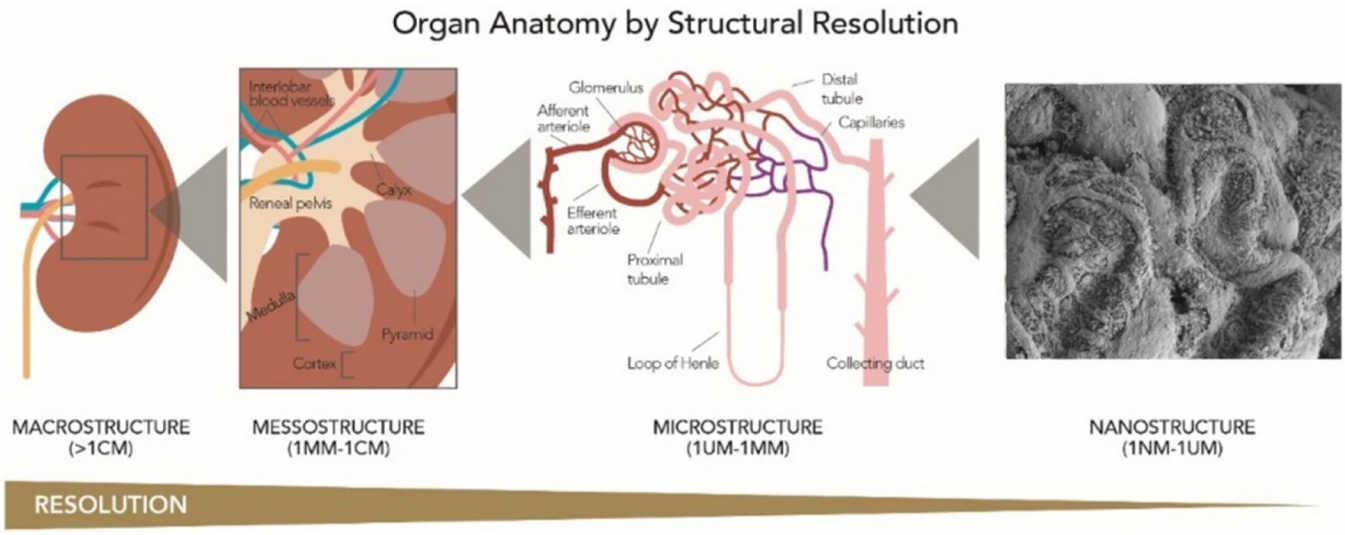

Figure 1. Organ Anatomy by Structural Resolution.

Organ complexity can be arranged into 4 primary structural resolutions, macrostructure, mesostructure, microstructure, and nanostructure. As an example, the kidney macrostructurally (resolution >1cm), is an organ with three major tubular structures connecting to the body's vascular supply and renal network. Mesostructural elements (1mm-1cm) help transport key products to and from the functional kidney units. On the microstructural level (1μm-1mm) are a network of complex structures that make up the kidney's functional unit: the nephron made up of the proximal and distal convoluted tubules, the loop of Henle, and the collecting duct. Finally, the kidney nanostructure (1nm -1μm), can be characterized, with its unique extracellular matrix (ECM) components, diffusion channels, and enzymes (the SEM image is reprinted under creative commons license from reference[15]. Copyright 2018, Springer Nature).

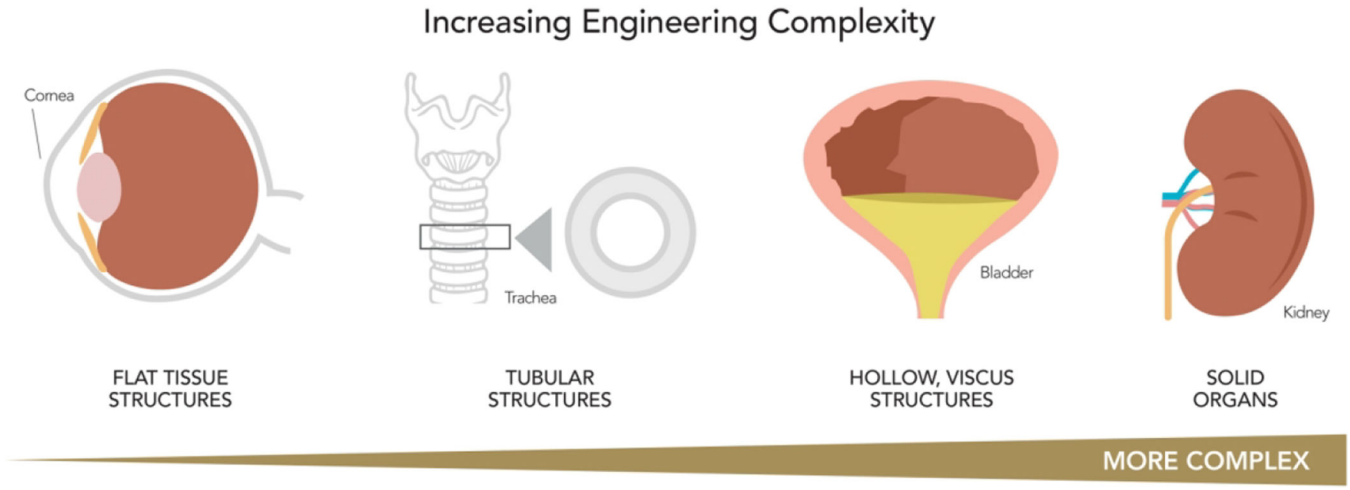

Figure 2. Organ Anatomy by Structural Complexity.

There are four general levels of tissues and organ macrostructural complexity: flat tissue structures, such as the skin or cornea; tubular structures, such as blood vessels; hollow structures, such as the bladder; and solid organs, such as the kidney. Tissue engineering complexity generally increases along this continuum as increased metabolic functions and structural requirements are needed for targeted for repair of the tissue or organ (adapted with permission from ref[7]. Copyright 2012 Science Translational Medicine).

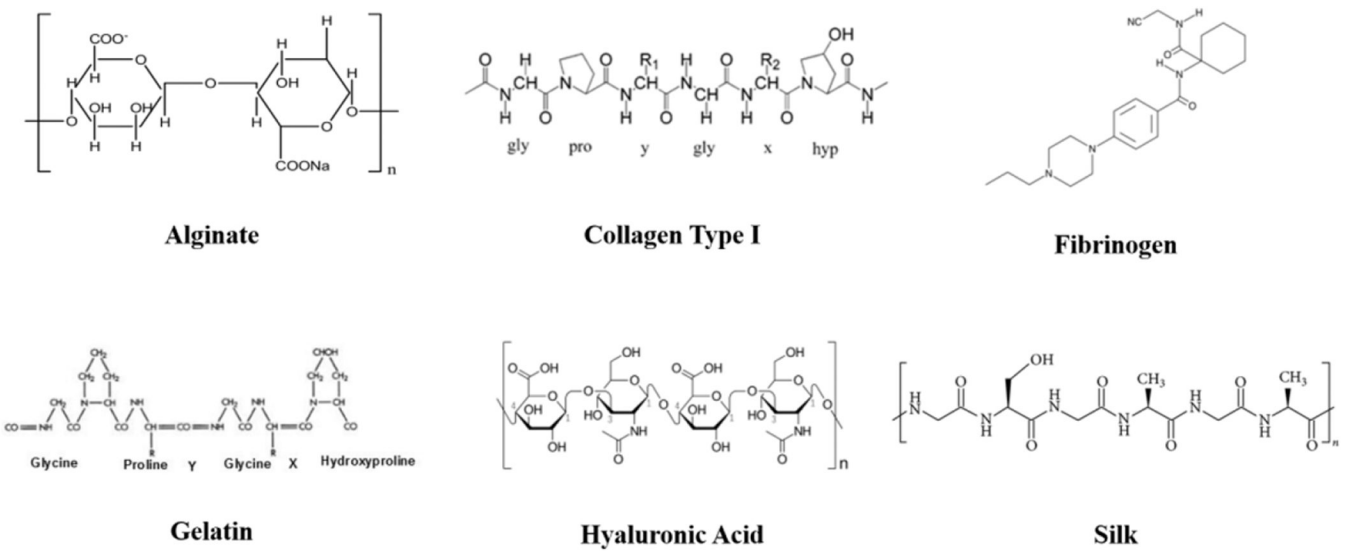

Figure 3.
Natural Polymers Chemical Structure.

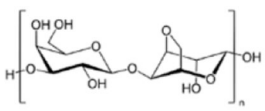

Agarose

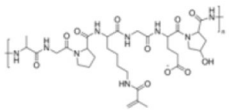

GelMA

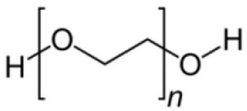

Polyethelene Glycol

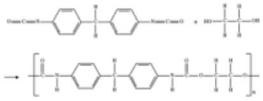

Polyurethane

Figure 4.
Synthetic Polymers Chemical Structure.

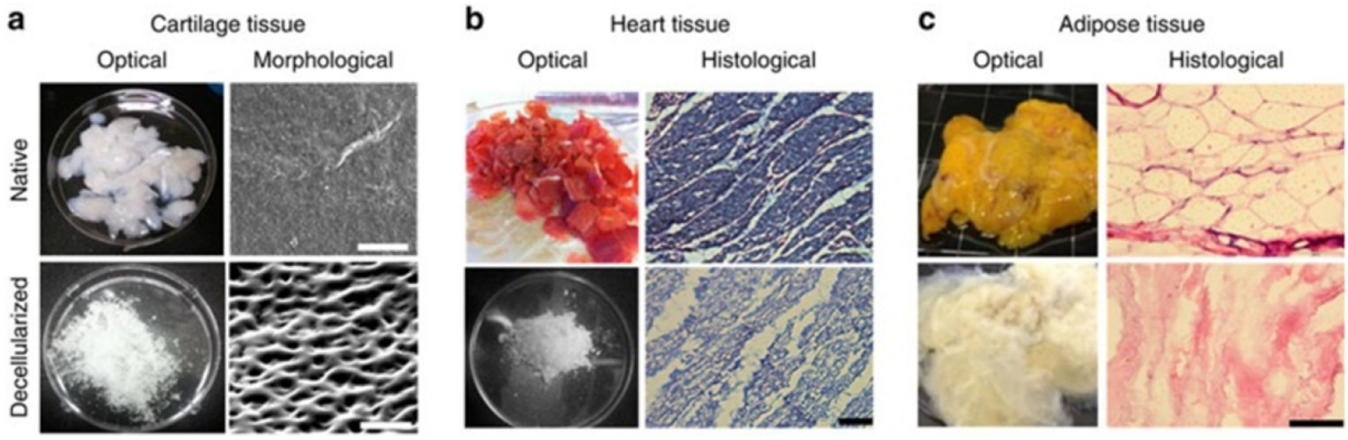

Figure 5. Decellularization of tissues with biochemical analysis.

Images of decellularized (a) cartilage tissue (scale bar, 50 μm), (b) heart tissue (scale bar, 100 μm), and (c) adipose tissue (scale bar, 100 μm). (Reprinted with permission from ref[43]. Copyright 2014 Nature Communications).

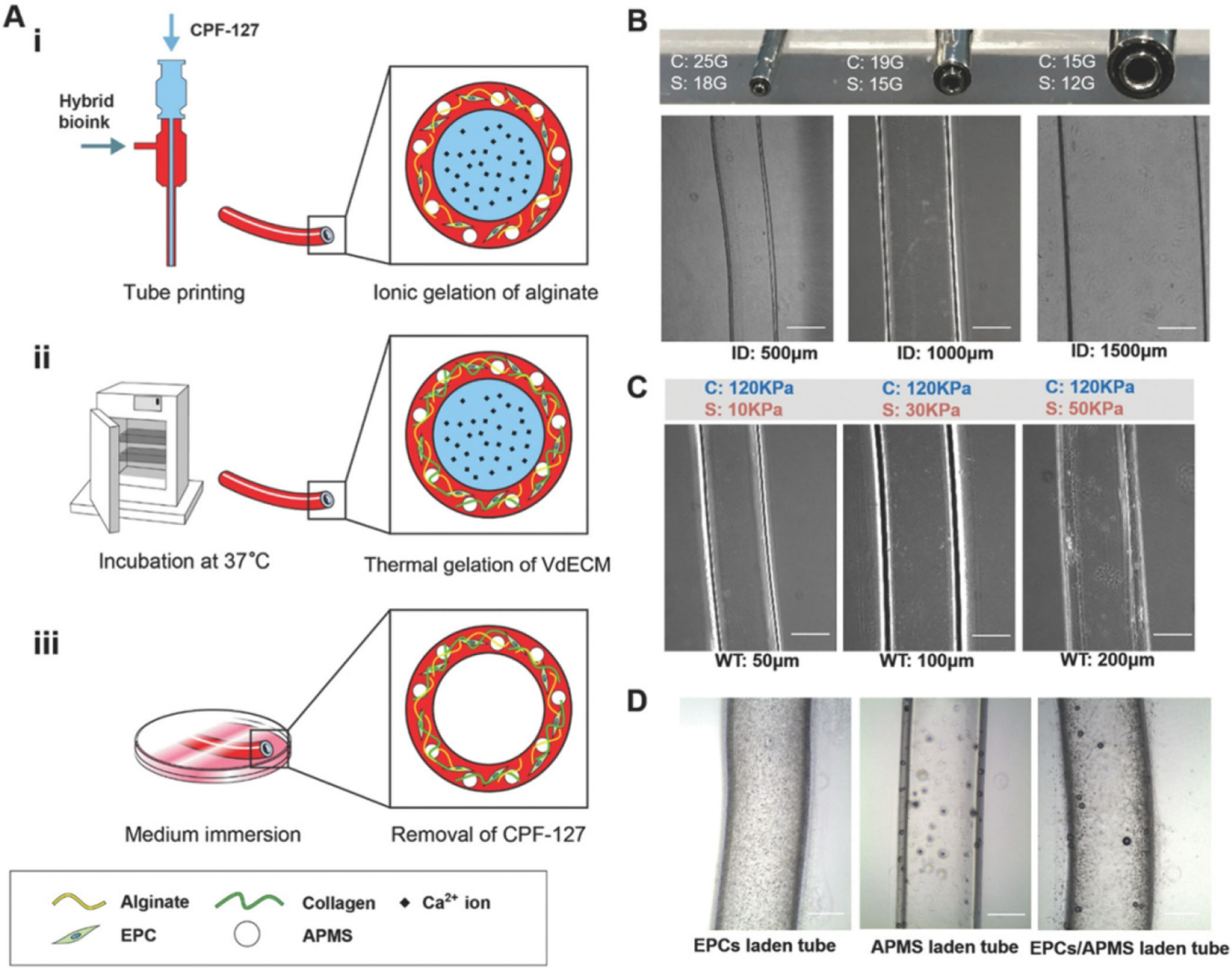

Figure 6. Coaxial Printing.

A) A schematic depiction of the coaxial printing process fabrication process. Alginate gelation is realized in coaxial printing (i), thermal crosslinking of collagen fibers is then induced by incubation at 37 °C (ii), followed by immersion in medium to the and obtain a hollow tubular shape (iii). B) Combining a variety of core and shell allows for printing tubes with different inner diameters. C) By adjusting the flow rate in the shell nozzle permits tubular structures with unique wall thicknesses with a 15/19 gauge coaxial nozzle. D) The 15/19 gauge coaxial nozzle produced successful tubular, vessel like structures with EPCs, AMPS, and EPC/AMPS laden BBVs (scale bar: 500 μm). (Reprinted with permission from ref[138]. Copyright 2019 Advanced Functional Materials)

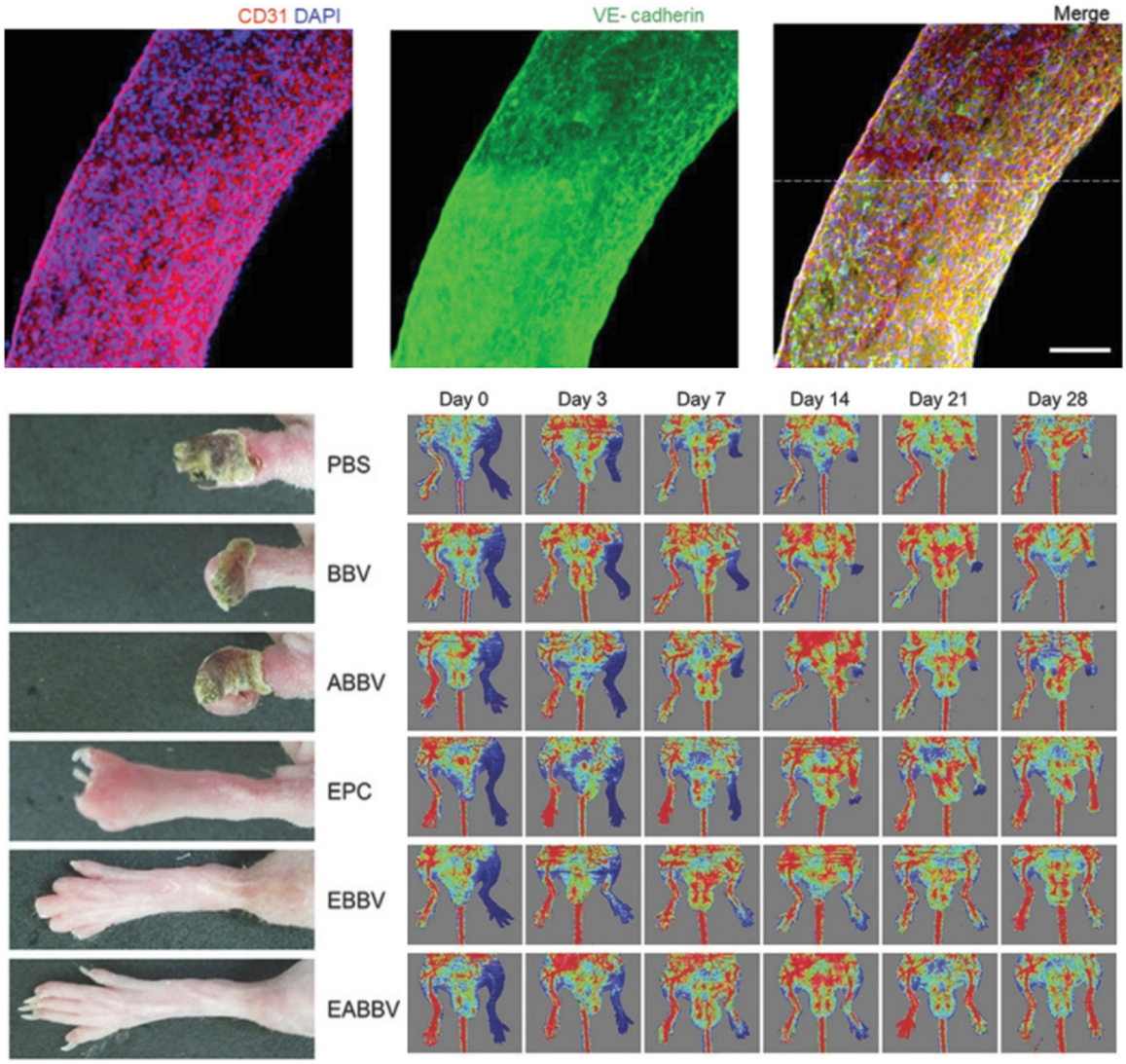

Figure 7. Coaxial blood vessel bioprinting.

Maturation of coaxial cell printed vasculatures. The formed endothelium layer in the luminal wall of tube expressed VE-cadherin on day 7 (scale bar: 100 μm) (Reprinted with permission from ref[134, 138]. Copyright 2019 Advanced Healthcare Materials). Assessment of functional recovery in a murine hind limb ischemia model with representative images of six treatment groups with transplanted coaxially printed vessel-like constructs showing different outcomes, including limb loss, foot necrosis, toe loss, and limb salvage. Blood perfusion was evaluated by laser Doppler perfusion imaging analysis in the ischemic limbs of the mice transplanted with PBS, BBV, ABBV, EPCs (EPC), EBBV, and EABBV. (Reprinted with permission from ref[134]. Copyright 2019 Advanced Functional Materials).

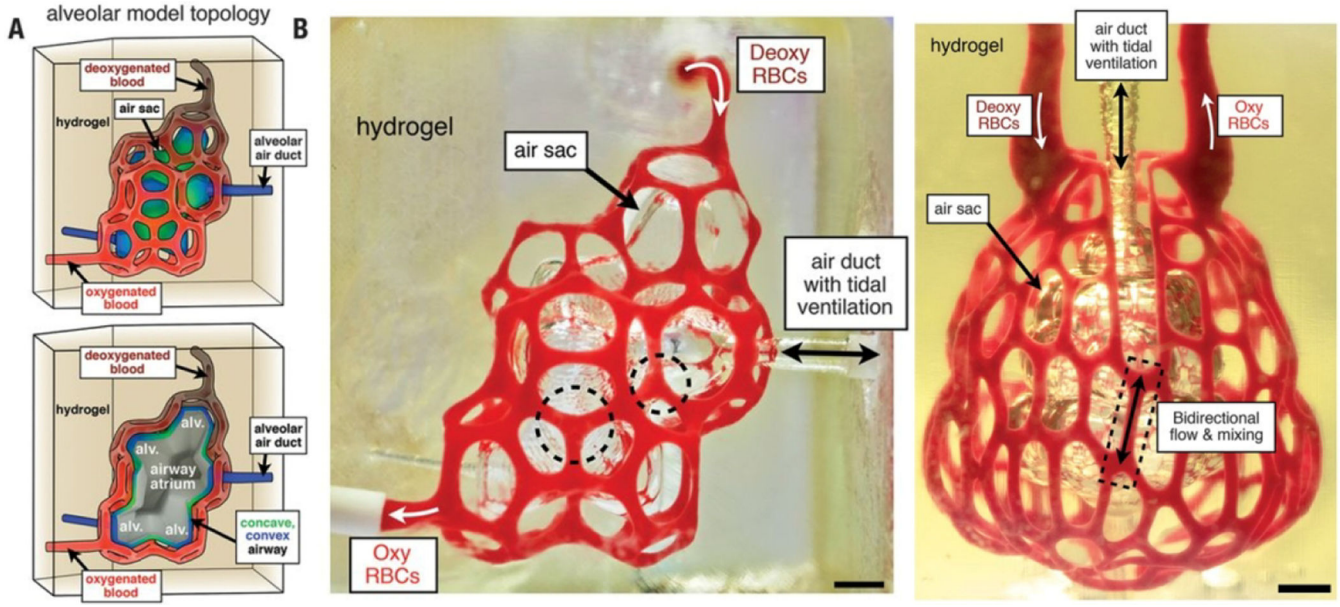

Figure 8. SLATE printed lung structure with oxygenation and tidal ventilation with vascularized alveolar topologies.

(A) A design of the alveolar model offset to derive an unsheathing vasculature, and a cutaway view to illustrate the shared airway atrium of the model alveoli. (B) A Photographs of a bioprinted construct during RBC perfusion with the air sac ventilated with O_2 (scale bar, 1 mm). (Reprinted with permission from ref[140]. Copyright 2019 Science).

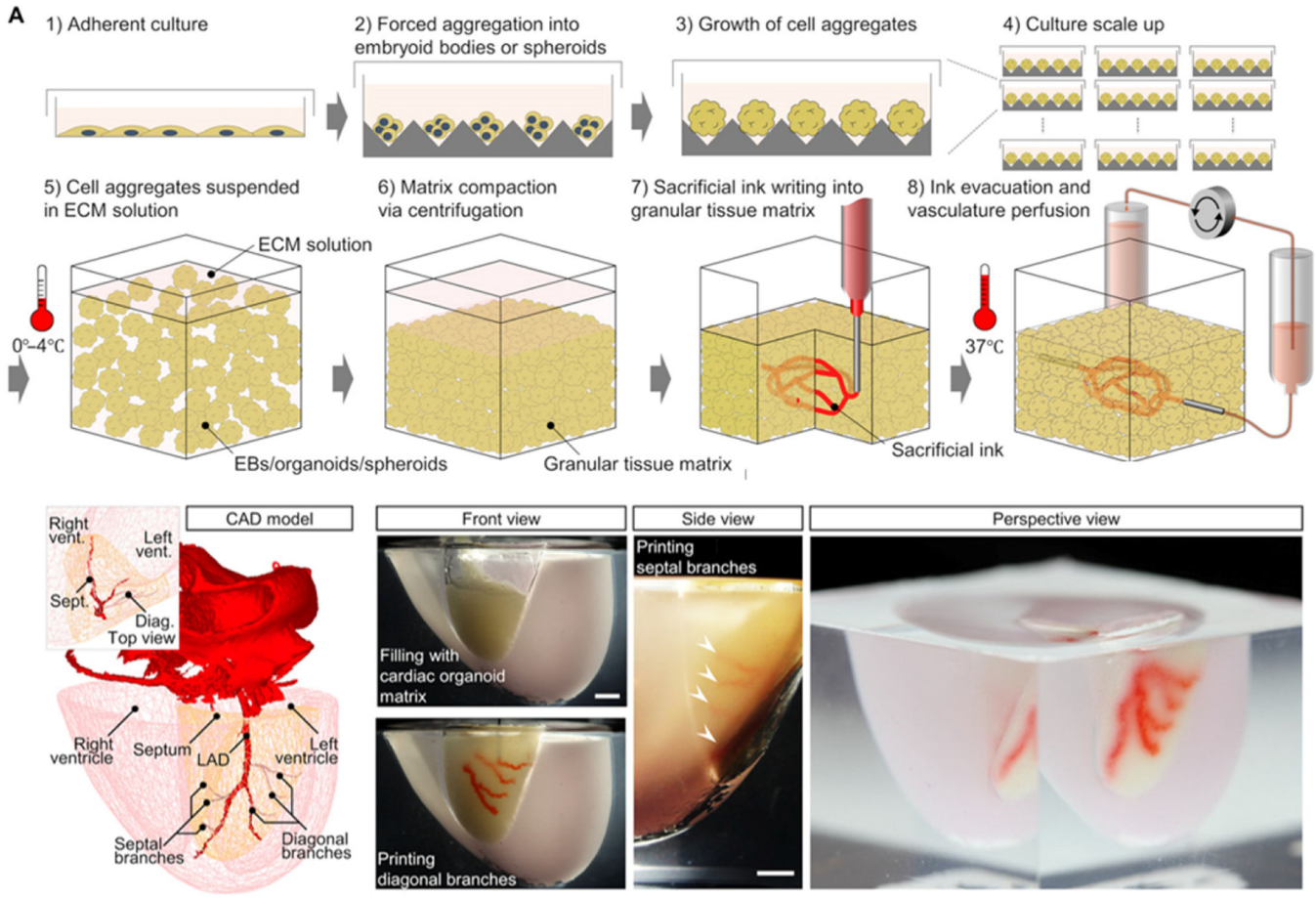

Figure 9. SWIFT indirect printing method.

An illustration of the SWIFT process, step-by-step. A 3D CAD model of a normal human heart was downloaded from the NIH 3D Print Exchange. A scale mold was formed using human CT imaging data, and the left anterior descending artery, diagonal and septal branches were printed by embedding into the septal-anterior wall wedge of the cardiac tissue matrix. Scale bar, 5 mm. (Reprinted with permission from ref[144]. Copyright 2019 Science Advances).

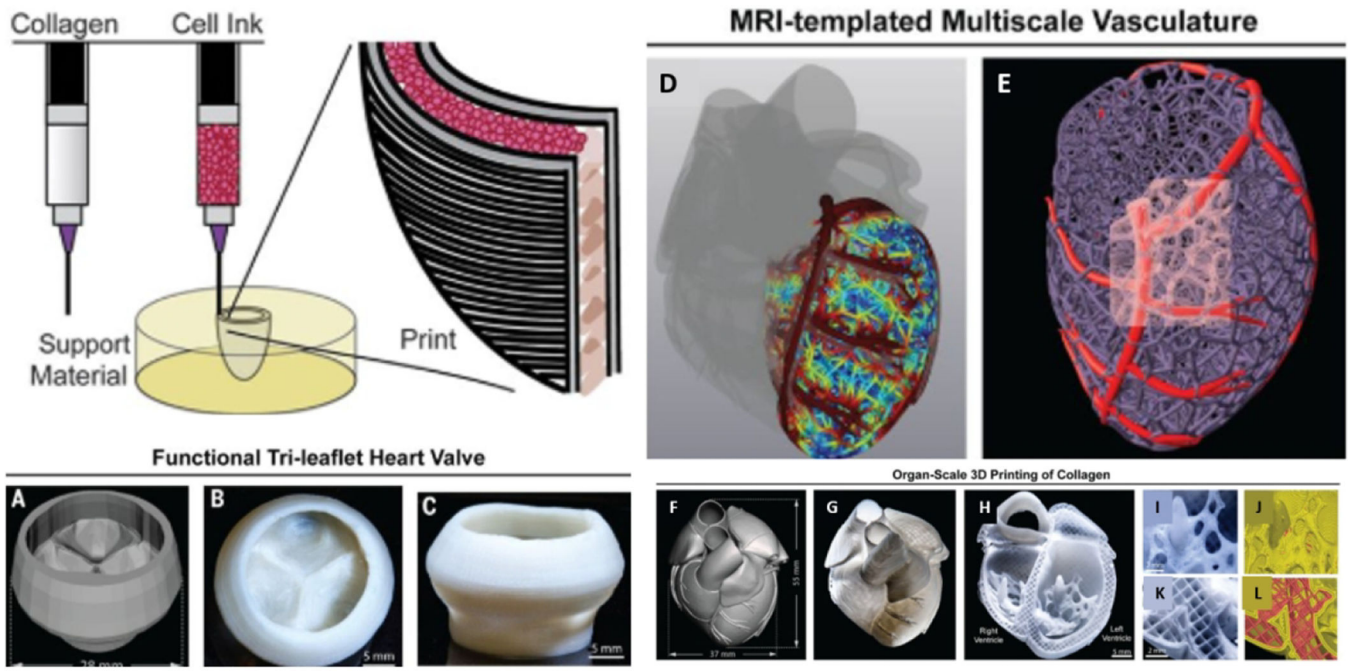

Figure 10. 3D Bioprinted neonatal-scale human heart fabricated using the FRESH 3D bioprinting technique.

First, an schematic of the dual-material FRESH printing method using a collagen bioink and a high-concentration cell ink. (A) 3D model of an adult human tri-leaflet vale, followed by top (B) and side (C) views of a FRESH-printed collagen heart valve. (D, E) A 3D human heart model derived from MRI, with a multiscale vascular network (left ventricle). The coronary artery is the template that guides smaller-scale vessels, which progressively decrease in diameter. (F) An MRI-derived 3D human heart scaled to neonatal size followed by the (G) FRESH-printed collagen heart. (H) Cross-sectional view of the fresh bioprinted heart. High-fidelity images of the trabeculae (I) and associated G-code (J). High-fidelity image of the septal wall (K) and G-code (L). (Reprinted with permission from ref[167]. Copyright 2019 Science).

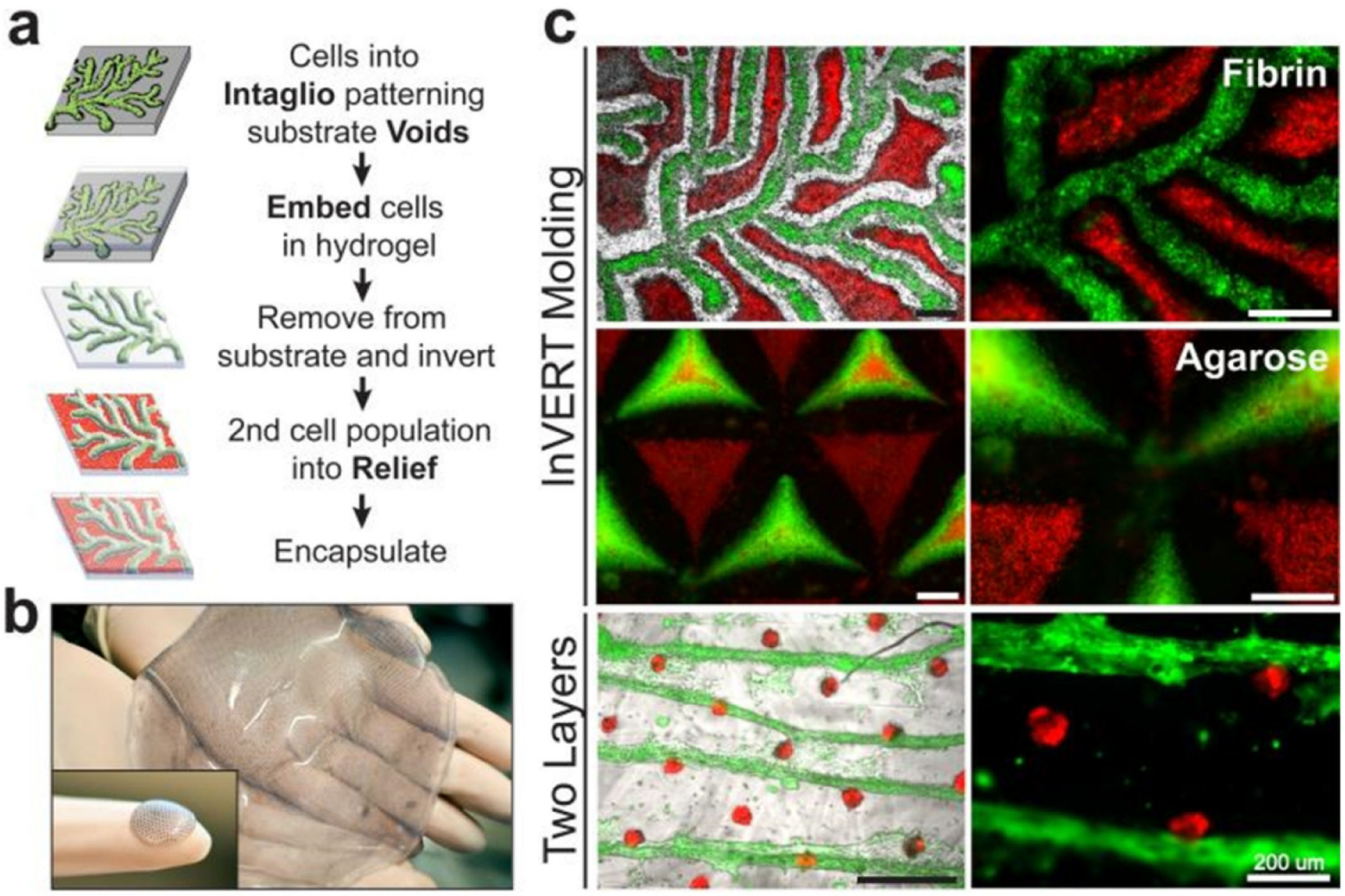

Figure 11. Liver fabrication using InVERT molding.

(a) The diagram describes InVERT (Intaglio-Void/Embed-Relief Topographic molding) molding, with cell populations displayed red (relief phase) and green (intaglio phase). (b) This method allows for construct formation up to 14cm in diameter. (c) InVERT molding allows for multi-compartmental patterning of a range materials. Labeled cells: endothelial cells (green); fibroblasts (red); are patterned in fibrin gel using a branching substrate (top) or in agarose using a substrate molded using a corner cube bike reflector (middle). Manual stacking allows for layering of the molded cell layers for multilayer patterning (scale bars 500 μm). (Reprinted with permission from ref[180]. Copyright 2013 Nature Communications).

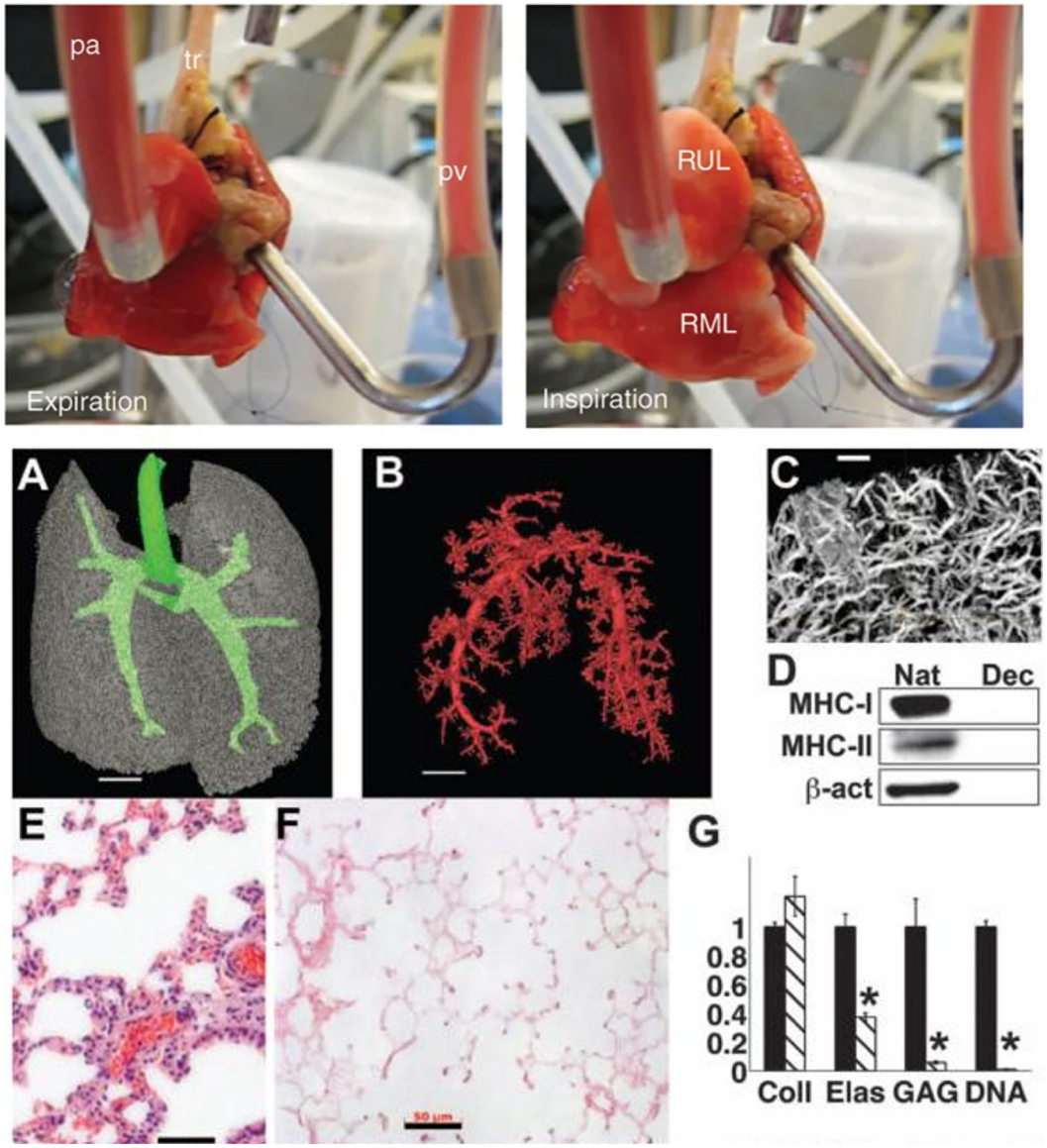

Figure 12. Lung Decellularization.

Regenerated lung constructs attached to an *in vitro* lung bioreactor (pa, pulmonary arterial cannula; pv, pulmonary venous cannula; tr, trachea) during inspiration (right; RUL, right upper lobe; RML, right middle lobe) and expiration (left). (Reprinted with permission from ref[182]. Copyright 2010 Nature Medicine). (A) A three-dimensional micro-CT rendering of the acellular matrix airway compartment, with large airways shown in green, compared with (B) angiography of the vascular compartment (red) (4 mm scale bar). (C) Smaller vessels are visualized with micro-CT (500 μm scale bar). (D) Immunoblot for MHC-1, MHC-II, and β-actin demonstrate removal of cellular proteins during decellularization. Next, they compared Hematoxylin and eosin (H&E) stained native rat lung (E) and decellularized lung matrix. (F) (50 μm scale bar). (G) Quantification of Collagen, elastin, glycosaminoglycan, and DNA contents of the native lung (black bars) compared to the acellular lung ECM matrix (hatched bars). (Reprinted with permission from ref[183]. Copyright 2013 Science).

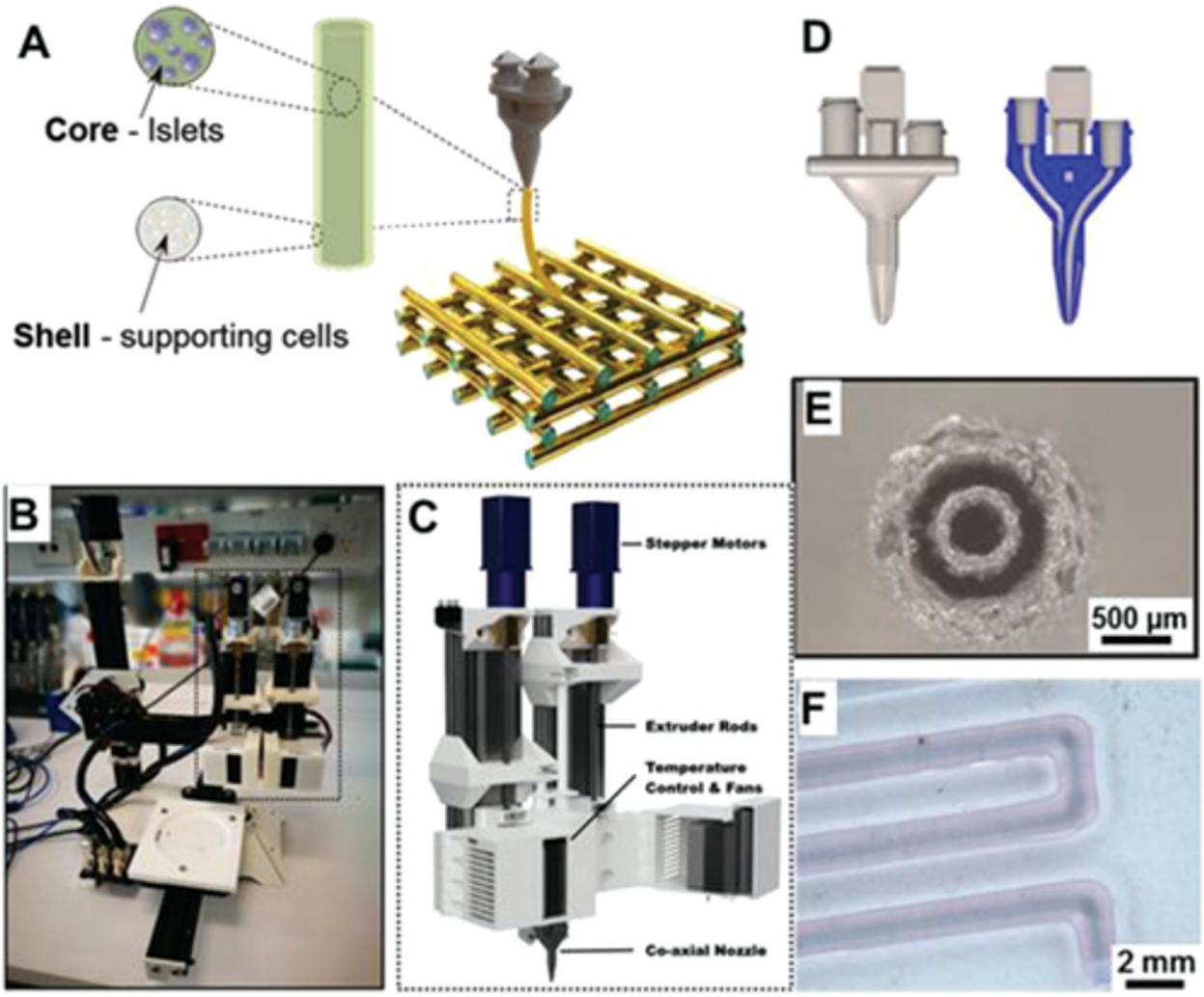

Figure 13. Pancreas Bioprinting.

Schematic representation of the proposed coaxial printing approach to establish vascularized bioartificial pancreatic constructs (A). Pancreatic insulin-secreting cells will be housed in the core component, which will be surrounded by EPC or Tregs cells. The Dual Ink Co-Axial Bioprinter (B), 3D models of the extruder heads (C) and the nozzle (D), microscope image of the coaxial structure of printing nozzle (E) and bright-field image of coaxial control strand printed with blue/red dye to visualize core and shell structure respectively (F) are displayed. (Reprinted with permission from ref[212]. Copyright 2019 Advanced Healthcare Materials).

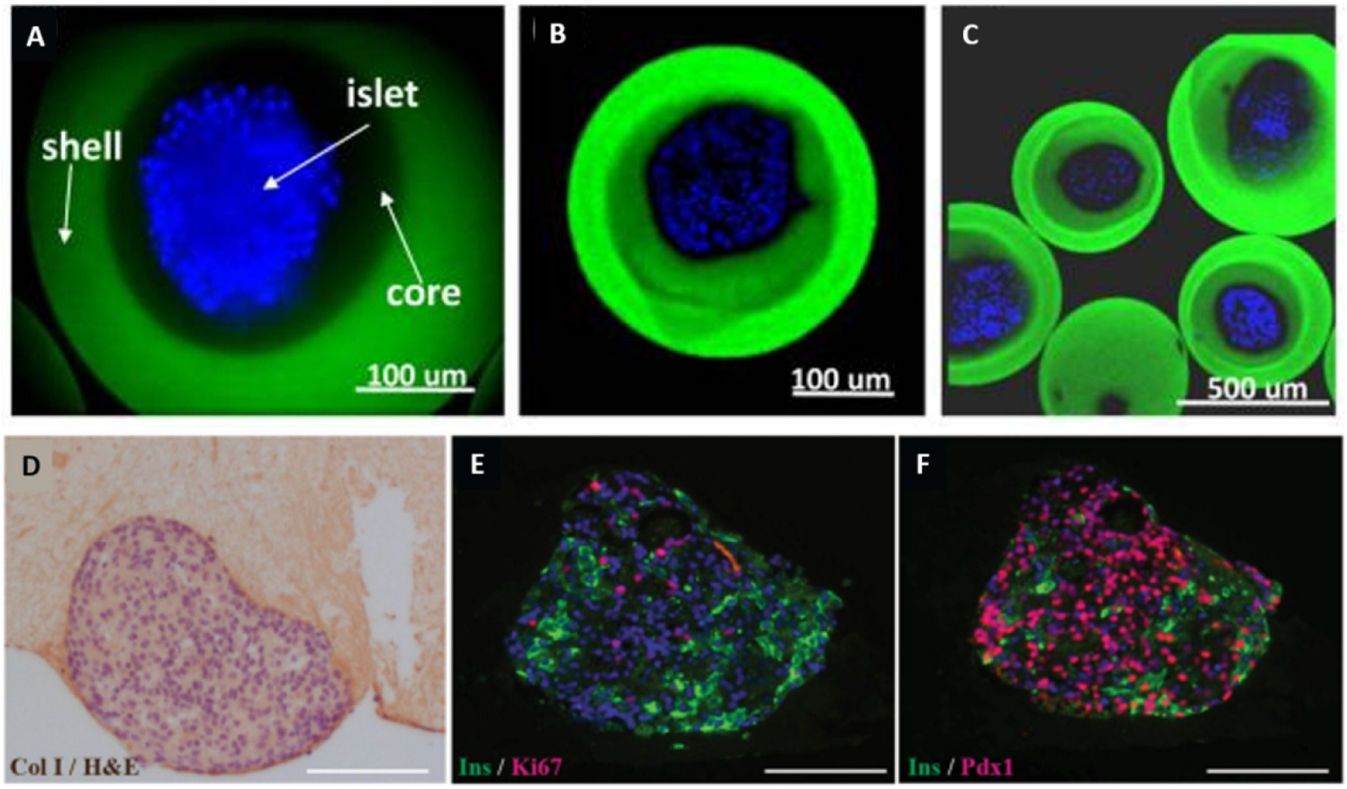

Figure 14. Pancreatic Islet Encapsulation.

(A-C) Comparison of islets encapsulated in regular capsules and core-shell capsules. 3D reconstructed confocal fluorescent images of islets encapsulated in core-shell capsules. The islets were stained blue, while the shell was labeled green. (Reprinted with permission from ref[208]. Copyright 2013 Advanced Healthcare Materials). (D-F) hPSC-derived ILCs were embedded in hP-HG for 4 days, fixed, embedded, and stained for Col I, Ins (green), Ki67 (red), or PDX1 (red nuclei). Images show healthy cell clusters containing non-proliferative Ins+ cells in the clusters and numerous PDX1+ Ins− progenitor cells and Ins+ PDX1+ beta-like cells. (Reprinted with permission from ref[209]. Copyright 2018 Scientific Reports).

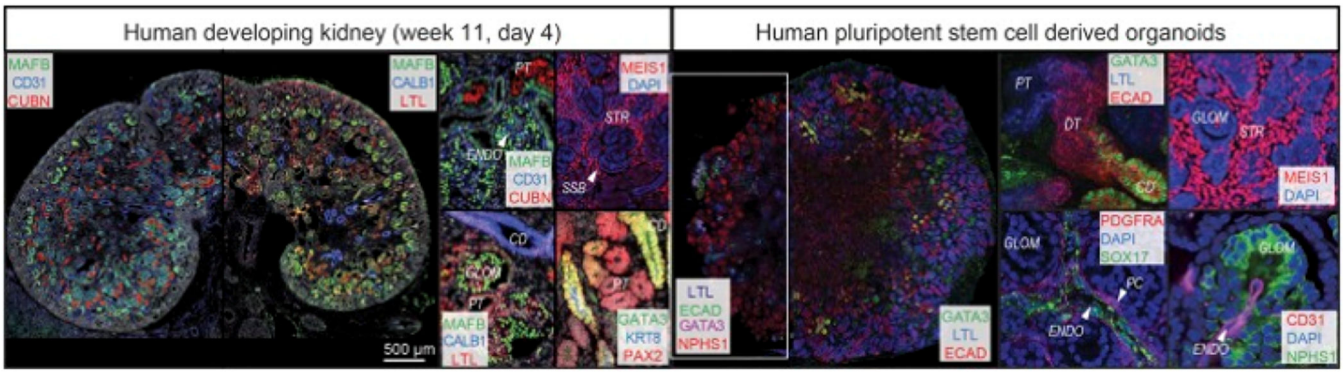

Figure 15. Kidney Organoids.

Kidney organoids derived from induced pluripotent stem cells shown to contain patterned nephrons, collecting ducts, renal interstitium, and endothelium similar to the native fetal human kidney. This figure provides a comparison between a normal human fetal kidney (left) and the kidney organoids (right) (Reprinted with permission from ref[219]. Copyright 2017 Journal of the American Society of Nephrology).

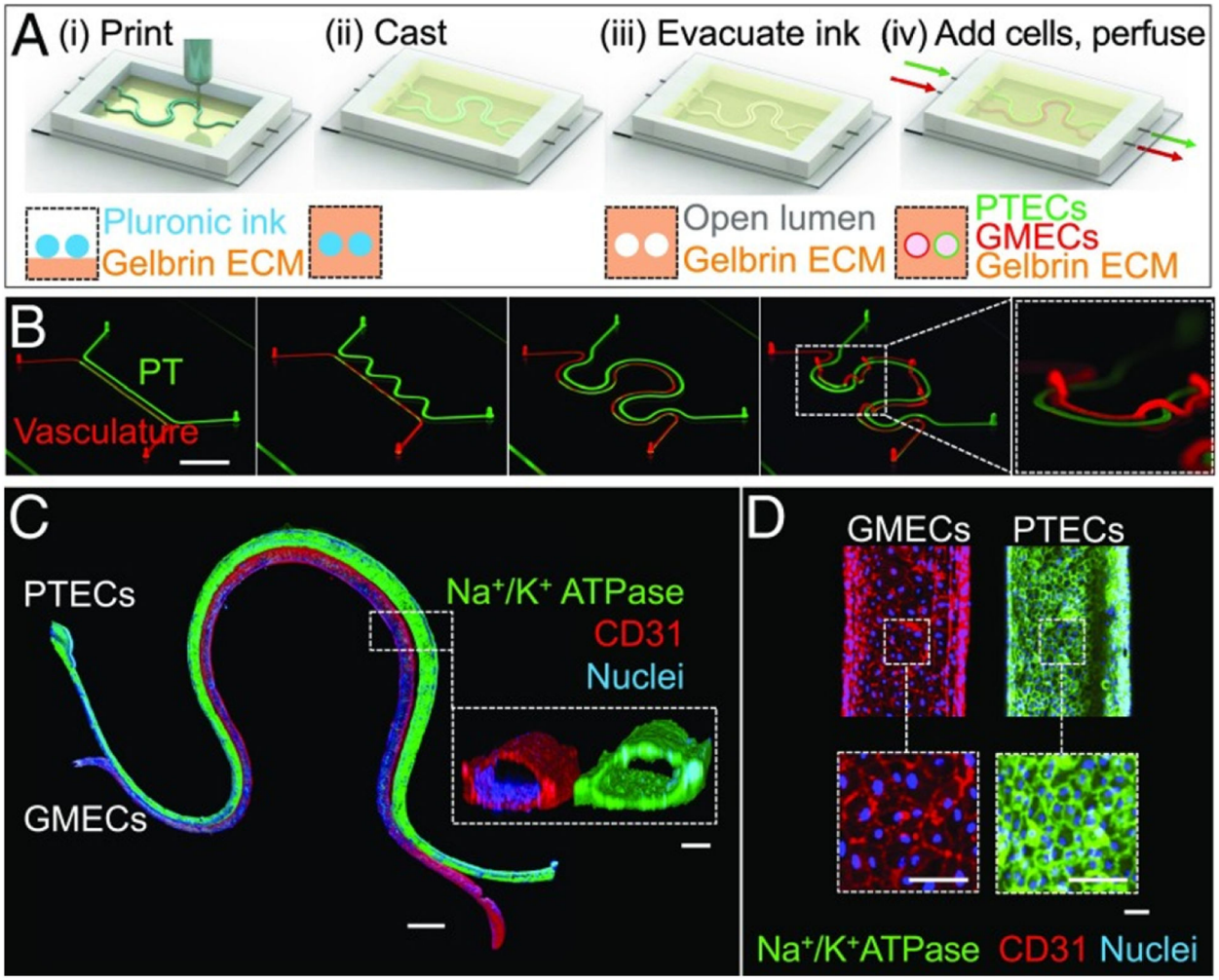

Figure 16. Kidney Tubule Bioprinting.

Design and fabrication bioprinted renal proximal tubule. (A) A schematic depiction of the fabrication process, demonstrating that (B) both simple and complex models can be printed (Scale bar: 10 mm.). (C) Immunofluorescence staining of the tissue with which Na^+/K^+ ATPase (green), CD31 (red), and nuclei (blue) (Scale bar: 1 mm.). (D) Images taken at high-magnification after staining (Scale bars: 100 μm.). (Reprinted with permission from ref[234]. Copyright 2019 PNAS).

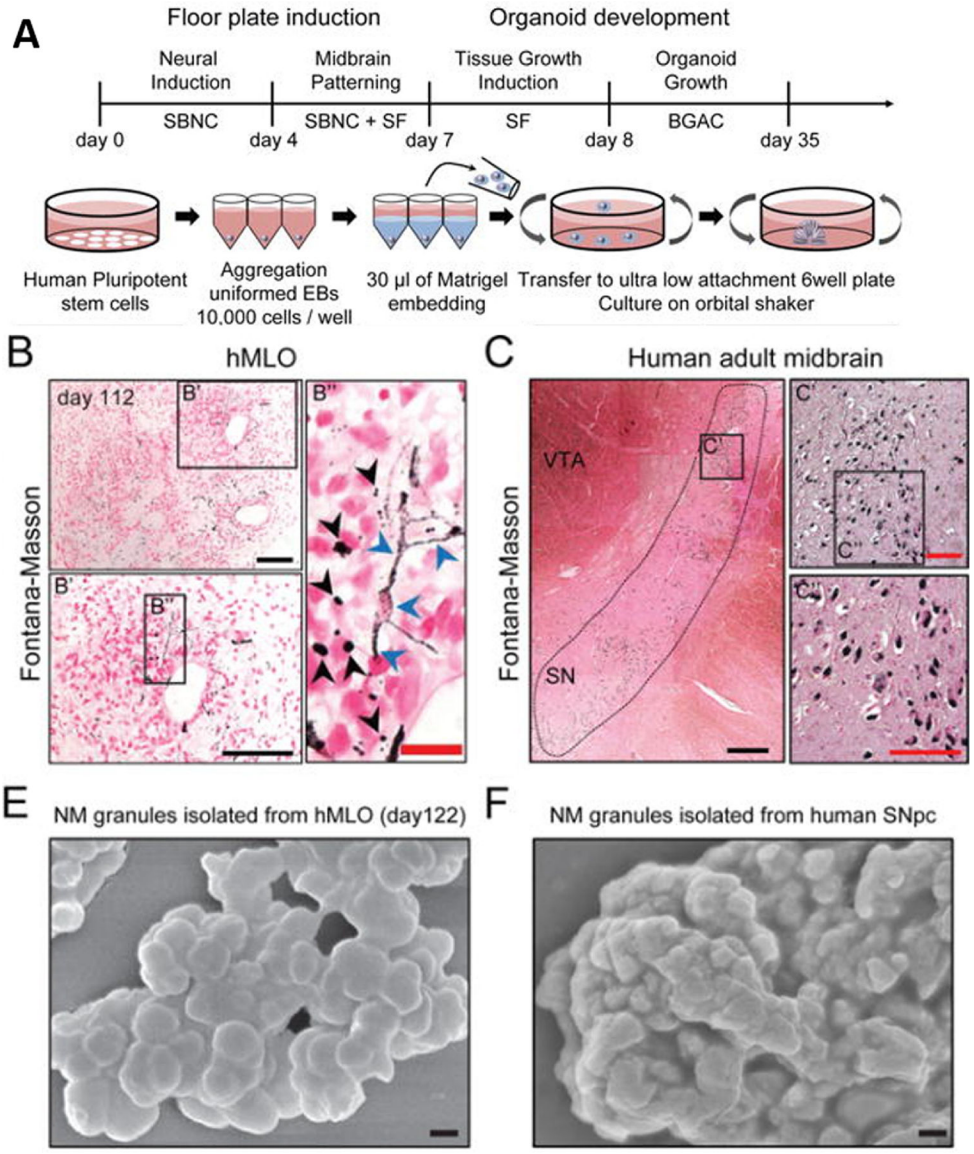

Figure 17. Midbrain Organoid.

(A) Schematic diagrams illustrating the overall strategy to midbrain organoids.

(B) Fontana-Masson staining to reveal NM-like granules in both intra- (blue arrows) and extracellular compartments (black arrows) of the organoids compared with (C) Fontana-human midbrain tissue. (E) SEM image of isolated NM granules from the organoids, compared with (F) Huma midbrain tissue. (Reprinted with permission from ref[244]. Copyright 2016 Cell Stem Cell).

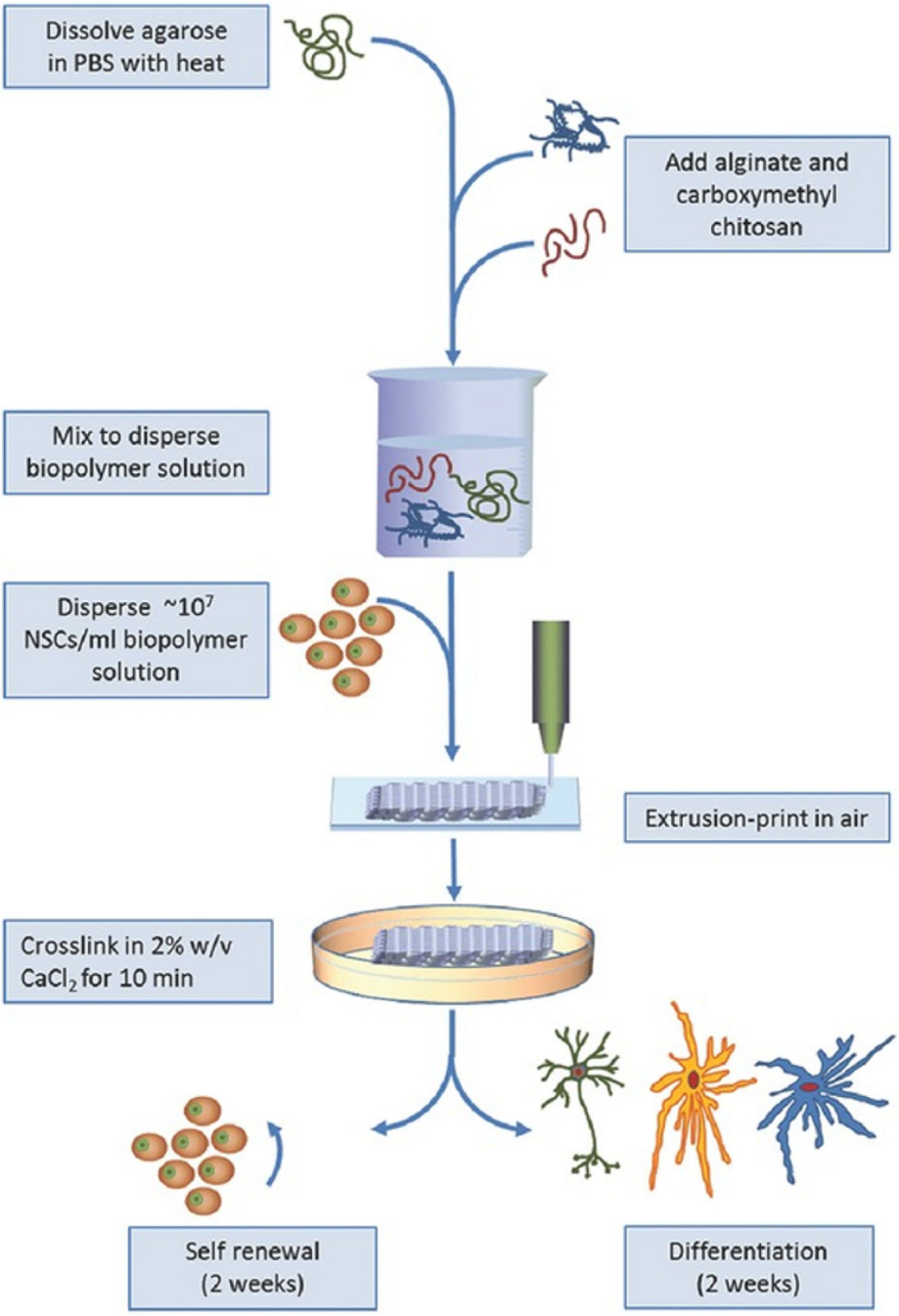

Figure 18. Brain bioprinting strategy

A Schematic illustration of the major steps for direct-write printing of bioprinted brain constructs with an optimized bioink with encapsulated neural stem cells for 3D culture and differentiation. (Reprinted with permission from ref[254]. Copyright 2016 Advanced Healthcare Materials).

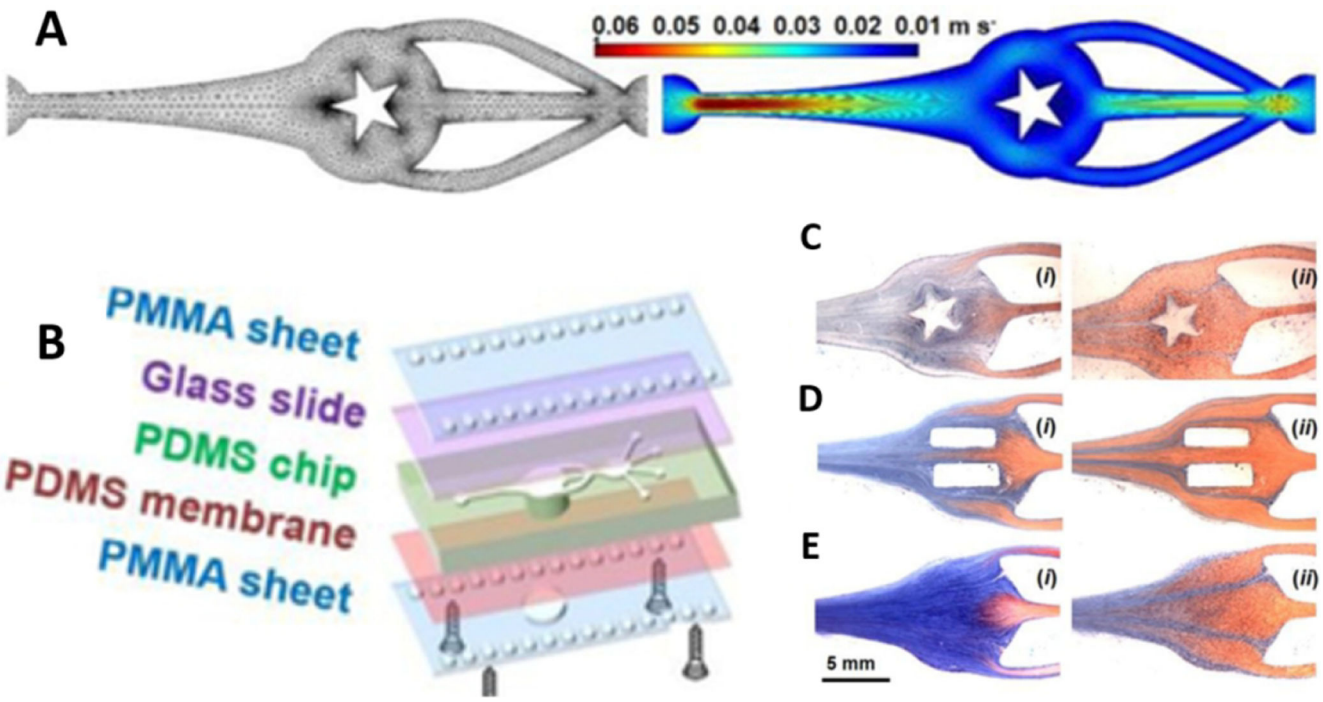

Figure 19. Microfluidic Bioprinting.

(A) Schematic diagram of the microfluidic chip with four inlets and one shared outlet. (B) A model of the closed chamber under sinusoidal fluid flow, and images (C-E) demonstrating the role of mixing and washing of streamline flow in GelMA solution, with a star pattern or two rectangular patterns vs. no pattern. (Reprinted with permission from ref[264]. Copyright 2018 Advanced Materials).

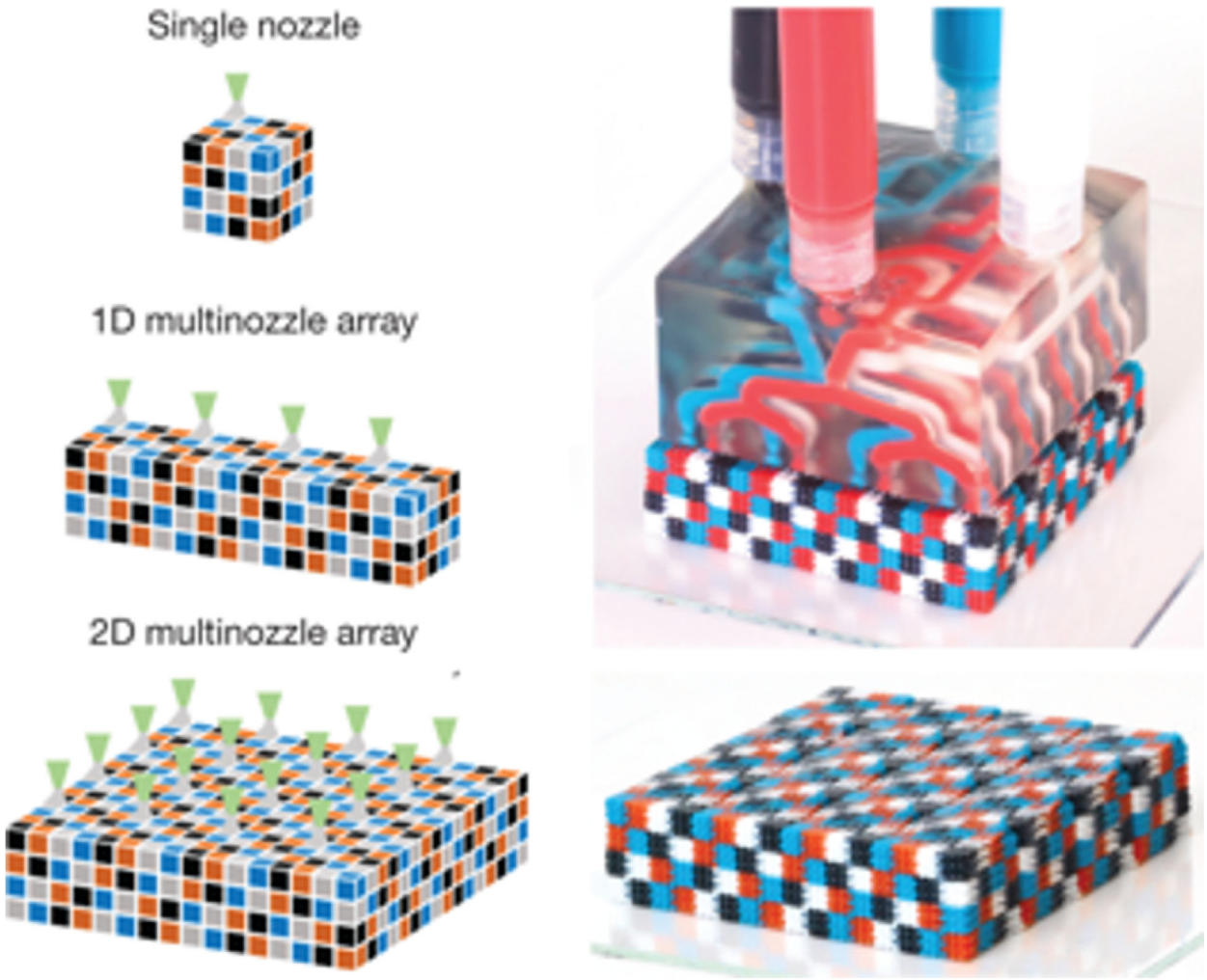

Figure 20. Multimaterial Multi-nozzle 3D Print Heads for Voxalated Printing

(Left) A summary image of the voxelated architecture printed using a single 0D nozzle (top), the 1D (middle), and 2D (bottom) MM3D print heads. Finally, an image of voxelated material fabricated by MM3D printing using a 4 × 4-nozzle, four-material, 2D print head. (Reprinted with permission from ref[265]. Copyright 2019 Nature).

Table 1.

Summary of hydrogel formulation by bioink, year, and target organ

Bioink	Formulation	Crosslinking Mechanism	Bioprinting Method	Target Organ	Structural Elements Targeted	Year	Reference
Agarose	agarose 1% collagen .8%, agarose 1% chitosan .33%	Covalent and Physical	Extrusion	General	Microstructure and Nanostructure	2015	[28]
	3% agarose with 3% alginate printed into a gluorcarbon support liquid	Physical	Extrusion	Vascular	Mesostructure (Blood vessel)	2013	[29]
	3% agarose	Physical	Extrusion	Vascular	Mesostructure (blood vessel)	2013	[30]
Alginate	3% Alginate	CaCl2	Extrusion	Liver	Microstructure (Liver)	2017	[31]
	1.5% RGD-Coupled Alginate	CaCl2 and Sodium Borohydride and barium chloride	Microvalve	Liver	Microstructure (Liver)	2015	[32]
	4% Alginate, 5% Gelatin	CaC12	Extrusion	Pancreatic	Microstructure (Islet of Langerhans)	2015	[33]
	.06 g/mL Gelatin, .05 g/mL Alginate	CaC12	Extrusion	Cardiac	Mesostructure (Heart Valve)	2013	[34]
	7.5% Aglinate	CaC12	Extrusion	Cardiac	Microstructure (Cardiac Muscle)	2012	[35]
Cell aggregate	Media	None	Microvalve	Kidney	Microstructure	2013	[36]
	Agarose	Physical	Extrusion	Neuro	Mesostructure	2013	[37]
	Agarose	Physical	Extrusion	Vascular	Mesostructure	2009	[38]
	Media	None	Extrusion	Cardiac	Microstructure	2008	[39]
Collagen	890uL type I collagen gel, 60uL sodium hydroxide, 250 uL sodium bicarbonate	Physical	Extrusion	Lymphatic	Macrostructure, Microstructure, and Nanostructure (Thyroid Gland)	2017	[40]
	.2% Collagen	NaHCO3	Microvalve	Bladder	Mesostructure	2010	[41]
Decellularized matrix	Liver ECM, Cardiac ECM, Skeletal Muscle ECM	Physical	Extrusion	Liver	Nanostructure	2015	[42]
	Cardiac ECM,	Physical	Extrusion	Heart	Microstructure and Nanostructure	2014	[43]
Fibrin	15% Gelatin and Fibrin 50mg/mL	Thrombin and CaCl2	Extrusion	Kidney	Microstructure	2016	[44]
	elatin (35~45 mg/ml), fibrinogen (20–30 mg/ml), HA (3 mg/ml) and glycerol (10% v/v)	Thrombin	Extrusion	Muscle	Macrostructure (Ear) Microstructure (Muscle Fibers)	2016	[45]
	10mg/mL Fibrinogen	Thrombin	Extrusion	Pancreatic	Mesostructure and Microstructure	2016	[46]
Gelatin	HyStem Gelatin and HA	Thiol	Extrusion	Cardiac	Microstructure and Nanostructure	2015	[47]
Gellangum	.5% RGD-Gellan Gum	CaCL2	Extrusion	Neural	Mesostructure and Microstructure	2015	[48]
Hyaluronic Acid	HAMa	Photo-Crosslink	Extrusion	Cardiac	Mesostructure and Microstructure	2014	[49]

Bioink	Formulation	Crosslinking Mechanism	Bioprinting Method	Target Organ	Structural Elements Targeted	Year	Reference
	GelMA HAMa	Photo-Crosslink	Extrusion	Vascular	Mesostructure	2010	[50]
Matrigel	Matrigel	Physical	Inkjet	Lung	Microstructure	2015	[51]
	3/1 Matrigel to Alginate	Physical	Extrusion	Vascular	Microstructure	2014	[52]
Media	Spheroid	Physical	Needle Array	Cardiac	Microstructure	2017	[53]
	Spheroid	Physical	Needle Array	Liver	Microstructure	2017	[54]
	PBS and C2C12 Myoblasts	Physical	Inkjet	Muscle	Microstructure (myotube)	2013	[55]
Polyethylene glycol	2% Thyolate HA, 4% TetraPA	PEGDA	Extrusion	Vascular	Mesostructure	2010	[50]
Polyurethane	Polyurethane and Matrigel	Physical	Laser	Cardiac	Mesostructure	2011	[56]